Phenomenology of Asymptotic Safety

Erik Gerwick

A thesis submitted in fulfilment of the requirements
for the degree of Doctor of Philosophy
to the
University of Edinburgh
August 2011

Abstract

In this work we explore the collider prospects for the asymptotic safety scenario being realized as a quantum theory of gravity. Testing gravity at colliders becomes a real possibility in the case of extra dimensional models, or with additional physics leading to a fundamental scale of gravity significantly lower than the Planck mass. We present several approximations for the full non-perturbative renormalization group running, and show how these can be implemented at the level of the graviton wave-function renormalization. The issue of scale identification of the physical process with the renormalization group scale k is clarified and several different choices are compared. The various approximations are resolved and shown in most cases to generate scheme independent results. On the phenomenological side, we investigate two separate observables. First, at tree-level we present results on LHC di-muon production due to asymptotically safe gravitons. By including fixed point scaling Kaluza-Klein modes, the predicted signal is enhanced and simultaneously problems associated with the breakdown of perturbative unitarity are reduced. At the one-loop level, we outline our calculation for the contribution to electro-weak precision observables originating from asymptotically safe gravity. New bounds are derived which show different behavior as a function of the number of extra dimensions compared with previous effective field theory results. Finally, we comment on possible further directions for exploring the frontier of collider physics and quantum gravity.

Declaration

A large potion of this work is from the paper produced by my collaboration with Daniel Litim and Tilman Plehn on "Asymptotically Safe Gravitons at the LHC" [1]. A smaller but still significant portion of this thesis is based on work I did as part of Ref. [2], where in the write-up I was assisted by Tilman Plehn. Some parts of the introduction are based on the proceedings in Ref. [3], written in collaboration with Tilman Plehn. Chapter 2 is loosely structured around a set of notes that I took during lectures given by Daniel Litim on quantum gravity, which I have cited in Ref. [4]. In Chapter 5, I received assistance from Michael Rauch in developing my own Monte Carlo tool and analysis package for investigating LHC signals, although all of the code is my own. I also benefitted from cross-checks with the private code of Tilman Plehn. Some of the discussion is motivated by material from my paper along with Tilman Plehn and Steffen Schumann [5]. In the appendix, I have presented some calculations in a simplified gravitational theory which were in the same set of lectures by Daniel Litim in Ref. [4]. Finally, I have benefitted from numerous informal interactions which are acknowledged in my publications.

E. Gerwick
August 2011

Acknowledgements

First of all, I thank my supervisor Tilman Plehn for providing me an incredible PhD experience where I essentially felt like part of two great programs; first at the University of Edinburgh and later with the pheno group in Heidelberg. I especially thank Tilman for his always welcoming hospitality in Heidelberg, his infectious optimism, for striking a nice balance between giving me my independence but never letting me feel like I was without his support, and importantly for breaking my long standing addiction with writing in the passive voice. I also especially thank my primary collaborator Daniel Litim. Without his patient style, deep theoretical insights, and our occasional 1 AM skype calls, our paper would never have achieved its full potential. Also, I thank Daniel for welcoming me into the quantum gravity community and encouraging me to attend various asymptotic safety conferences, quite often in nice locations.

In Edinburgh, the PPT staff took an active interest in my education and mentorship even though my primary collaborations were elsewhere. In particular I would like to thank Arjun Berera, Thomas Binoth, Einan Gardi and Luigi Del Debbio for their strong role in my development as a physicist and their concern in general for the education of theory post-graduates. I thank my fellow students, Gavin Cullen, Liam Keegan and Eoin Kerrane and office-mate Enrico Rinaldi for plenty of interesting chats over the years and our always therapeutic PhD inspired commiseration. From the Heidelberg group, Dorival Goncalves-Netto, Bob McElrath, Ioan Wigmore, Davide Lopez-Val, Peter Schintel, Kentarou Mawatari, Michihisa Takeuchi, Christoph Engert and Steffen Schumann provided a wonderful environment for physics. I will always cherish our numerous mensa lunches, summer BBQs, Havana sunday brunches, lively discussions and occasional Mannheim excursions.

There are a number of my former educators without whose influence I would

certainly never have achieved this PhD. First of all, Pat Cannon at Corvallis High school for taking me as a pretty poor high school student and molding an enthusiastic physicist through two years of consistently high expectations. The skills learned in his AP physics class remain some of the most important to my everyday research. At Lewis and Clark College I thank especially Herschel Snodgrass, Michael Broide and Martin Olsson for inspired teaching and ultimately seeding my near obsession with theoretical physics which led directly to graduate school. I will always appreciate the complementary styles of Michael's emphasis on physical conceptual understanding and Herschel's commanding awe of beautiful mathematical physics. If I ever become an educator myself, I will certainly attempt to model my approach after these two great teachers.

Outside physics, I was incredibly lucky to find flatmates over the past 4 years, Alex Qaqaya, Matt Anker, Eoin Kerrane, Julia Kennedy, Ioan Wigmore and Henry Dodson, who all in their own special ways provided me with a sanity restoring home environment and many irreplaceable memories. I also benefitted from great friends over the past years, especially traveling comrades in Ben Elkind, Josh Schoonover, Geoff Creighton, Colin Pomeroy, James Pullen, Ali Stewart, Richard Miranda and Henry Dodson as well as always motivated gym buddies in Michael Briggs, Henry Pearce and Trevor Back. Without these "distractions" my energy would never have carried me through this PhD. A significant part of this thesis was written during the "most productive week ever" at the British National Library. This was as a result of exceptional hospitality by James Pullen, Richard Miranda, Ali Stewart, Polly Bennett and Emily Richardson in a wonderful family-like environment in East London. Thank you to all.

A PhD of course never comes for free, and mine would not have been possible without a generous fellowship from the Scottish University Physics Alliance (SUPA). Moreover, I would like to specifically thank Avril Manners for her support and informal chats, in addition to setting me up with numerous speaking opportunities outside my normal graduate student responsibilities. Equally important, I would have been completely lost nearly my entire PhD without Jane Patterson. With Jane, a seemingly insurmountable bureaucratic task was often turned into a cheerful conversation. I cannot honestly remember a time when I came to her office and did not feel better (and calmer) walking away.

And finally, I thank my family in too many ways to list, though here are a few. Först, tack vare min mormor, morfar och hela den svenska familjen för trevlig sommarsemester de senaste 4 åren. My sister for her always uplifting and quite often philosophical phone chats. My father for inspiring me with the long hot tube talks about various aspects of time-travel, relativity and Star Trek. My mother for her high expectations and never letting me coast through school. And finally, both of my parent for there constant unconditional love and support. I dedicate this thesis to them.

Contents

List of Figures

List of Tables

Chapter 1

Introduction

Because truths we don't suspect have a hard time
making themselves felt, as when thirteen species
of whiptail lizards composed entirely of females
stay undiscovered due to bias
against such things existing,
we have to meet the universe halfway.
Nothing will unfold for us unless we move toward what
looks to us like nothing: faith is a cascade.

-Alison Fulton "Cascade Experiment"

1.1 LHC: A Window into Quantum Gravity?

In the summer of 2011, with the arrival of the first successful inverse femto-barn of proton-proton data, the Large Hadron Collider's (LHC) stated goal of exploring the frontier of TeV scale physics is finally coming to fruition. First and foremost, the LHC program expects to reveal the nature of electroweak symmetry breaking [9][10]. This may be the scalar Higgs boson predicted in the Standard Model or something more complicated acting like the Higgs. However, as the history of physics has shown, quite often the primary motivation for an experiment is not the *a postori* justification. In other words, in addition to identifying the mass of the Higgs boson, we hope that the LHC discovers the next paradigm in high-energy physics.

Typically at the LHC, searches for a new paradigm originate in the more humble pursuit of new particles. Connecting particles to paradigms and vice versa is thus the primary occupation of particle phenomenologists. To streamline this process, assumptions based on the expected nature of new physics is often used [11]. An example is dark matter, where the fact that these particles are relatively stable suggests looking at deviations from the SM prediction for missing energy. There is a balance though. By making model assumptions we limit the size of the net cast on beyond the Standard Model theories. For example, searching for jets plus missing energy is ineffective for other viable dark matter models like gravitino dark matter [12][13]. At the LHC then, we would like to cover all bases and include searches with varying amounts of model assumption.

One such model is the recently revived paradigm of extra dimensions [14][15][16][17][18]. In this thesis we primarily discuss flat extra dimensions where only gravity propagates in the additional space. These models predict a large number of gravitationally interacting massive particles in addition to the (indirectly measured) massless graviton responsible for general relativity [19][20]. At colliders like the LHC, these new particles can be seen in two ways. Either we produce them directly and they escape as missing energy [21], or the massive graviton decays back to observable particles creating an excess in some distribution [22]. The later is theoretically more interesting as the signal probes off-shell effects of massive gravitons.

Searches for virtual gravitons are plagued with theoretical ambiguities [23]. As will be discussed in detail, the signal is sensitive to the regime where the effective description of extra dimensions breaks down and the dynamics of quantum gravity become relevant. In order to proceed, we can compute observables in the low energy limit, and reformulate searches for extra dimensions in terms of generic four-point operators. The advantage here is that no input about the speculative nature of quantum gravity is necessary. However, the downside is that the resulting bounds on extra dimensions carry an inherently unquantified theoretical uncertainty. Alternatively, we can maintain the full dynamics of the extra dimensions, but cut-off divergent integrals explicitly "by hand". This implies that the majority of the signal comes from exactly that region of momentum space where the cutoff is placed. An unknown dependence on the details of UV physics is then implicit in most observables. Neither of these methods is fully

convincing in the search for extra dimensions.

In this thesis, we present an improvement to this search by making the additional assumption that in the UV gravity possesses an interacting fixed point [24]. This situation is typically referred to as Asymptotic Safety, as it generalizes the more well-known Asymptotic Freedom. Moreover, we will see that asymptotic safety provides robust predictions for the behavior of extra dimensional gravitons, meaning that it may be possible to actively search for and rule out these new particles at the LHC.

Along with providing their own unique predictions, a crucial benefit of assuming asymptotic safety is an improvement in theoretical uncertainty in searches for extra dimensions. The reason for this is that the conventionally divergent momentum integral in our approach is regulated by renormalization effects at the fixed point. In addition, we present a new calculation for the indirect electroweak constraints originating from contributions to gauge boson self energies. Naively this amplitude is power divergent, but with a fixed point becomes finite and independent of the UV cut-off. However, the sensitivity to the fixed point region is enhanced compared with the tree-level. We present this calculation as a proof of concept that our techniques can be extended to observables beyond tree-level.

This thesis is arranged as follows. In Chapter 2 we build the necessary technology to analyze gravity in perturbation theory. We will see the appearance of divergences in this straight-forward approach and understand the notion of gravity as an effective theory. Moving beyond perturbation theory we outline the growing evidence that gravity may be a continuum quantum field theory. In Chapter 3, we present the modern paradigm of large extra dimensions, and exhibit in detail the Kaluza-Klein reduction needed to derive the 4-dimensional particle spectrum. In particular, we derive the spectrum in two gauges as we use both in our computations. The experimental constraints on extra dimensions are outlined. We devote a sizable portion of this section to a discussion on the ambiguities associated with virtual graviton exchange.

We present our work melding the asymptotic safety scenario with extra dimensions starting in Chapter 4. In order to make sense out of the generally complicated form of the asymptotic safety running coupling we build a number of approximate solutions. A sizable effort is then made to cross-check these

approximations and also to establish some semblance of scheme independence. Finally we calculate tree-level and one-loop amplitudes in our formalism. The phenomenological implications are given in chapter 5. We demonstrate that asymptotic safety can lead to observable and experimentally interesting results. Finally, in chapter 6 we conclude this work and offer some possible future directions.

As of now, there is no definitive evidence for beyond the Standard Model physics at the LHC, yet there is still reason to believe that the next revolution in physics is approaching. Regardless of the outcome, stringent bounds will be placed on many popular models of beyond the Standard Model physics. Whether or not TeV scale extra dimensions exist in nature is a question the LHC can answer, and as this thesis shows may also deepen our understanding of quantum gravity.

Chapter 2

Field Theory Methods in Gravity

2.1 Introduction

In this section, starting from minimal requirements for gravity we build a consistent action. Our approach is meant to evoke the thought process which might be followed by a particle physicist inspired by the successful quantization of Non-Abelian gauge theories like QCD. Basic arguments in dimensional analysis will help us determine the fate of such actions under quantization. We will see explicitly how and where a straight-forward quantization of gravity fails.

The motivation for this extended foray into perturbative gravity is two-fold. First, it allows a pedagogical introduction into the technical aspects of gravity, which will prove useful in Chapter 4 when we discuss higher dimensional realizations. Many aspects of 4-dimensional gravity carry-over and assist our understanding here. The second and more immediate motivation is that by understanding the downfall of a perturbative description of gravity, we obtain a better position for achieving a non-perturbative quantization scheme. An comprehensive and pedagogical reference is Ref. [25].

2.1.1 Einstein-Hilbert Action

In order to build a field theory for gravity we first enumerate the field-content. The dynamical field is the metric $g_{\mu\nu}(x)$, which initially is nothing more than a necessary tool for defining invariant scalar products. The commutativity of the scalar product requires $g_{\mu\nu} = g_{\nu\mu}$. In addition, invariance under similarity

transformations demands $g \equiv \det g_{\mu\nu} = \pm 1$ where in order to describe Minkowski space $g = -1$. Finally, $g_{\mu\nu}$ must be dimensionless.

We can conveniently deduce the transformation laws of the metric by noting that the basis vectors defining two sets of coordinates x and y are related by a Jacobian

$$dx^\mu = \frac{dx^\mu}{dy^\nu} dy^\nu. \tag{2.1}$$

The transformation of the tensor $x^\alpha x^\beta$ and the invariance of the scalar product under basis changes requires that the metric between the two systems transform as

$$g^{\mu\nu} = \frac{\partial y_\alpha}{\partial x_\mu} \frac{\partial y_\beta}{\partial x_\nu} g^{\alpha\beta}. \tag{2.2}$$

According to Einstein's equivalence principles, a freely falling observer in a gravitational field cannot locally be distinguished from free space. Mathematically this is reflected in that the gravitational action is invariant under arbitrary local coordinate transformations. This symmetry corresponds to a variation in the space-time coordinate

$$x_\mu \to x_\mu + \delta x_\mu = x_\mu + \xi_\mu(x), \tag{2.3}$$

where $\xi(x)$ is a function of the original coordinates. For the metric tensor in the coordinate system defined by ξ_μ this leads to the variation

$$\delta g_{\mu\nu}(x) = \xi^\rho \partial_\rho g_{\mu\nu} + \partial_\mu \xi^\rho g_{\rho\nu} + \partial_\nu \xi^\rho g_{\mu\rho}. \tag{2.4}$$

In contrast to Yang-Mills theory, enforcing general covariance on an action requires several steps.

- Replace normal space-time derivatives with covariant derivatives, acting on a general rank-2 tensor as,

  $$\nabla_\mu T^\rho{}_\nu = \partial_\mu T^\rho{}_\nu + \Gamma^\rho{}_{\tau\mu} T^\tau{}_\nu - \Gamma^\tau{}_{\nu\mu} T^\rho{}_\tau. \tag{2.5}$$

  The connection $\Gamma^\mu_{\nu\rho} \equiv \frac{1}{2} g^{\mu\tau}(\partial_\rho g_{\nu\tau} + \partial_\nu g_{\rho\tau} - \partial_\tau g_{\rho\nu})$ does not itself transform as a tensor.

- The flat metric $\eta_{\mu\nu}$ must everywhere be replaced with a general metric $g_{\mu\nu}$.

- Under (2.3) the measure transforms as

$$d^4x' \to \frac{\partial x'}{\partial x} d^4x'. \tag{2.6}$$

  This can be made invariant with the replacement $d^4x \to \sqrt{-g}\, d^4x$ as g transforms identical to $g_{\mu\nu}$.

These previous conditions are necessary for general covariance in a pre-existing action, whereas we would also like to construct a kinetic term for the gravitational field. The relevant question is to identify the gravitational equivalent to the field strength tensor $F_{\mu\nu}$. The more complicated transformation law (2.4) as well as the index structure of $g_{\mu\nu}$ allow for a tensor with more symmetry. The Riemann tensor

$$\mathcal{R}^{\mu}{}_{\nu\rho\sigma} = \partial_\sigma \Gamma^{\mu}{}_{\nu\rho} - \partial_\rho \Gamma^{\mu}{}_{\nu\sigma} + \Gamma^{\alpha}{}_{\nu\sigma}\Gamma^{\mu}{}_{\alpha\rho} + \Gamma^{\alpha}{}_{\nu\rho}\Gamma^{\mu}{}_{\alpha\sigma} \tag{2.7}$$

is the analogous field tensor in gravity[1]. However, the Ricci Scalar, obtained from the Riemann tensor as $\mathcal{R} \equiv g^{\nu\rho}\mathcal{R}^{\mu}{}_{\nu\rho\mu}$, is the invariant object featured in the correct (low energy) Lagrangian

$$\mathcal{L} = \sqrt{-g}\frac{1}{16\pi G_N}\mathcal{R}, \tag{2.8}$$

where we have defined the experimentally measured Newton's constant $G_N \equiv 1/M_{\rm Pl}^2$ in natural units. At first glance this action looks strange in dimensional analysis as $[G_N^{-1}] = 2$, and we may conclude this term is super-renormalizable. However, the equations of motion for the gravitational field generate a dynamical coupling to matter. From the definition of the symmetric energy-momentum tensor

$$T_{\mu\nu} = \frac{2}{\sqrt{-g}}\frac{\delta S}{\delta g^{\mu\nu}}, \tag{2.9}$$

taking the variation of (2.8) coupled to matter yields Einstein's Equations

$$\left(\mathcal{R}_{\mu\nu} - \frac{1}{2}g_{\mu\nu}\mathcal{R}\right) = 8\pi G_N\, T_{\mu\nu}, \tag{2.10}$$

[1] A perfectly valid generally covariant Lagrangian at this point would be $\mathcal{L} = \sqrt{-g}R^{\mu}{}_{\nu\rho\sigma}R_{\mu}{}^{\nu\rho\sigma}$, analogous to the YM kinetic term $\sim F^2$. If this were the action chosen by nature, then gravity in pertubation theory would be similar to YM theories by naive power-counting.

where $\mathcal{R}_{\mu\nu} = R^{\alpha}{}_{\mu\alpha\nu}$. The constant G_N^{-1} is the pre-factor in (2.8) precisely because G_N acts as the coupling constant of the gravitational field to the energy momentum tensor on the RHS of Einstein's Equations.

2.1.2 Quantization

In order to quantize gravity we first perform the flat space expansion of the metric

$$g^{\mu\nu} = \eta^{\mu\nu} + \sqrt{8\pi G_N} h^{\mu\nu}. \tag{2.11}$$

The field $h_{\mu\nu}$ is the propagating spin-2 graviton which is now canonically normalized. The lowest order equations of motion obtained from (2.10) and (2.11) for the graviton field are

$$\begin{aligned} &\Box h_{\mu\nu} - \partial_\mu \partial^\alpha h_{\alpha\nu} - \partial_\nu \partial^\alpha h_{\alpha\mu} + \partial_\mu \partial_\nu h^\alpha_\alpha \\ &\qquad - \eta_{\mu\nu} \Box h^\alpha_\alpha + \eta_{\mu\nu} \partial^\alpha \partial^\beta h_{\alpha\beta} = \sqrt{8\pi G_N} T_{\mu\nu} \ . \end{aligned} \tag{2.12}$$

We deduce the action leading to (2.12) as

$$\mathcal{L} = -\frac{1}{2} h^{\mu\nu} \Box h_{\mu\nu} + \frac{1}{2} h \Box h - h^{\mu\nu} \partial_\mu \partial_\nu h + h^{\mu\nu} \partial_\mu \partial^\alpha h^\nu_\alpha - \sqrt{8\pi G_N} h^{\mu\nu} T_{\mu\nu}. \tag{2.13}$$

The slightly circumvent logic (Einstein–Hilbert action→ Einstein's equation → linearized Einstein's equation → linearized Einstein–Hilbert action) leading us to (2.13) is necessary because the energy momentum tensor is generated through (2.9) when computing the equations of motion. Had we inserted the graviton decomposition into the Einstein–Hilbert action directly, the resulting linearized Einstein equations would describe a freely propagating field. Thus, in the linearized action, the coupling to matter at the level of the action is inserted by hand. Reproducing Einstein's Equations at the linearized level forces us to introduce a non-renormalizable interaction[2], the last term in (2.13).

The action (2.13) carries a linearized version of the gauge symmetry

$$\delta h_{\mu\nu} = -\partial_\mu \xi_\nu - \partial_\nu \xi_\mu, \tag{2.14}$$

[2]Graviton self-interactions are also generically non-renormalizable as the three-graviton vertex contains two derivatives and hence has dimension 5.

we obtain by inserting (2.11) in (2.4). In order to extract the propagator we fix the gauge. For pure gravity this gauge fixing is simple, and completely analogous to Yang-Mills theories. A convenient choice which generalizes nicely to higher dimensional gravity is the unitary gauge where

$$\partial_\mu h^\mu_\nu = \frac{1}{2}\partial_\nu h^\mu_\mu. \tag{2.15}$$

Two notable points are as follows. First, this choice eliminates the last two kinetic terms in (2.13), and the remaining tensor is easily inverted. Second, a symmetric tensor contains 10 components, while (2.15) eliminates 4. An additional 4 degrees of freedom are dropped by noting that (2.15) under a linearized gauge transformation produces the condition $\Box\xi_\nu = 0$. Thus, there are only 2 remaining propagating degrees of freedom as we expect for a massless boson in 4-dimensions.

We use a second gauge choice for loop calculations in the D dimensional theory, the DeDonder gauge, where we include a generic ghost contribution $\mathcal{L}_{gh}$, and defining

$$C_\mu \equiv \frac{1}{\sqrt{2}}(\partial_\alpha h^\alpha_\mu - \frac{1}{2}\partial_\mu h) \tag{2.16}$$

add to the action a term $\mathcal{L}_{gh} = -C_\mu C^\mu$. We will see how the KK reduction of the D dimensional action in these respective gauges leads to differently suited sets of Feynman rules.

2.1.3 Divergences

A simple way to compute loops in gauge theories is the background field method [26]. This proves effective in gravity as well due to the diffeomorphism invariance realized at the linear level (2.14). Suppose we start with an action containing operators $\mathcal{O}_i$. Once we compute loops in the background field method, divergences are proportional to some set of gauge invariant operators $\bar{\mathcal{O}}_i$. If all $\bar{\mathcal{O}}_i$ are contained in the original Lagrangian $\mathcal{O}_i$, then the action is termed perturbatively renormalizable as all divergences can be soaked up with redefined couplings. If the $\bar{\mathcal{O}}_i$ generate new operators on the other hand, then in order to eliminate the divergence we must introduce additional terms. Now the quantum theory containing only $\mathcal{O}_i$ is inconsistent.

Using these methods and considering the one-loop graviton self-energy for the

Einstein-Hilbert action it was shown in Ref. [27] that a divergence

$$\delta\mathcal{L} = \frac{1}{8\pi^2}\frac{1}{D-4}\sqrt{-g}\left[\frac{1}{120}\mathcal{R}^2 + \frac{7}{20}\mathcal{R}_{\mu\nu}\mathcal{R}^{\mu\nu}\right] \tag{2.17}$$

is produced which cannot be reabsorbed into the definition of (2.8). However, there is a solution, $\delta\mathcal{L}$ in this case vanishes on shell as a solution to the classical field equations. This means that if we redefine our field $g_{\mu\nu} \to g_{\mu\nu} + \delta g_{\mu\nu}$ where,

$$\delta g_{\mu\nu} = \frac{1}{D-4}\frac{1}{20}\left(-7\mathcal{R}_{\mu\nu} + \frac{11}{3}\mathcal{R}g_{\mu\nu}\right) \tag{2.18}$$

then the vacuum equations of motion for $g_{\mu\nu}$ in (2.10) are preserved and the one-loop divergence is eliminated. However, in the presence of matter where $T_{\mu\nu} \neq 0$, the counter-term does not vanish on-shell, and the necessary field redefinition is not possible. At the two loop level in pure gravity, it was shown in Ref. [28] that the counter-term

$$\delta\mathcal{L} = \sqrt{(-g)}\frac{1}{d-4}\frac{1}{(16\pi^2)^2}\frac{209}{2880}\mathcal{R}_{\mu\nu}{}^{\sigma\rho}\mathcal{R}_{\sigma\rho}{}^{\kappa\tau}\mathcal{R}_{\kappa\tau}{}^{\mu\nu}, \tag{2.19}$$

is generated, and crucially this does not vanish for solutions to the vacuum field equations. Not surprisingly, loop correction in gravity produce fatal divergences.

One possible way out is to include higher derivative terms in the original action, and hope that there exists some special set which is closed under perturbative quantization. In fact, it was proposed and later shown that there is a set of higher derivative invariants, which along with (2.8) generate a closed set of counter-terms to all loop orders. This Lagrangian found in Ref. [29] is

$$\mathcal{L} = \sqrt{(-g)}\left[\frac{1}{16\pi G_N}\mathcal{R} - a\mathcal{R}^2 - b\mathcal{R}_{\mu\nu}\mathcal{R}^{\mu\nu}\right], \tag{2.20}$$

where a and b are dimensionless couplings. This is not heralded as a successful theory of quantum gravity for an important reason. The scalar part of the graviton propagator from (2.20) is

$$\Delta(p) = \frac{1}{p^2 - \alpha G_N p^4}, \tag{2.21}$$

where α is an $\mathcal{O}(1)$ coefficient depending on a and b. For large energies

where $p^2 G_N \sim 1$ we see that the propagator changes sign so that the high-energy spectrum of this theory contains a ghost obeying the wrong relation between spin and statistics. However, it was later found in Ref. [30] with modern BRST techniques that an action containing all diffeomorphism invariant terms is perturbatively renormalizable and contains ghost free propagators. Renormalizablility in this case is not surprising as all divergences must be proportional to an invariant and we may redefine our infinite number of couplings to cancel these. What is non-trivial is that unitarity is preserved in the propagator only for the inclusion of an infinite number of terms. An obvious downside is that an infinite number of experiments are needed to fully specify the theory. A theory with well behaved UV behavior despite a complete lack of predictive power is generally referred to as *weakly* perturbatively renormalizable.

Despite the breakdown of perturbative gravity in the UV, there remains some hope for a theory of quantum gravity that is both ghost-free and weakly coupled in the UV (for a recent example see Ref. [31]). However, even if gravity as a field theory has no sensible UV behavior, it is still possible to discuss quantum gravity as an effective field theory.

2.1.4 Gravity as an Effective Theory

The Standard Model is likely to be a low-energy effective theory. This picture neatly explains the perturbative renormalizablity of all measured operators in terms of the Wilsonian renormalization group, and succinctly determines the plethora of observed global symmetries. Furthermore, the first instance of definitive beyond the standard model physics, neutrino oscillations and their implied masses, follow directly from the least suppressed higher dimensional operator. Constraining (or better yet determining) the EFT scale of these operators is a crucial phenonological pursuit.

For some presumably large physical cut-off scale Λ, contributions to observables from higher dimensional operators at the characteristic energy scale E are suppressed by powers of E/Λ. While renormalizibility is a virtue when computing loops, it does not assist the determination of the scale when such a description breaks down[3]. Conversely, the merit of non-renormalizable interactions is that

[3]Although the SM is certainly expected to break-down above the Planck scale, the only intrinsic limit on the validity of the perturbative description of the SM is the Landau pole in

they transparently predict their own demise, when $E/\Lambda \sim 1$. This defines an upper-bound on the scale of new physics. For this specific purpose, gravity is more helpful than the SM. Perturbation theory ceases to be a good description when the dimensionless expansion parameter $E^2 G_N \sim 1$. Consequently, for experiments at energies far below this scale the effective operator expansion of gravity is well defined [32][33].

In order to proceed, all operators consistent with general covariance should be included in the a generalized gravitational Lagrangian

$$\mathcal{L} = \sqrt{-g}\left[\frac{1}{16\pi G_N}\mathcal{R} + c_1\mathcal{R}^2 + c_2\mathcal{R}_{\mu\nu}R^{\mu\nu} + c_3\nabla^2\mathcal{R} + \cdots\right]. \tag{2.22}$$

The Riemann tensor squared term is not included as the linear combination of the Ricci tensor, Ricci Scalar and Riemann tensor is equal to a topological (Gauss-Bonet) invariant. There are very weak constraints on the size of the dimensionless coefficients $c_1, c_2 < 10^{74}$ from cosmology [32]. We calculate the first order quantum effects by considering one-loop diagrams, analogous to QED, which modify the graviton propagator and vertex with matter. The modification to the Newtonian potential is obtained by considering the exchange of a graviton between two massive bodies, where an effective vertex is inserted twice and the one loop propagator is used for the virtual graviton. This calculation is done in Ref. [32] at leading order in G_N for the Newtonian potential,

$$V(r) = \frac{G m_1 m_2}{r}\left[1 - \frac{G(m_1+m_2)}{c^2 r} - \frac{167}{30\pi}\frac{G\hbar}{c^3 r^2} + \cdots\right] \tag{2.23}$$

where we have temporarily moved away from Planck units. The second term in brackets corresponds to a relativistic correction which is found in classical General Relativity. However, the third term is due to genuine quantum effects in gravity.

The important point is that the potential decreases as r gets small. We may absorb the quantum effects in G_N and define an effective coupling $G_N(r)$ valid up to energy scales $E \sim r^{-1}$

$$G(r) = G\left(1 - \frac{167}{30\pi}\frac{G_N\hbar}{r^2}\right). \tag{2.24}$$

the electro-weak gauge couplings.

This is in opposition to the effects of QED vacuum polarization, which give a one loop effective coupling to the fine structure constant $\alpha \sim e^2$,

$$e^2(\mu) = e^2(\mu_0)\frac{1}{1 - \frac{e^2(\mu_0)}{6\pi^2}\log\left(\frac{\mu}{\mu_0}\right)} \tag{2.25}$$

which increases for large energies μ. The effect of electron-positron pair creation is a screening of the electric charge. The coupling increases as we move closer to the bare charge. In contrast, gravitational effects appear as anti-screening, analogous to QCD. In the one loop approximation the gravitational coupling gets arbitrarily weak for energies

$$\frac{1}{r} \sim \sqrt{\frac{30\pi}{167 G_N \hbar}}. \tag{2.26}$$

At such high energies, we of course over-extend the expected region of validity for our one loop calculation. Instead we compute the contribution by inserting our effective coupling into the one loop propagator recursively,

$$\begin{aligned} G(r) &= G\left(1 - k\frac{G_N\hbar}{r^2}\right) + G\left(1 - k\frac{G_N\hbar}{r^2}G\left(1 - k\frac{G_N\hbar}{r^2}\right)\right) + \cdots \\ &= \frac{G}{1 + \frac{167}{30\pi}\frac{G_N\hbar}{r^2}} \end{aligned} \tag{2.27}$$

where we have defined $k \equiv 167/(30\pi)$ and resummed the geometric series. Now we can take the $r \to 0$ limit. Apparently, the resummed coupling still shows strong anti-screening behavior for large energies.

To conclude, an effective theory approach towards gravity allows us to unambiguously compute the leading order quantum corrections to the gravitational potential between two sources. Moreover, the fact that the effective force due to quantum corrections between particles decreases at shorter distances suggests the possibility of soft scattering amplitudes in the UV. We cannot naively extend this to energies greater than the denominator of the higher order effective interactions. At these energies our ordering principle is rendered meaningless and in general, all effective operators consistent with the symmetries must be included in a calculation.

In this thesis we summarize current evidence that applying non-perturbative methods to gravity, the hints of improved UV behavior provided by effective field theoy in (2.27) can be solidified into a coherent framework of UV finiteness under the rubric of asymptotic safety. We will argue consequently that gravitational field theory can be thought of as more than an effective theory in the special case where the renormalization group trajectory ends on a UV fixed point[4]. In the next section we present the ground work which allows us to investigate the non-perturbative nature of gravity.

2.2 Asymptotic Safety

One of the great lessons of quantum field theory is that observable quantities depend on the scale at which they are viewed. In other words, when claiming the numerical value of a dimensionless parameter it is necessary to specify the energy scale of the measurment. Physically, quantum mechanics demands that an interacting bare particle be thought of as a cloud of virtual particles. These virtual effects determine the physically measured mass and couplings in non-trivial ways. Quantitatively the dynamics of the measured parameters in the Lagrangian are determined by the renormalization group (RG) flow. In other words, the RG flow describes the entire structure of the virtual cloud surrounding our bare fields.

We frequently employ the prototypical example of the RG with QCD as a toy model. The Yang-Mills coupling is classically scale invariant. However, once we include quantum effects, the coupling decreases with energy and vanishes exactly in the limit of arbitrarily small distances. The fact that as the energy increases, the coupling approaches the origin indicates that QCD contains a free-field UV fixed point. Synonymous to this is that QCD is an asymptotically free theory.

Asymptotic freedom is only one of many possible fates for a generic coupling in the UV. In general, a coupling may also increase without bound, settle on some periodic behavior or lead to a non-zero UV fixed point. The last choice is an example of asymptotic safety, a generalization of asymptotic freedom to the

[4]There is even a precedent for extending effective theories with non-renormalizable interactions to arbitrarily high energies. The Gross-Neveu model, N interacting Dirac fermions with a $O(2N)$ global symmetry, in $2+1$ dimensions [34] is an example where a straight-forward perturbative quantization fails as expected but the non-perturbative handle provided by the $1/N$ expansion allows a simple proof of renormalizability to all orders [35].

case where the UV fixed point remains interacting. In the next section we will describe the general features of an interacting fixed point in gravity.

2.2.1 Fixed point for Newtons Constant

In $4+n$-dimensional gravity the coupling constant G_D carries mass dimension $-2-n$. Since the renormalization group flow deals exclusively with phyisical, dimensionless parameters, we define a dimensionless coupling using an at this stage arbitrary scale μ.

$$g \equiv \mu^{n+2} G_D \tag{2.28}$$

In perturbative gravity we expand in g so that some energy scale when $\mu^{-2-n} \sim G_D$, our calculation is bound to fail. However, we anticipate that Newtons constant G_N is in fact a function of μ, and in order to make connection with RG based literature [36] we define the wave-function renormalization $Z^{-1}(\mu)$.

$$G(\mu) = G_N \, Z^{-1}(\mu) \tag{2.29}$$

We supply a suitable renormalization condition fixing $Z^{-1}(\mu_0) = 1$ at the energy scale μ_0. This condition allows us to define the low energy Newtons constant in 4-dimensions as the experimentally measured $6.67 \times 10^{-11} \mathrm{m}^3/\mathrm{kg\ s}^2$. In practice we will always take $\mu_0 \sim 0$ and define the IR regime of gravity as the energy range where $Z^{-1}(\mu) \approx 1$. At the level of the Lagrangian, $Z^{-1}(\mu)$ appears in the kinetic operator for the graviton and therefore renormalizes the graviton two-point function. The scale dependence of $Z^{-1}(\mu)$ determines the rescaling of the fields once quantum effects are included in the path integral. For sufficiently small rescaling perturbation theory remains applicable. More precisely we define the anomalous dimension

$$\eta \equiv -\frac{d \log Z}{d \log \mu} \, . \tag{2.30}$$

which is so named as it measures the rate of deviation from canonical dimension for the fields. We are generally interested in the fixed-point situation where the dimensionless renormalized coupling goes to a finite value. For gravity this implies that the dimensional renormalized Newton's constant approaches 0 in the UV at a rate determined by η. This value constitutes the first genuine observable we discuss in the context of asymptotic safety.

To gain more traction with this idea, we consider the generic scale derivative of g, the beta function of the corresponding coupling in quantum field theory

$$\beta_g \equiv \mu \frac{dg(\mu)}{d\mu} = (n + 2 + \eta)\, g(\mu). \tag{2.31}$$

In deriving (2.31) we use the definitions given by (2.28), (2.29) and (2.30). There are two possible fixed points associated with (2.31). Most simply if $g \to 0$ we encounter the Gaussian (non-interacting) fixed point where $\mu \to 0$. Identifying $\mu = E$ with the center-of-mass energy of the process at hand, we see from our effective field theory logic delineated in (2.22) that this constitutes the regime where a perturbative expansion is applicable and corresponds to the region of classical general relativity.

A more interesting possibility presents itself by observing that (2.31) has a second fixed point when the anomalous dimension is negative and given by the value $\eta = -2 - n$. This implies that the dimensional Newtons constant scales in the UV exactly to cancel the canonical scaling factor, or in other words $G_N Z^{-1}(\mu) \sim \mu^{-2-n}$. We see the essence of the fixed point by considering the real space 2-point scalar correlation function for a theory with $\eta = -2 - n$. The effective propagator once we identify the graviton momentum p^2 with the RG scale μ^2 becomes p^{-4-n}. The Fourier transform defining the real space correlator is

$$\Delta(x) \sim \int \frac{d^{4+n}p}{p^{4+n}} e^{i\mathbf{p}\cdot\mathbf{x}} \sim \log(\Lambda\, x)\,, \tag{2.32}$$

where Λ is some at this stage arbitrary scale. In (2.32), the residual interaction of the theory become effectively 2-dimensional. Interestingly, this feature is confirmed by Lattice studies of gravity deemed Causal Dynamical Triangulations (CDT) [37].

In order to fully classify fixed points, we need, in addition to the fixed point coupling and anomalous dimension, the value of the *critical exponent* defined by

$$\theta = -\frac{\partial \beta}{\partial g}\bigg|_{\mu_\star}\,. \tag{2.33}$$

The critical exponent for the UV fixed point in gravity is computed by setting g equal to its fixed point value $g_\star$ in (2.33). For real critical exponents, the magnitude determines the rate of approach to fixed point scaling and more

importantly the sign indicates whether the trajectories ending on the fixed point are stable under small perturbations.

Before we outline the conditions for asymptotic safety, we briefly generalize the above discussion to the case where there are an arbitrary number of couplings in the theory, each providing their own dynamics.

2.2.2 Fixed point for general action

In an EFT approach to gravity one generally orders operators as in (2.22) in terms of their canonical dimension. At high energies this ordering principle is insufficient and all operators allowed by symmetries should be included. The coefficient of each operator then obeys its own RG equation

$$\beta_i = \frac{dg_i}{d\log\mu}\{g_0, g_1 \cdots\} \tag{2.34}$$

which in the general case depends on every other coupling in the theory. For a given truncation of operators, the space of all couplings constitutes *theory space*. An interacting (or Non-Gaussian) fixed point occurs at any point where all the β_i vanish and at least one g_i is non-zero. We will denote this point $\bar{g}_\star$. At $\bar{g}_\star$ we identify as a generalization of (2.33), a so-called *stability matrix*

$$\begin{aligned} M_{ij} &= \left.\frac{\partial\beta_i}{\partial g_j}\right|_{\bar{g}_\star} \\ &= -d'_{(i)}\delta_{ij} + N(g_0, g_1, \cdots)\,. \end{aligned} \tag{2.35}$$

where $d'_{(i)}$ is the canonical dimension of the i-th coupling with no implicit summation. The function N generalizes the anomalous dimension and encapsulates the entire quantum structure of the theory. As an example, in gravity since $[R] = 2$ and $[R^2] = 4$, the canonical dimension for these operators in $4 + n$ dimensions is $2+n$ and n respectively. All higher dimensional operators have negative canonical dimension in 4-dimensions. The eigenvalues of the stability matrix determine the stability of the fixed point, and are the critical exponents θ_i of $\bar{g}_\star$.

There is some set of trajectories through theory space which emanate from $\bar{g}_\star$. As all the β_i are smooth functions in the g_i and μ, these curves form a manifold, dubbed the UV critical surface. The dimensionality of this manifold Δ_{UV} is then given by the number of directions attracted to the fixed point in

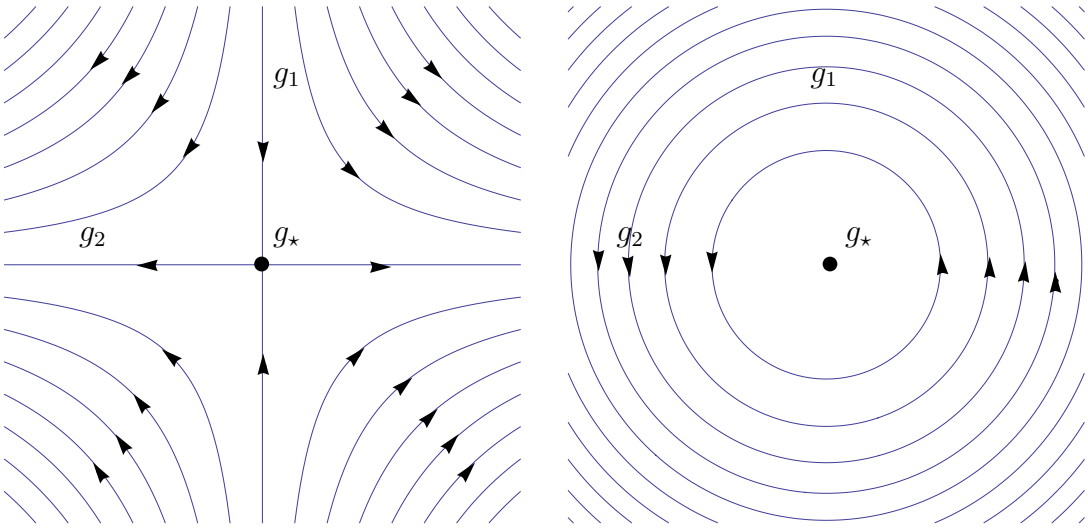

Figure 2.1: Simple illustration of a a) 1-dimensional b) 0-dimensional UV critical surface in a 2-dimensional theory space. A 2-dimensional surface corresponds to all flows ending on the UV fixed point.

its linearized vicinity. If a coupling g_i has $\theta_i < 0$ ($\theta_i > 0$) this coupling is called UV attractive (repulsive). Hence, the dimension of Δ_{UV} is identical to the number of UV attractive critical exponents in the theory *i.e.* the number of eigenvalues of the stability matrix with negative real part. Physically, Δ_{UV} counts the parameters in the theory which are not fixed by the requirement that the RG flow ends on a UV fixed point. These couplings can only be determined through experimental measurement. In the next section we will use these definitions to define an acceptable theory of quantum gravity which is asymptotically safe.

2.2.3 Criteria for the Scenario

We are in a position to state the two criteria for asymptotic safety in quantum gravity first enumerated by Weinberg [24]. In order for gravity to be an acceptable and predictive quantum field theory it must;

1. Contains a UV fixed point in all couplings,

2. Allow a finite dimensional UV critical surface at this fixed point.

The second requirement does not necessarily mean that a finite number of terms are present in the correct UV action, only that in this case the *a priori*

independent couplings must actually be functions of only a finite number [38]. This criteria is the weakest form of in principle predictivity for a continuum quantum field theory.

2.2.4 Evidence for Asymptotic Safety

As we noted in Sec. 2.1.3, in order to investigate the high energy behavior of gravity we need to either compute the gravitational path integral directly or find a useful non-perturbative expansion. The former is the inspiration for numerical lattice based investigations in gravity called causal dynamical triangulations (CDT) [37]. We will only mention in passing that there seems to be some evidence for asymptotic safety in CDT as the spectral dimension of space-time was found in agreement with (2.32) in Ref. [37]. In order to gain a handle on gravity without resorting to lattice simulations we need clever techniques.

There are several examples of gravity related field theories which are finite in the UV by virtue of a non-trivial fixed point. The first example is Einstein Hilbert gravity in $D = 2 + \epsilon$ dimensions. It is well known that gravity in $D = 2$ is a topological invariant, but the same cannot be said for gravity for $D = 2 + \epsilon$. Furthermore, perturbation theory is valid in $D = 2$ since G_N is dimensionless. The gravitational β-function was calculated at 1-loop [39] and later at 2-loops [40] as

$$\beta_g = \epsilon g - bg^2 + \mathcal{O}(g^3). \tag{2.36}$$

For $\epsilon = 0$, the β-function is a downward facing parabola, exactly like QCD. Thus the theory in $D = 2$ dimensions is asymptotically free. However, as soon as the theory moves a small distance away from $D = 2$, an interacting fixed point occurs at $g_\star = \epsilon/b$ in the one loop approximation. In this sense, the lack of perturbative renormalizability for $D > 2$ gravity is seen as a result of the $D = 2$ Gaussian fixed point being continuously shifted off the origin as ϵ grows. As we will see this is in agreement with results from renormalization group studies for gravity in $D = 4$. Another expansion finding a fixed point is found by minimally coupling N scalar fields to the metric, and performing a $1/N$ expansion [41][42].

It was only with the addition of exact renormalization group techniques from Ref. [43] and Ref. [44] that a rigorous computation of the non-perturbative β-function became possible [45][46][47]. Details on these techniques are given in

the appendix. More modern computations now include higher order invariants up to R^8 terms [48], also including couplings to matter [49], and truncations proportional to invariants which do not vanish in perturbation theory [50]. Also, the fixed point structure in 4-dimensions persists in higher dimensional gravity theories [51]. In all cases so far, a fixed point with the requisite properties for asymptotic safety was found. More importantly, the critical exponents indicate that for R^N operators with $N > 2$, the critical exponents are UV repulsive and the magnitude of the exponents θ_i grow as a positive power of N [48]. This is strong mathematical evidence that the UV critical surface is finite dimensional. While no rigorous proof demonstrates that the fixed point is truly robust against even higher invariants, there is are still many promising paths for improving the study of asymptotic safety.

2.3 Conclusions

Starting from field theory we examined how gravity, defined as the Einstein-Hilbert action, fails in perturbation theory. This does not mean that gravity does not make sense as a quantum field theory, only that it cannot be applied at arbitrarily high energies. Attempts to cure the poor UV behavior of gravity in perturbation theory have been plagued by among other field theory nightmares, unphysical ghosts. It is safe to say that so far no consistent perturbative quantization of gravity has been found without appealing to non-field theory based objects (*i.e.* string theory).

Moving beyond perturbation theory there is hope that gravity may be an acceptable and predictive theory within the asymptotic safety scenario. There is growing evidence that these criteria are realized in many approximations and as of this writing no solid counter-example to the conjecture is known. However, in order to establish the asymptotic safety scenario at a level more than mathematical existence, we require some form of experimental input. For this purpose, recent developments on low scale gravity models in extra dimensions prove useful.

In low scale gravity models, the topic of the next chapter in this thesis, the energy where fixed point scaling is realized may be as low as a TeV. With these fortuitous circumstances, effects from the large anomalous dimension may be

observable at the LHC. This idea was first pointed out in Ref. [52] and Ref. [53]. Further non-collider based applications of asymptotic safety include cosmology [54][55], black holes [56][57][58] and dark energy [59].

Chapter 3

Extra Dimensions and KK states

Not into space. Into the space between spaces.

-Prof. Oxley in "Indiana Jones and the Kingdom of the Crystal Skull"

3.1 Introduction

The tantalizing possibility of extra spacial dimensions has trickled through the thoughts of theoretical physicists beginning with their original proposal by Kaluza [60]. It was hoped that seemingly different 4-dimensional forces such as electromagnetism and gravity could be neatly unified in a 5-dimension pure gravitational multiplet. The 5 degrees of freedom associated with a massless graviton in 5-dimensions decomposes to 4-dimensions as a scalar ϕ, vector A_ν and tensor $h_{\mu\nu}$. The tensor is the massless graviton and the vector may be identified as the photon.

In order to explain the non-observation of these additional dimensions, the idea of compact extra dimensions proved useful [61]. As opposed to observed spacial dimensions which possess no boundary, these extra dimensions might contain an intrinsic size along with boundary conditions specifying their topology. At length scales large compared with the size of the extra dimensions, all effects of the higher dimensional theory are visible through effective contact interactions. The only macroscopic force law in this case is the normal Newtonian potential

$$F(r) \sim \frac{m_1 m_2}{r^2}. \tag{3.1}$$

As the Compton wavelength of a probing particle reaches this size, the higher dimensional force law

$$F(r) \sim \frac{m_1 m_2}{r^{2+n}}, \tag{3.2}$$

takes effect. In the far UV the imbedding of the extra dimension is irrelevant and all spacial dimensions are treated on equal footing.

In order do enforce dimensional consistency in (3.2), we see from (3.1) that the numerator must soak up a dimensional quantity. The only two scales in this set-up are the fundamental scale of gravity M_* and the radii R of the additional dimensions. The interplay between these two scales leads us to the next section on Large Extra Dimensions and in particular the idea of extra dimensions as a solution to the hierarchy problem.

3.2 Large Extra Dimensions

The theoretical progeny from the original ideas of extra dimensions have inspired many beyond the SM scenarios in recent years. In [62] the idea of TeV scale extra dimensions was first introduced in the context of Supersymmetry breaking. Later, the inspiration provided by string theory [63] and in particular the invention of D-branes [64] provided a consistent framework for SM imbeddings. In this thesis we explore one of the simplest modern realizations, the so-called AADD model [14][15]. For completeness we note that in addition to the AADD model, extra dimensions proved remarkably useful in other aspects of model building with warped [16][17] and Universal Extra Dimension [18]. The later two ideas are mentioned only fleetingly in the remainder of this work.

Before defining the large extra dimensional paradigm in detail, we discuss the original motivation for these models. Quite subjectively, the vast disparity between the electroweak scale around 100 GeV and the measured Planck scale at 10^{19} GeV is aesthetically unappealing. While not a fundamental problem itself, when taken together with a light SM Higgs scalar, this discrepancy becomes harrowing to any theorist. Large extra dimensions solve this issue simply by asserting that the observed vast difference between these scales is an artifact of low energy observers.

3.2.1 The Hierarchy Problem

The only particle not yet observed in the Standard Model is the Higgs boson. In addition to illuminating the mechanism for electro-weak symmetry breaking, observation of the Higgs may provide the first evidence for the existence of a fundamental scalar field. As it turns out, the spin of a fundamental field crucially determines the effect of loop corrections on the measured or renormalized mass in the theory.

One-loop self-energies for spin-$\frac{1}{2}$ and spin-1 particles depend logarithmically on the scale of new physics. To see that this can be at most logarithmic, consider the massless case where the fields enjoy chiral symmetry and gauge invariance respectively. In this limit, the mass renormalization vanishes to all orders in perturbation theory in order to preserve these symmetries. This implies that any mass renormalization be proportional to the original particle mass, and thus by power counting can be at most logarithmically divergent. In the language of 't Hooft, these fields are deemed *technically natural*. Colloquially, we refer to mass terms for these fields as being *protected* from large radiative corrections.

Scalar fields on the other hand do not enjoy any additional symmetry in the massless limit. For the standard model Higgs, Pauli-Villars regulated self energy corrections from additional loops produces the following mass renormalization

$$\begin{aligned} m_H^2 &= m_{H,0}^2 + \delta m_H \\ &= m_{H,0}^2 + m_{H,0}^2 \frac{3g^2}{32\pi^2} \frac{\Lambda^2}{m_W^2}, \end{aligned} \tag{3.3}$$

where Λ is the scale of new physics and only the contribution from W loops is included. If this scale is the EFT cut-off at the GUT or Planck scale, then the measured Higgs mass m_H must be a careful cancellation between $m_{H,0}$ and δm_H of the order 10^{-30}. Furthermore, in reality (3.3) receives contributions from all massive particles in the SM (and beyond), so this cancellation is even more suspect. Often, such an unnatural cancellation between the bare Higgs mass and the self energy correction is called excessive *fine tuning*.

Now, a caveat is that if we use dimensional regularization instead of Pauli-Villars, all quadratically divergent self energy integrals vanish. However, supposing that the cut-off scale Λ represents the scale where new particles appear, then the self energies due to these new particles naively acts as a quadratically

divergent loop contribution even within dimensional regularization. In either case, the question of why the Higgs mass is so light is not answered within the Standard Model without appealing to the fine-tuning argument mentioned above. This constitutes the hierarchy problem.

Two major paradigms conceived as solutions to the hierarchy problem are Technicolor and Supersymmetry. Both models enforce the stability of the Higgs mass, through an order TeV compositeness scale or a new symmetry which protects the scalar mass respectively. As we will see in the next section, extra dimensions also provide a solution to the Hierarchy problem, and more importantly motivate the search for quantum gravitational physics far below the naive Planck scale.

3.2.2 Model details

The ADD model in its simplest manifestation consists of an arbitrary number of toriodially compactified extra dimensions. First we outline some notation. We write the 4-dimensional coordinates as x_μ, while the $(4+n)$-dimensional coordinates are y_a, such that $z_M = x_\mu + y_a$. For indices we use Greek indices for 4-dimensions $\mu, \nu, \alpha = 0, 1, 2, 3$ and denote extra dimensional coordinates with lower case Roman letters $a, b, c = 5, 6, 7, \cdots n$. These are unified to capital Roman letters $A, B = 0, 1, 2, 3, 5, \cdots n$.

Coordinate transformations no longer mix all spacial components. The following are requirements on the extra-dimensional space described by metric g_{ij}.

- *spatial*: the signature for the n extra dimensions is $(-1, -1, \cdots)$.
- *separable*: the extra dimensions must be orthogonal to the brane so that the measure $d^{4+n}z$ is well defined. In other words, the metric decomposes as a product space $g^{(4+n)} = g^{(4)} \otimes g^{(n)}$.
- *flat*: the dimensions must be flat so that they can be integrated out explicitly in the action. In standard gravity the same is true unless sources induce $T_{ij} \neq 0$. We therefore restrict matter to the $y_i = 0$ brane:

$$T_{AB}(x; y) = \eta^\mu_A \, \eta^\nu_B \, T_{\mu\nu}(x) \, \delta^{(n)}(y) = \begin{pmatrix} T_{\mu\nu}(x) \, \delta^{(n)}(y) & 0 \\ 0 & 0 \end{pmatrix}. \tag{3.4}$$

The assumption of an infinitely thin brane for our 4-dimensional world might have to be weakened to generate realistic higher-dimensional operators for flavor physics or proton decay [65, 66]. Einstein's equation purely in the extra dimensions

$$\mathcal{R}_{jk} - \frac{1}{n+2} g_{jk} \mathcal{R} = 0, \tag{3.5}$$

contracted with g^{jk} requires $\mathcal{R} = 0$. The full Ricci scalar is then

$$\mathcal{R} = g_{MN}\mathcal{R}^{MN} = g_{\mu\nu}\mathcal{R}^{\mu\nu} + g_{ij}\mathcal{R}^{ij} + g_{i\mu}\mathcal{R}^{i\mu} = g_{\mu\nu}\mathcal{R}^{\mu\nu} = \mathcal{R}^{(4)} \ , \tag{3.6}$$

using $g^{jk}\mathcal{R}_{jk} = 0$ along with the fact that $g_{\mu i}$ no longer transforms under general coordinate transformations.

- *compact/periodic*: the simplest compact space is a torus with periodic boundary conditions and a radius R of the compactified dimension $y_i = y_i + 2\pi R$.

At the classical level, compact extra dimensions lead to the following relationship between the 4-dimensional and D-dimensional gravitational constant. Starting with the action in D-dimensions we have

$$\begin{aligned} S_D &= \frac{1}{M_*^{n+2}} \int d^{4+n}x \sqrt{-g}\mathcal{R} && (3.7) \\ &= \frac{1}{M_*^{n+2}} \int d^n y \, d^4x \sqrt{-g^{(4)}}\mathcal{R}^{(4)} \\ &= \frac{V_n}{M_*^{n+2}} \int d^4x \sqrt{-g^{(4)}}\mathcal{R}^{(4)} && (3.8) \end{aligned}$$

In the the final line of (3.8) we reproduce experimentally measured Einstein gravity provided we identify $M_*^{n+2} = M_{\rm Pl}^2 V_n$. In the case of the simplest toriodal compactification with equal radii R we have

$$V_n = (2\pi R)^n. \tag{3.9}$$

Therefore, if the radius of the extra dimensions is large in Planck units, then the fundamental scale of gravity can be significantly lower than 10^{16} TeV. Now we make connection with the original inspiration for these models, namely that for a fundamental Planck scale of the order of a TeV, the size of the extra dimensions

can be small enough to have avoided detection thus far. In this case the mass renormalization to the scalar higgs mass should be proportional to $M_*^2/(16\pi^2)$ as opposed to $M_{\rm Pl}^2/(16\pi^2)$ and the amount of fine tuning is eliminated or greatly reduced.

This leads us to the basis of extra dimensions as a solution to the hierarchy problem: our 4-dimensional Planck scale $M_{\rm Pl}$ is not the fundamental scale of gravity. It is merely a derived parameter which depends on the fundamental $(4+n)$–dimensional Planck scale and the geometry of the extra dimensions, *e.g.* the compactification radius of the n–dimensional torus. Matching the two theories translates into

$$M_{\rm Pl} = M_* \, (2\pi R M_*)^{n/2}. \tag{3.10}$$

If the proportionality factor $(2\pi R M_*)^{n/2}$ is large we can postulate that the fundamental Planck scale M_* be not much larger than 1 TeV. In that case the UV cutoff of our field theory is of the same order as the Higgs mass and there is no problem with the stability of the two scales.

Assuming $M_* = 1$ TeV we can solve the equation above for the compactification radius R — transferring the hierarchy problem into space-time geometry:

n	R
1	10^{12} m
2	10^{-3} m
3	10^{-8} m
...	...
6	10^{-11} m

At least in the simplest model $n = 1$ is ruled out by classical bounds on gravity. A possible exception is if there is a larger than expected mass-gap between massless and massive excitations [23]. For larger values of n we need to test Newtonian gravity at small distances [67][68][69] and we discuss these constraints in Sec. 3.4. Note that the analysis in this section is purely classical, and it is obvious that its physical degrees of freedom do not survive compactification. For this we resort to the original ideas of Kaluza and Klein and decompose the higher-dimensional gravitational theory as an effective 4-D theory with residual gauge symmetries.

3.3 Kaluza-Klein States

With a clear geometrical picture of large extra dimensions, we now perform a KK reduction and identify the propagating degrees of freedom in the 4-dimensional effective theory. Physically this corresponds to classifying components of the higher dimensional metric as representations under the 4-dimensional Poincaré group. In a fully modern treatment, this procedure was carried out in [19, 20], although we follow closely the approach of Ref. [7].

3.3.1 Spectrum

Just as with the 4-dimensional case, we expand about a flat background η_{MN} and define the D-dimensional graviton field h_{MN} so that $g_{MN} = \eta_{MN} + \kappa_D h_{MN}$. Here we define the D-dimensional coupling constant $\kappa_D = 32\pi/M_*^{n+2}$. The D-dimensional action is

$$S = \int d^4x d^n y \mathcal{L}_D \tag{3.11}$$

with $\mathcal{L}_D$ the D-dimensional generalization of (2.13)

$$\mathcal{L}_D = -\frac{1}{2}h^{AB}\Box h_{AB} + \frac{1}{2}h\Box h - h^{AB}\partial_A\partial_B h + h^{AB}\partial_A\partial_M h^{MB} - \kappa_D h^{AB}T_{AB}. \tag{3.12}$$

Periodic boundary conditions allow us to Fourier decompose the y component of the graviton field

$$\begin{aligned} h_{AB}(z) &= \sum_{m_1=-\infty}^{\infty} \cdots \sum_{m_n=-\infty}^{\infty} \frac{h_{AB}^{(\vec{n})}(x)}{\sqrt{(2\pi R)^n}} e^{in_j y_j/R} \\ &= h_{AB}^{(0)}(x) + \sum_{n_1=1}^{\infty} \cdots \sum_{n_n=1}^{\infty} \frac{1}{\sqrt{(2\pi R)^n}} \left[h_{AB}^{(\vec{n})}(x) e^{in_j y_j/R} + h_{AB}^{\dagger(\vec{n})}(x) e^{-in_j y_j/R} \right], \end{aligned} \tag{3.13}$$

where $h_{AB}^{(\vec{n})}(x)$ is a four dimensional bosonic field with mass $\vec{n}\cdot\vec{n}/R^2$. The second step is possible because $h_{AB}(z)$ is real.

To avoid confusion we emphasize that $h_{AB}^{\dagger(\vec{n})}(x)$ does not constitute an additional degree of freedom in the theory. The internal index $\vec{n}$ can be thought of as a discretized momentum index, such that $h_{AB}^{(\vec{n})}(x)$ and $h_{AB}^{\dagger(\vec{n})}(x)$ differ only

by the sign of the extra-dimensional momentum $h^{\dagger(\vec{n})}_{AB}(x) = h^{(-\vec{n})}_{AB}(x)$. This is also obvious from the fact that $h^{(\vec{n})}_{AB}(x)$ and $h^{(\vec{n}')}_{AB}(x)$ are not distinct field excitations. It is now simple to work out the form of Einstein's equations in terms of the field $h^{(\vec{n})}_{AB}(x)$. For example, the first term in (3.12) decomposes as

$$\begin{aligned}
\Box^{(4+n)} h_{AB}(z) &= \sum_{n_j} \frac{1}{(2\pi R)^{n/2}} \partial_C \partial^C \left[h^{(\vec{n})}_{AB}(x)\, e^{i(n\cdot y)/R} \right] \\
&= \sum_{m_j} \frac{1}{(2\pi R)^{n/2}} \partial_C \left[\left(\delta^C_\mu \partial^\mu h^{(\vec{n})}_{AB}(x) + \delta^C_j h^{(\vec{n})}_{AB}(x) \frac{i n_j}{R} \right) e^{i(n\cdot y)/R} \right] \\
&= \sum_{m_j} \frac{1}{(2\pi R)^{n/2}} \left[\Box^{(4)} - \frac{n^j n_j}{R^2} \right] h^{(\vec{n})}_{AB}(x)\, e^{i(n\cdot y)/R}
\end{aligned} \tag{3.14}$$

An independent check on the consistency of this method is that the 4-dimensional massive graviton field $h^{(\vec{n})}_{\mu\nu}(x)$ only has a Pauli–Fierz mass term, $\propto [h_{\mu\nu} - \eta_{\mu\nu} h]$ and no mass terms originating from mixed index derivatives. This is required for a consistent massive spin-2 field [70].

In order to derive the propagator for the 4-dimensional fields $h^{(\vec{n})}_{AB}(z)$ we fix the gauge using a generalization of the 't Hooft ξ for spontaneously broken gauge theories. We add the gauge fixing term

$$\mathcal{L}_{GF} = -\frac{F^2}{\xi}, \tag{3.15}$$

with

$$F = \partial^\mu \bar{h}_{\mu N} + \xi \partial^i (h_{iN} - \frac{1}{2\xi} \eta_{iN} h), \tag{3.16}$$

and

$$\bar{h}_{MN} = h_{MN} - \frac{1}{2} \eta_{MN} h. \tag{3.17}$$

The DeDonder and Unitary gauge for the 4-dimensional theory correspond to $\xi = 1$ and $\xi = \infty$ respectively. We now derive the decomposed effective 4-dimensional action in both gauges. In the remainder of this work we will suppress the extra dimensional label $(\vec{n})$ for notational clarity.

3.3.2 DeDonder Gauge

We decompose the action first in the DeDonder gauge. This corresponds to the only value of ξ which maintains Lorentz invariance in (3.16), and the resulting term is the generalization of the 4-dimensional gauge fixing used in (2.16). The still D-dimensional action is

$$\mathcal{L} = -\frac{1}{2} h^{AB} \Box h_{AB} + \frac{1}{4} h \Box h \,. \tag{3.18}$$

In order to proceed it is helpful to write the D dimensional graviton field in matrix notation in terms its 4-dimensional irreducible components.

$$h_{AB} = \begin{pmatrix} h_{\mu\nu} - \frac{1}{2}\eta_{\mu\nu}\phi & \frac{1}{\sqrt{2}} A_{i\mu} \\ \frac{1}{\sqrt{2}} A_{\nu j} & \phi_{ij}, \end{pmatrix}. \tag{3.19}$$

Inserting (3.19) into (3.18) conveniently produces diagonal kinetic terms. Upon integrating over the extra coordinates we obtain the canonically normalized kinetic Lagrangian for the various fields

$$\begin{aligned} \mathcal{L} = \sum \Bigg(& h_{\mu\nu}(\Box + m_{\mathrm{KK}}^2) h^{\mu\nu} - \frac{1}{2} h (\Box + m_{\mathrm{KK}}^2) h \\ & + \phi_{ij}(\Box + m_{\mathrm{KK}}^2)\phi_{ij} - \frac{1}{2}\phi(\Box + m_{\mathrm{KK}}^2)\phi + A_{i\mu}(\Box + m_{\mathrm{KK}}^2) A_i^{\mu} \Bigg). \end{aligned} \tag{3.20}$$

The corresponding propagators for tensor, vectors and scalars we obtain by inverting the kinetic terms.

$$\Delta^{\mathrm{DeDonder}}_{\mu\nu\alpha\beta}(p, m_{\mathrm{KK}}) = \frac{1}{2}\delta^{(\vec{n},-\vec{n})} \Delta_G (\eta_{\mu\alpha}\eta_{\nu\beta} + \eta_{\mu\beta}\eta_{\nu\alpha} - \eta_{\mu\nu}\eta_{\alpha\beta}) \tag{3.21}$$

$$\Delta^{\mathrm{DeDonder}}_{i\mu j\nu}(p, m_{\mathrm{KK}}) = \delta^{(\vec{n},-\vec{n})} \delta_{ij}\eta_{\mu\nu}\Delta_G \tag{3.22}$$

$$\Delta^{\mathrm{DeDonder}}_{ijkl}(p, m_{\mathrm{KK}}) = \frac{1}{2}\delta^{(\vec{n},-\vec{n})} \Delta_G \left(\delta_{ik}\delta_{jl} + \delta_{il}\delta_{jk} - \frac{2}{\delta + 2}\delta_{ij}\delta_{kl} \right). \tag{3.23}$$

Here we define $\Delta_G = (p^2 - m_{\mathrm{KK}}^2)^{-1}$. By subtracting the trace in the definition of (3.19) we avoid unwanted mixing between $h_{\mu\nu}$ and ϕ coming from the decomposed

second term in (3.18). In physical terms, the DeDonder gauge choice maintains translation invariance in the extra dimensions and corresponds to a freely floating brane in the extra dimensions. In this sense the dynamics of the brane are decoupled from the gravitational sector. The degrees of freedom are as follows. First we have the ± 2 components of the massive graviton with 2 polarizations. Next, there are the n massless components of the vector each containing 2 degrees of freedom. Finally, there are the $n(n+1)/2$ scalar components in the symmetric tensor ϕ_{ij}.

Since the brane moves in the extra dimensions, we must also consider its action. For this purpose it is helpful to follow the lead of Ref. [71] and define the brane coordinates $y_\mu(x) = (x^\mu, (\tau)^{-1/2}\xi^i(x))$ where τ is the brane tension. Since this choice of coordinates breaks translation invariance, the $\xi^i(x)$ correspond to n Goldstone modes. The induced metric of the brane then simply defines the brane dynamics through minimal coupling. We do not provide details on this procedure here as our chosen processes are insensitive to the brane dynamics assuming the particular energy hierarchy delineated in Ref. [72]. We mention their existence though as they correspond to an additional n degrees of freedom. From this result and the previous paragraph we see that the total number of physical degrees of freedom in the DeDonder gauge is $(n^2 + 5n + 4)/2$.

Finally, we note that this choice demands ghost fields $\eta, \bar{\eta}$ be included in the original Lagrangian. For gravity these are spin-1 anti-commuting fields with propagator $\Delta_{\mu\nu} = \eta_{\mu\nu}/k^2$ around flat space [73]. As with QCD in Feynman gauge, ghosts modify gauge boson legs in diagrams involving self interaction vertices. For our considerations in this work, tree-level virtual graviton exchange and one-loop self energy corrections, these conditions are never satisfied and we do not need to specify specifically the ghost-gravity interactions. Moreover, even for real-graviton emission, the ghost contribution only comes in at next-to-leading order in the gravitational coupling.

3.3.3 Unitary Gauge

The goldstone modes associated with the breaking of translation invariance are eaten by the massive vectors in the unitary gauge. Explicitly, the KK decomposition proceeds as follows. Fixing the gauge parameter $\xi \to \infty$ gives

a translation breaking gauge fixing operator

$$\mathcal{L}_{GF} = (\partial^i h_{iN})^2 \to m_{\rm KK}^2 h_{ij}^2 + m_{\rm KK}^2 h_{i\mu}^2 \,, \tag{3.24}$$

after integrating over the extra dimensions. The result in (3.24) corresponds to the eaten Goldstone modes needed to form the massive tensor and n massive vectors. The kinetic action now reads

$$\mathcal{L}_D = -\frac{1}{2} h^{AB} \Box h_{AB} + \frac{1}{2} h \Box h - h^{AB} \partial_A \partial_B h + h^{\mu B} \partial_\mu \partial_\nu h_B^\nu \tag{3.25}$$

which when inverted for the propagators in terms of the same 4-dimensional fields gives

$$\Delta^{\rm unitary}_{\mu\nu\alpha\beta}(p, m_{\rm KK}) = \frac{1}{2}\delta^{(\vec{n},-\vec{n})}\Delta_G(t_{\mu\alpha}t_{\nu\beta} + t_{\mu\alpha}t_{\nu\beta} - \frac{2}{n+2}t_{\mu\nu}t_{\alpha\beta}), \tag{3.26}$$

$$\Delta^{\rm DeDonder}_{i\mu j\nu}(p, m_{\rm KK}) = \delta^{(\vec{n},-\vec{n})} P_{ij} t_{\mu\nu} \Delta_G, \tag{3.27}$$

$$\Delta^{\rm DeDonder}_{ijkl}(p, m_{\rm KK}) = \frac{1}{2}\delta^{(\vec{n},-\vec{n})}\Delta_G \left(P_{ik}P_{jl} + P_{il}P_{jk} - \frac{2}{\delta+2} P_{ij}P_{kl} \right), \tag{3.28}$$

using the notation of Ref. [7] that

$$t_{\mu\nu} = \eta_{\mu\nu} - \frac{p_\mu p_\nu}{m_{\rm KK}^2}, \qquad P_{ij} = \delta_{ij} - \frac{n_i n_j}{n^2}. \tag{3.29}$$

Here $n_i/R = p_{i\perp}$ is the momentum component perpendicular to the brane. The two gauges are identical up to longitudinal terms. The interpretation of the unitary gauge is that the brane breaks translation invariance in the extra dimensions, and the resulting n goldstone bosons are eaten by the now massive vectors. Note that the denominator of (3.27) matches that of a massive weak gauge boson in the (electroweak) unitary gauge. The counting of degrees of freedom are as follows. There are now 5 corresponding to the massive graviton which has eaten a massive vector, leaving an additional $n-1$ vectors. This is evident by rewriting the fields in terms of the mass eigenstates as in Ref. [19]. The scalars maintain the same number $n(n-1)/2$ so we obtain $(n^2+5n+4)/2$

as in the DeDonder gauge.

In passing we note that strictly speaking the two gauge choices describe the same physics, but in the DeDonder gauge, fluctuations of the brane can be decoupled from the interaction of the massive spin-2 graviton and spin-1 gravi-photons. For loop calculations, the longitudinal modes of the spin-2 graviton lead to IR divergences which must be regulated, carried through the calculation and eventually checked for cancelation in the end for a genuine physical observable. In practice, this is a poor choice for sufficiently involved loop calculations. We find that the DeDonder gauge where IR divergences are prohibited by naive IR power counting provides the simplest set-up for loop computations.

Finally, interactions between KK particles and the SM are determined either by expanding the minimally coupled gravity-matter interactions in the decomposed fields, or through the standard operator $h_{MN}T^{MN}$ for a suitably brane confined energy momentum tensor. The definition of T^{MN} guarantees that these are equivalent. We derive the necessary vertices in the appendix. Note that at lowest order matter interacts solely with the tensor mode through the energy momentum tensor. In addition to simplifying computations, this has the positive effect of eliminating equivalence principle violating fields which may in principle appear with the interactions of the KK scalar 0-modes.

As we enumerated the particle content of the AADD model, we now outline some of the constraints on the many experimental predictions.

3.4 Search for Extra Dimensions

Perhaps the most appealing aspect of AADD models is that they provide several entirely orthogonal experimental predictions [74]. These can be divided into two classes, those which are sensitive to the first massive KK excitation, deemed IR constraints, and those probing higher modes in the KK tower. The later are further divided into loop-based indirect constraints and direct constraints from collider production. The main focus of this thesis is collider experiments, but first we briefly overview the other classes of experimental constraints.

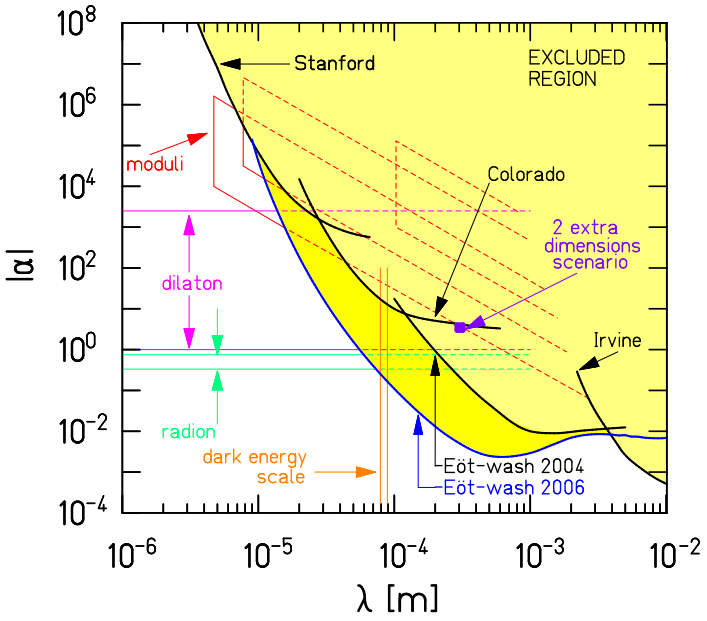

Figure 3.1: Constraints on deviations to the Newtonian force law taken from Ref. [6].

3.4.1 IR Constraints on Extra Dimensions

First, as mentioned in Sec. 3.2.2, differences from the 4-dimensional force law are tested in gravitational experiments at small distance scales. We parameterize deviations from the Newtonian potential as

$$V(r) = V_N(r)(1 + \alpha\, e^{-r/\lambda}), \tag{3.30}$$

where α and λ are calculated in the specific theory. For extra dimensions we identify $\lambda = R$ and α is the degeneracy of the first KK excitation. The most recent bounds are summarized in Fig. 3.1 taken from [6]. From this data for example with $n = 6$ extra dimensions, the constraint is $M_* > 6.4$ TeV using the relation in (3.10) between M_* and R.

The second class of low energy constraints are due to the abundance of new light particles. Such states are constrained by astrophysics [75] and cosmology [76][77] in a similar manner as for example axions [78]. These carry different types of bounds compared to the direct tests. For $n > 4$ extra dimensions, R^{-1} need

to be bigger than a few TeV. For 2 and 3 extra dimensions the constraints are many TeV. With these constraints taken seriously, we are at odds to reconcile the hierarchy problem with extra dimensions. However, since these constraints are generically low-energy, dealing with the first massive KK excitation, we can perfectly well adjust this to fit within the above constraints, but leave the rest of the model untouched [23]. Therefore we turn to the UV side of theory and constraints originating from the lowered cut-off in the standard model.

3.4.2 Indirect Constraints on Extra Dimensions

With the cut-off scale of the SM at the TeV, we expect extra dimension to generate higher dimensional operators suppressed by a TeV energy scale. However, we know from proton decay, flavor physics and the observation of neutrino masses that the suppression scale should not be less than 10^{12}, 10^{2-3} and 10^{11} TeV respectively [74]. This generically occurs in theories of new physics at a low scale, and there certainly exist circumventions most simply by enforcing new additional flavor symmetries.

There are also indirect constraints coming from operators which appear in the SM and are measured precisely. Two examples are the muon $g-2$ [79] and electroweak precision constraints. In the former, constraints are generally weaker around 400 GeV on the generic scale of strong gravity. For higher numbers of extra dimensions $n > 6$ this is pushed up to the TeV level. Electroweak precision computations in Ref. [80] and later in Ref. [81] found strong multi TeV level constraints in the *STU* fomalism [82]. However, the validity of these computations was questioned in Ref. [7], which then computed new bounds using the $\bar{\epsilon}$ parameter with

$$\bar{\epsilon} = \frac{\Pi(m_W^2)}{m_W^2} - \frac{\Pi(m_Z^2)}{m_Z^2}. \tag{3.31}$$

Here $\Pi(m_W^2)$ is the $W^\pm$ boson self-energy evaluated at the scale m_W. Physically, this tests the value of the tree-level SM weak mixing angle using the forward-backward asymmetry in $Z \to l^+l^-$. Note that $\bar{\epsilon}$ is closely related though not identical to the Peskin-Takeuchi T parameter used previously. Generically, theories of higher numbers of extra dimensions are primarily constrained by low energy precision experiments. For recent examples in the warped case see Ref.

[83] and Ref. [84]. We will present the constraints on M_* for various numbers of extra dimensions together with our results implementing the asymptotic safety scenario.

3.4.3 Real Emission Searches

Of the two classes of collider observables we first consider the real emission of Kaluza–Klein gravitons at the LHC [19, 20]. The outgoing gravitons cannot be detected directly and appear as missing transverse momentum or missing transverse energy $\not{E}_T$. One likely process to radiate a gravitons is single jet production [85]. For the graviton–jet final state an obvious irreducible background is $q\bar{q} \to Zg$ where the gluon is emitted from an initial-state quark and the Z decays invisibly. This background is known to next-to-leading order [86], but at large partonic energies the rate prediction becomes increasingly uncertain, due to large logarithms. Extracting new physics from pure QCD signatures at the LHC is therefore always difficult.

Due to the structure of the parton densities of quarks and gluons inside a proton, Tevatron searches for large extra dimensions concentrate on $\gamma\not{E}_T$ final states. Similarly, at the LHC a one photon final state could be resolved in the detectors optimized for Higgs searches in the $H \to \gamma\gamma$ decay channel. Hard single photon events would constitute a revealing signature for physics beyond the Standard Model.

Similarly, the Drell–Yan process $q\bar{q} \to \gamma^*, Z \to \ell^+\ell^-$ with two leptons (electrons or muons) in the final state is the arguably best known hadron collider process [87]. A large amount of missing energy in this channel would be a particularly clean signal for physics beyond the Standard Model at the LHC [88]. Depending on the detailed analysis, both of these electroweak signatures do have smaller rates than a jet+graviton final state, but the lack of QCD backgrounds and QCD-sized experimental and theory uncertainties result in discovery regions of similar size [19][21].

Going back to the theoretical basis, the partonic cross section for the emission of one graviton is not the appropriate observable. We are interested in is the entire

KK tower contributing to the missing energy signature

$$d\sigma^{\text{tower}} = \sum_{\vec{n}} d\sigma^{\text{graviton}} = \int dN \; d\sigma^{\text{graviton}}, \tag{3.32}$$

where $\int dN$ is an integration over an n-dimensional sphere in KK density space. Here we define

$$\int dN \equiv S_{n-1} \; |\vec{n}|^{n-1} \; d|\vec{n}|, \qquad\qquad S_{n-1} = \frac{2\pi^{n/2}}{\Gamma(n/2)}. \tag{3.33}$$

In the ultraviolet the sum over $\vec{n}$ is truncated to those states which satisfy kinematic constraints. In particular, the KK mass satisfies $m_{\text{KK}} = |\vec{n}|/R < \sqrt{s}$ where $\sqrt{s}$ is the partonic center of mass energy (related to the proton center of mass energy via $s = (E_{\text{COM}})^2 \; x_1 x_2$).

We rewrite the KK state density as a mass density kernel using $dm_{\text{KK}}/d|\vec{n}| = 1/R$

$$dN = S_{n-1} \, R^n \, m_{\text{KK}}^{n-1} \, dm_{\text{KK}} = \frac{S_{n-1}}{(2\pi M_*)^n} \left(\frac{M_{\text{Pl}}}{M_*}\right)^2 \; m_{\text{KK}}^{n-1} \, dm_{\text{KK}} \; . \tag{3.34}$$

This implies for the production of a Kaluza–Klein tower

$$d\sigma^{\text{tower}} = d\sigma^{\text{graviton}} \; \frac{S_{n-1} \, m_{\text{KK}}^{n-1} \, dm_{\text{KK}}}{(2\pi M_*)^n} \; \left(\frac{M_{\text{Pl}}}{M_*}\right)^2 \; . \tag{3.35}$$

The key aspects of this formula are:

- The factor M_{Pl} from the KK tower summation can be absorbed into the one-graviton matrix element squared. The effective coupling of the entire tower at the LHC energy scale E is then $E/M_* \gtrsim 1/10$ instead of E/M_{Pl}, *i.e.* roughly of the same size as the Standard Model gauge couplings.

- In particular for larger n the integral is infrared finite with the largest contributions arising from higher mass modes. This is the effect that KK modes are more tightly spaced as we move to higher masses and even more so for an increasing number of extra dimensions n.

- The m_{KK} integration at least on the partonic level — *i.e.* without the parton

Table 3.1: Real emission constraints on the Fundemental scale M_* (in TeV) taken from Ref. [8].

Experiment and channel	$n = 2$	$n = 3$	$n = 4$	$n = 5$	$n = 6$
LEP Combined	1.60	1.20	0.94	0.77	0.66
CDF monophotons, 2.0	1.08	1.00	0.97	0.93	0.90
DØ monophotons, 2.7	0.97	0.90	0.87	0.85	0.83
CDF monojets, 1.1 fb^{-1}	1.31	1.08	0.98	0.91	0.88
CDF combined	1.42	1.16	1.06	0.99	0.95

densities — can be done without specifying the process.

$$\int dN = \int_0^{\Lambda} \frac{S_{n-1}}{(2\pi M_*)^n} \left(\frac{M_{\text{Pl}}}{M_*}\right)^2 m_{\text{KK}}^{n-1}\, dm_{\text{KK}} = \frac{S_{n-1}}{(2\pi M_*)^n} \left(\frac{M_{\text{Pl}}}{M_*}\right)^2 \frac{\Lambda^n}{n} \tag{3.36}$$

The scale Λ in this case is related to the kinematics of the problem and is roughly the hard scale E of the partonic collision. Therefore the result is insensitive to physics far above the LHC energy scale.

Finally, we conclude the discussion on the real emission of graviton by providing a table of constraints based on the previously mentioned processes taken from Ref. [8].

3.4.4 KK Integral and Virtual Graviton Exchange

Virtual gravitons at the LHC demand a markedly different analysis since by definition they do not produce gravitational missing energy. These signals are gravitons which decay within the detector into observable states. In the Standard Model some of these final states, leptons and weak gauge bosons, can only be produced by a $q\bar{q}$ initial state. Since at LHC energies the protons mostly consist of gluons, graviton signatures get a head start. The Tevatron mostly looks for two-photon or two-electron final states [89]. At the LHC the cleanest signal taking into account backgrounds as well as experimental complications is a pair of muons [90]. In Higgs physics the corresponding channel $H \to ZZ \to 4\mu$ is referred to as the 'golden channel', because it is so easy to extract.

In the Standard Model the Drell–Yan process mediates muon pair production via the s-channel exchange of on-shell and off-shell γ and Z bosons. Aside from

the squared amplitude for graviton production, these Standard Model amplitudes interfere with the graviton amplitude, affecting the total rate as well as kinematic distributions. This mix of squared amplitudes and interference effects make it hard to apply any kind of golden cut to cleanly separate signal and background. One useful property of the s-channel process is that the final state particles decay from a pure d-wave (spin-2) state. This results in a distinctive angular separation $\Delta\phi$ of the final state muons [91].

Since the properties of each KK mode are identical other than mass, for a given inclusive process, we generically sum over all modes. This is a distinct feature of extra dimensional theories which we now discuss in detail. Consider an s-channel graviton exchange

$\mathcal{M}$ =

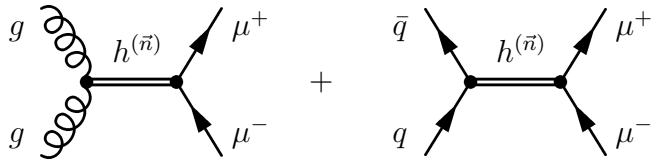

where any graviton in the KK tower can appear as an intermediate state. These states must be summed at the amplitude level. Since this KK sum involves a very large number of states ($\sim 10^{32}$) [92] with mostly regular spacing well below any experimental resolution, we replace it with an integral

$$\frac{1}{M_{\rm Pl}^2}\sum_{n_1=-\infty}^{\infty}\cdots\sum_{n_n=-\infty}^{\infty}\cdots \quad\longrightarrow\quad \frac{S_{n-1}}{M_*^{n+2}}\int dm_{\rm KK}\, m_{\rm KK}^{n-1}\,\cdots\,. \tag{3.37}$$

Absorbing the geometric size of the extra dimensions R into the coupling, $M_{\rm Pl} = M_*(2\pi R M_*)^{n/2}$, the tower of KK states now couples proportional to M_*. It is instructive to go back to the full $(4+n)$-dimensional theory, where we only have the fundamental Planck scale M_* and the gravitons propagating in the the full (brane + bulk) space. In this case the sum leading to (3.37) is merely a loop integral over the unfixed bulk momentum, with the appropriate powers of M_* in front. The power of M_* is fixed by the higher-dimensional coupling, $[\kappa_D] = -(2+n)$.

From the KK graviton Feynman rules [19, 20] it follows that for a massless Standard Model ($T^\mu_\mu = 0$) and energy-momentum conservation ($k_\mu T^{\mu\nu} = 0$), the tensor structure of the graviton matter coupling simplifies significantly. Tree–level

graviton exchange is described by the amplitude $\mathcal{A} = \mathcal{S} \cdot \mathcal{T}$, where

$$\mathcal{T} = T_{\mu\nu} T^{\mu\nu} - \frac{1}{2+n} T^{\mu}_{\mu} T^{\nu}_{\nu} \tag{3.38}$$

is a function of the energy-momentum tensor, and

$$\mathcal{S}(s) \equiv \frac{S_{n-1}}{M_*^{n+2}} \int dm \, \frac{m^{n-1}}{s - m^2 + i\epsilon} \, . \tag{3.39}$$

defines the *summed KK kernel*. The amplitude (3.39) is ultraviolet divergent for $n \geq 2$. For $0 < n < 2$ the integral (3.39) converges. By dimensional analysis the amplitude behaves as [1]

$$\mathcal{S}(s) = \frac{S_{n-1}}{M_*^4} \left(\frac{s}{M_*^2} \right)^{n/2-1} C \, , \tag{3.40}$$

where the coefficient C may be divergent. We can compute the amplitudes for $n > 2$ by analytic continuation of the result from $0 < n < 2$, corresponding to dimensional regularization. In this case one finds $C_{\rm DR} = \pi^{n/2} \Gamma\left(1 - \frac{n}{2}\right)$. For odd dimensions $C_{\rm DR}$ is finite, but remains divergent for even dimensions. Alternatively, an upper limit of the integration Λ may be placed in (3.39), in which case $C \to C(\Lambda/\sqrt{s})$. In either case the regularized version of the effective operator takes the form

$$\mathcal{S} = -\frac{S_{n-1}}{M_*^4} \left(\frac{\Lambda}{M_*} \right)^{n-2} C \tag{3.41}$$

for sufficiently small $s/M_*^2 \ll 1$ where Λ stands for the UV cutoff scale introduced to regularize C,

$$C = \int_0^\infty dx \, x^{n-3} \, F(x) \, , \tag{3.42}$$

and $F(x)$ denotes the explicit regularization for the integral ($x = m/\Lambda$). The coefficient C now parameterizes the effective operator in terms of the (unknown) UV completion of the theory. There are several ways to implement a UV cutoff [19, 90, 89, 85, 93]. For a sharp cutoff the UV modes are suppressed by hand above $m = \Lambda$ and $F_{\rm sharp}(x) = \theta(1 - x)$. This leads to

$$C_{\rm sharp} = \frac{1}{n-2} \, . \tag{3.43}$$

Note that the strong UV divergence of the single graviton amplitude (3.39) is now parameterized by the strong sensitivity of (3.41) on the UV cutoff scale Λ. Note additionally that the logarithmic divergence at $n = 2$ becomes a simple pole in the coefficient (3.43).

On dimensional grounds and to lowest order in $s \ll M_*$, the effective operator representing s-channel graviton exchange is written

$$\mathcal{S} = -\frac{4\pi}{M_{\rm eff}^4}\,. \tag{3.44}$$

This parameterization using the scale $M_{\rm eff}$ is commonly applied in the literature. In general, the mass scale $M_{\rm eff}$ cannot be determined from low-energy considerations alone, but requires input from the full quantum dynamics at the Planck scale. The regularization (3.42) also fixes the mass scale $M_{\rm eff}$ in (3.44) as

$$\left(\frac{M_*}{M_{\rm eff}}\right)^4 = \frac{S_{n-1}}{4\pi}\left(\frac{\Lambda}{M_*}\right)^{n-2} C\,. \tag{3.45}$$

We will study in this thesis how quantum gravity regularizes the amplitude (3.39) dynamically, provided that the high-energy behavior of gravity is governed by a renormalization group fixed point.

3.5 Conclusions

In this chapter we saw that the decomposition of a D-dimensional massless graviton into 4-dimensional fields produces massive scalar, vector and tensor excitations. We specified two specific gauge choices, the DeDonder and Unitary gauge, and found that the propagators in these two cases are identical up to longitudinal terms. In the DeDonder gauge, the Goldstone modes are treated somewhat separately from the gravitational physics. Although unequal terms between the two gauges must drop out for any physical observable, there are substantial differences in the complexity based on this choice. In the next chapter we will compute observables in both gauges based on technical convenience.

The massive spectrum of particles in AADD like models is interesting not only from a theoretical point of view, but from the experimental perspective as well since these have observable consequences. In the simplest geometry where the KK

modes are compactified on a n-dimensional torus, the spectrum of massive modes follows the pattern of integer multiplets on S_{n-1}. Summing over these modes is well approximated as an integral, and once all powers of $m_{\rm KK}$ are accounted for, the integral is divergent in $n > 1$ dimensions. Withholding input from quantum gravity there are two options. First, the divergent KK integral may be replaced with a dimensionally consistent effective interaction as in (3.44). The search for extra-dimensions via virtual graviton exchange is transformed into a generic search for four-fermion or two-boson-two-fermion contact interactions. In other words, all dynamics associated with the KK gravitons are lost. Testing this hypothesis on LHC distribution is certainly meaningful, but does not really constitute a search for extra dimensions. The second option is to apply some type of cut-off regularization but keep the s dependence of the integral. Since the original integral is UV divergent this means cutting of the integral in exactly the regime where the contribution to the cross-section is largest. A large sensitivity to the details of UV physics is then reflected in the positive powers of the cut-off Λ_{KK}.

In the next chapter we will apply asymptotic safety inspired arguments in an attempt to remedy the divergent KK integral in models with $n > 1$ extra dimension. We will find that the cut-off on KK modes can be completely removed in this case, at both tree and one-loop level.

Chapter 4

RG Improved Gravitons

4.1 Introduction

Inspired by the previous chapters on asymptotic safety and extra dimensions, we attempt here to meld these two promising ideas. The reason for this undertaking is that KK gravitons on their own do not satisfactorily describe virtual graviton processes. By assuming the UV fixed point, we find first and foremost that the KK integral is cut-off independent. Moreover, we find in this chapter several other improvements with the UV fixed point.

The ordering of the chapter is as follow; first we develop some helpful approximations to the full anomalous dimension at the fixed point. Second, we carefully study the KK integral in the low $\sqrt{s}$-limit and derive a useful renormalization condition. This allows a full comparison of scheme (in)dependence among the various approximations. Finally, we compute the full amplitude for s-channel tree-level virtual graviton exchange and one-loop contribution to massive gauge boson propagators. These assist in the next chapter when we make phenomenological predictions.

4.2 Approximations of Asymptotic Safety

We require non-perturbative techniques in order to study gravity in the vicinity of the non-trivial fixed point. These are outlined in Appendix .1.4. Within this framework we recall a convenient form of the β-function in the minimal Einstein-

Hilbert truncation [94].

$$\beta_g = \frac{(1-4(4+n)g)(n+2)}{1-(2n+4)g} \tag{4.1}$$

Note that (4.1) is inherently an all-orders expression due to the factor of g in the denominator. Likewise, from the definition of the β-function in (2.31) we obtain an expression for the anomalous dimension

$$\eta(g) = -(n+2)\frac{2(n+6)g}{1-2(n+2)g}. \tag{4.2}$$

Integrating the differential equation in (4.1) produces

$$\ln\frac{\mu}{\mu_0} = \frac{1}{\theta_G}\ln\frac{g(\mu)}{g_0} - \frac{1}{\theta_{\rm NG}}\ln\frac{g_\star - g(\mu)}{g_\star - g_0}\,, \tag{4.3}$$

where we define the specific value of the non-Gaussian fixed point

$$g_\star = \frac{1}{4(4+n)}\,, \tag{4.4}$$

and the critical exponents for the two fixed points

$$\theta_{\rm G} = n+2\,, \qquad \theta_{\rm NG} = 2\frac{(n+4)(n+2)}{n+6}. \tag{4.5}$$

The magnitude of the critical exponents determine how quickly the RG flow approaches the respective fixed points. For all $n > 0$ we have $\theta_{NG} > \theta_G$. Note also that the critical exponents have opposite sign indicating that they are UV and IR attractive. We see in (4.2) that as g approaches its fixed point value $1/(4(4+n))$, the anomalous dimension η approaches the value $-2-n$ as required. We integrate (4.3) and obtain

$$\frac{\mu}{\mu_0} = \left(\frac{g(\mu)}{g_0}\right)^{1/\theta_{\rm G}} \left(\frac{g_* - g(\mu)}{g_* - g_0}\right)^{-1/\theta_{\rm NG}}, \tag{4.6}$$

which should be inverted in order to define the running coupling. However, without making some approximation for (4.6) this is not algebraically possible. Nevertheless, we can obtain a final expression for the wave-function renormaliza-

tion by integrating up to the scale μ the anomalous dimension

$$Z^{-1}(\mu) = Z^{-1}(\mu_0) \exp\left(\int_{\mu_0}^{\mu} dk\, \eta(k)\right). \tag{4.7}$$

In Section 2.2 we saw that in an entirely generic way, the renormalization group improved coupling $Z^{-1}(\mu)G_N$ for asymptotic safety approaches the non-trivial fixed point at a rate corresponding to an anomalous dimension of $\eta = -(2+n)$. In principle we can obtain the exact solution by inverting (4.6) with the critical exponents given in (4.5), plugging this in for the anomalous dimension (4.2) and integrating the result up to the scale μ in (4.7). However, even in the simplest Einstein-Hilbert truncation this is not analytically possible. Solving for $Z^{-1}(\mu)$ numerically on the other hand contains its own downsides. First of all, the expression itself will enter the KK integral, which in some case should be carefully evaluated via contour integration. Second, we would like to implement the running coupling in a Monte Carlo event generator, and a complicated numerical form for this expression will drastically slow down computational speed.

4.2.1 Phenomenological Models

In order to make progress we introduce three approximations for $Z^{-1}(\mu)$ which capture the correct dynamics of asymptotic safety while remaining sufficiently agile for use in our LHC computations. First of all, we define the Λ_T to be the crossover scale for fixed point scaling. Later we will make this definition more precise. The three requirements for an acceptable form of the wave-function renormalization are the following.

1. For $\mu < \Lambda_T$ we insist that Z^{-1} is classical so that $Z^{-1}(\mu \ll \Lambda_T) \approx 1$.

2. At high-energies $\mu \gg \Lambda_T$, $Z^{-1} \to 0$ with exactly the power law behavior

$$\frac{d\log Z}{d\log \mu} = D - 2 \tag{4.8}$$

3. The interpolation between the two regimes should be a smooth[1] function of μ.

[1]We will consider one example of a discontinuous function and mention how this can lead to unphysical results

With the previous three considerations we introduce first the linear approximation [1]

$$Z_{\text{lin}}^{-1}(\mu) = \frac{1}{1 + G_N \mu^{n+2}/g_*} \,. \tag{4.9}$$

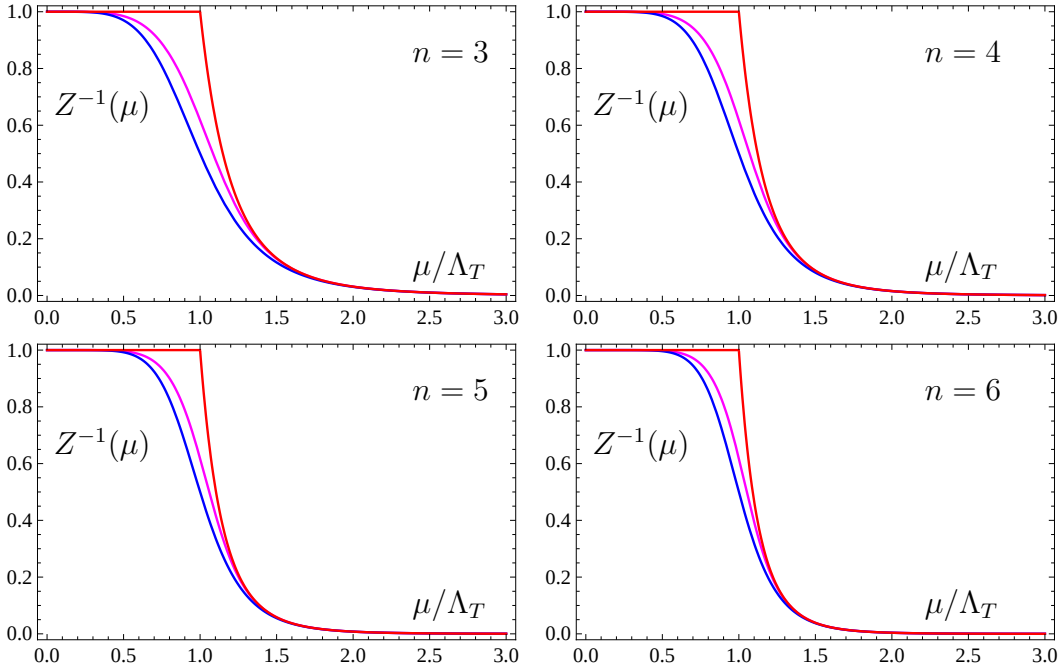

Figure 4.1: $Z^{-1}(\mu)$ representing the cross-over from classical to fixed point scaling for the quenched (red), linear (blue), quadratic (magenta) approximations and $n = (3, 4, 5, 6)$ extra dimensions. For ease of comparison we have set $\Lambda_T^{(0)} = \Lambda_T^{(1)} = \Lambda_T^{(2)}$ for all curves.

A second form we make use of is the quadratic approximation [1]

$$Z_{\text{quad}}^{-1}(\mu) = \sqrt{1 + \left(\frac{G_N \mu^{2+n}}{2g_*}\right)^2} - \frac{G_N \mu^{2+n}}{2g_*,} \,, \tag{4.10}$$

The steps necessary to derive (4.9) and (4.10) from (4.6) are found in Ref. [1]. Note that the cross-over width in (4.10) is smaller than the one in the linear approximation (4.9). In fact as evident in Fig. 4.2, the cross-over width of the solution (4.6) is bounded by the width of the linear cross-over (4.9) and the width of the quadratic approximation (4.10). In general, the fixed point value of the dimensionless coupling g^* contains gauge and cut-off dependency. Therefore, for

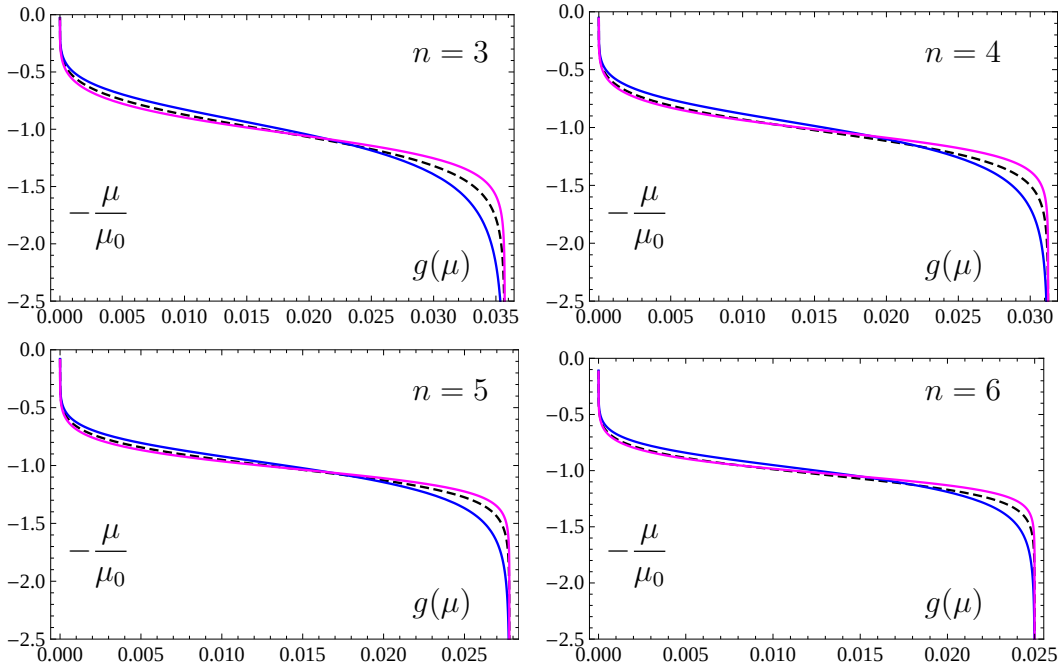

Figure 4.2: Comparison of RG flow equation (dashed) with the linear (blue) and quadratic (magenta) approximations for $n = (3, 4, 5, 6)$ extra dimensions. For increasing n the gap between the approximations diminishes.

our purposes we let $g_*/G_N = \Lambda_T^{n+2}$ where now Λ_T is treated as a parameter related to the fundamental scale of gravity M_* by an $\mathcal{O}(1)$ number. However, we separately label the transition scale $\Lambda_T^{(1)}$ and $\Lambda_T^{(2)}$ in the linear and quadratic approximations respectively.

Finally, we have the quenched approximation [52]

$$Z^{-1}_{\text{quen}}(\mu) = \begin{cases} 1 & \text{for } \mu < \Lambda_T^{(0)} \\ (\Lambda_T^{(0)})^{n+2}/\mu^{n+2} & \text{for } \mu \geq \Lambda_T^{(0)} \end{cases} \qquad \eta(\mu) = \begin{cases} 0 & \text{for } \mu < \Lambda_T^{(0)} \\ -2-n & \text{for } \mu \geq \Lambda_T^{(0)} \end{cases} \tag{4.11}$$

In the quenched approximation we identify the cross-over scale Λ_T with the parameter $\Lambda_T^{(0)}$ in (4.11). The implicit θ function used in the piecewise definition is non-analytic function of the RG scale μ. In contrast, the smooth approximations, (4.9) and (4.10), exhibit two useful properties. First that they contain no additional poles in the external momenta once this is identified with the RG scale μ. Second, they imply a KK kernel which falls of sufficiently quickly as a function of the momenta that the contour around the classical pole can be closed at ∞, and the Cauchy's theorem can be applied as usual. This will prove useful

when we evaluate tree-level and one-loop amplitudes.

In Fig. (4.1) we compare (4.9), (4.10) and (4.11) featuring identical scale Λ_T. In Fig. (4.2) we contrast the two smooth approximations with the shape of the full RG result obtained in the following way. First we invert (4.2) and define $g(\eta) = g(\log Z(\mu)_\mu)$. Now (4.9) and (4.10) may be used to define $g(\mu)$, itself inverted for the RG equation given in (4.3). Finally, the scale μ_0 is fixed so that the shapes are conveniently compared. In general, the deviation from the full result is modest for both the linear and quadratic approximation.

4.2.2 Scale identification

The tree-level single graviton amplitude in extra dimensions includes an integral over perturbative KK propagators. Quantum gravitational corrections are included by replacing perturbative propagators with quantum corrected running propagators, and perturbative vertex functions with running vertex functions. We include only the RG correction to the propagator, and ignore vertex corrections. This step requires that the RG scale μ is identified with the scale relevant for the physical process under investigation

$$\mu = \mu(\sqrt{s}, m), \tag{4.12}$$

in general depending on some combination of the center-of-mass energy $\sqrt{s}$ and the KK mass m. A discussion of a matching which involves several scales is given in Ref. [58] in the context of black hole production. The RG improved amplitude takes the form [1]

$$\mathcal{S}(s) = -\frac{S_{n-1}}{M_*^4}\left(\frac{\Lambda_T}{M_*}\right)^{n-2} C(s;\Lambda_T), \tag{4.13}$$

where

$$C(s;\Lambda_T) = \int_0^\infty dx \frac{x^{n-1}}{-s/\Lambda_T^2 + x^2}\, Z^{-1}\left(\mu = \mu(\sqrt{s}, m, \Lambda_T)\right), \tag{4.14}$$

and $x = m/\Lambda_T$. The energy dependence of (4.14) is encoded in the wave function factor $Z(\mu)$, itself defined via the running of the gravitational coupling.

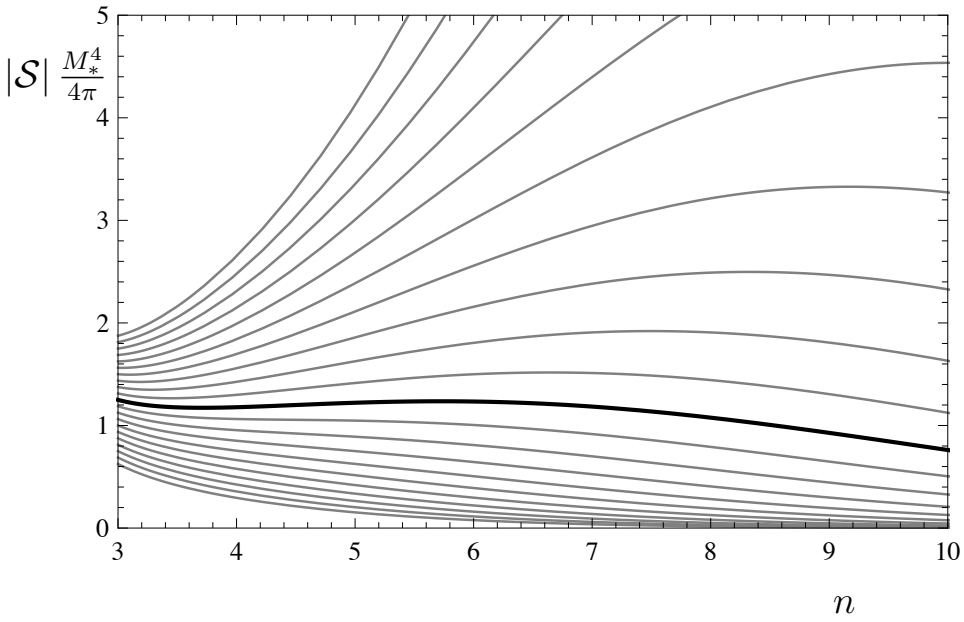

Figure 4.3: The n-dependence of the amplitude $|\mathcal{S}|\,M_*^4/(4\pi)$ defined in (4.13). Thin grey lines cover $\Lambda_T/M_* = 0.5$ to 1.5 in steps of 0.05 (from bottom to top). Close to $\Lambda_T/M_* = 1$ (thick black line), the overall n-dependence of the amplitude is very weak. From Ref. [1]

4.2.3 Low-Energy Matching

First, we analyze the virtual graviton exchange (4.13) and (4.14) in the limit of small center-of-mass energy where $\sqrt{s} \ll M_*, \Lambda_T$. Withholding input from quantum gravity the integration over the KK gravitons is cut off and we obtain the well-known result (3.43). We apply the renormalization group corrections predicted by asymptotically safe gravity. In the limit of small $\sqrt{s} \ll M_*$, the matching (4.12) becomes

$$\mu = m\,, \tag{4.15}$$

so that the RG scale is matched to the KK mass. For the now s independent number (4.14), we find

$$C = \int_0^\infty dx\, x^{n-3}\, Z^{-1}(x\,\Lambda_T)\,. \tag{4.16}$$

where $x = m/\Lambda_T$. The scale-dependence of the wave function factor Z^{-1} acts as the regulator $F(x)$ in (3.42). The coefficient (4.16) is computed for a given renormalization group trajectory $G(\mu) = G_N Z^{-1}(\mu)$ or in other words once we integrate over μ. We can analytically compute (4.16) in the three approximations using the identification (4.15). In the quenched approximation (4.11), we find [95]

$$C_{(0)} = \frac{1}{n-2} + \frac{1}{4} \equiv C_{\rm EFT} + C_{\rm UV}\,. \tag{4.17}$$

The first term $C_{\rm EFT}$ is identical to the contribution within effective theory (3.43), provided the effective theory cutoff coincides with the energy scale where gravity becomes non-perturbative. The second term $C_{\rm UV}$ originates solely from the KK gravitons with mass $m > \Lambda_T$ ($x > 1$). The cross-over point is for $n = 6$ extra dimensions, below which the IR contribution is larger. For more dimensions the UV regime dominates. For the linear approximation (4.9), we have [1]

$$C_{(1)} = \frac{1}{4}\Gamma\left(\frac{n-2}{n+2}\right)\,\Gamma\left(\frac{n+6}{n+2}\right) \,=\, \frac{1}{4} + \frac{2}{3}(\frac{\pi}{n})^2 + \mathcal{O}\left(\frac{1}{n^3}\right). \tag{4.18}$$

We see that (4.18) reaches the same limit as (4.17). For the quadratic approximation (4.10), we obtain [1]

$$C_{(2)} = -\frac{\Gamma\left(\frac{n+4}{n+2}\right)\Gamma\left(-\frac{4}{n+2}\right)}{(n+2)\,\Gamma\left(2\frac{n+1}{n+2}\right)} \,=\, \frac{1}{4} + \frac{1}{2n} + \mathcal{O}\left(\frac{1}{n^2}\right). \tag{4.19}$$

The large-n limit implies that $C_{(0)} \geq C_{(2)} \geq C_{(1)}$, which furthermore holds for all $n > 2$. In the next section we choose to match these coefficients through the definition of the scale $\Lambda_T^{(i)}$.

Finally we discuss and illustrate in Fig. 4.3 the n-dependence of the amplitude (4.13). The phase space factor S_{n-1} grows until $n \approx 8$. The coefficients (4.17), (4.18), and (4.19) decrease until $n \approx 10$ and stay at their asymptotic value thereafter. Roughly speaking the product does not depend on n for intermediate values $n = 3...8$ so that the main dependence of (4.13) is in the prefactor $(\Lambda_T/M_*)^{n-2}$. Therefore, the signal will depend greatly on the value of Λ_T in $4+n$ dimensions.

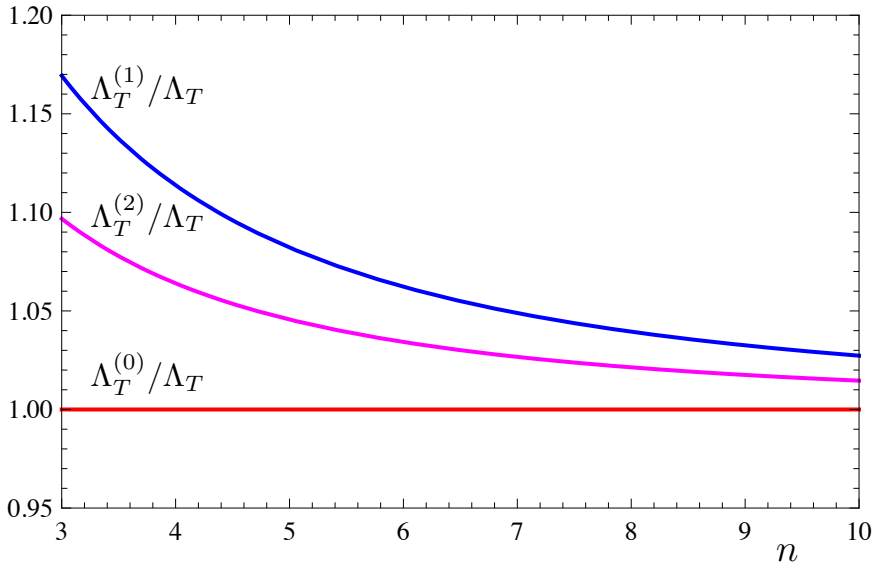

Figure 4.4: The variation between the fundamental cross-over scale Λ_T and the RG parameters Λ_T^{RG} appearing in the quenched ($\Lambda_T^{(0)} = \Lambda_T$, red), linear ($\Lambda_T^{(1)}$, blue) and quadratic ($\Lambda_T^{(2)}$, magenta) approximations. The scale parameters differ at the 10% level for $n = 3, 4$, and rapidly approach each other with increasing n. From Ref. [1].

4.2.4 Universality

In the previous section we labelled the transition scales in the linear, quadratic and quenched approximation as $\Lambda_T^{(1)}$, $\Lambda_T^{(2)}$ and $\Lambda_T^{(0)}$ respectively. The reason for this is that the specific transition scale, especially in the case of a smooth function is not well defined, and in general will depend on the form of the function itself. Although the transition scales in the various approximations are related in magnitude, we allow them to be independent. The issue remains as to how these scales should be related by the underlying physics.

For this purpose we turn to some wisdom provided by perturbative quantization. As summarized in for example [96], a superficially divergent one-loop scattering amplitude regulated by some cut-off scale Λ is made independent of Λ by introducing a running coupling constant. In addition, the independence demands a *renormalization condition* enforced at the level of an observable. In QED, where the scattering amplitude is well defined at vanishing center-of-mass energy, $s = 0$ is used as the renormalization point, sometimes referred to as the

Thompson limit. We would like to find a similar way to assure that the low energy scattering amplitude involving virtual gravitons does not depend on the approximations used. This suggest that we adjust the parameters $\Lambda_T^{(1)}$, $\Lambda_T^{(2)}$ and $\Lambda_T^{(0)}$ in order to define an analogous condition.

We compare different approximations for the RG improved couplings for a given cross-over scale Λ_T. The definition of Λ_T is fixed through the low-energy amplitude $\mathcal{S}(s=0)$. We further choose that Λ_T coincides with the scale $\Lambda_T^{(0)}$ set in the quenched approximation, as the transition scale in this case is the most well-defined. The definition of the corresponding scale $\Lambda_T^{(i)}$ in terms of Λ_T for a smooth crossover of Newton's coupling is then obtained from [1]

$$(\Lambda_T)^{n-2}\, C_{\text{quench}}(s=0;\Lambda_T) = (\Lambda_T^{(i)})^{n-2}\, C_{(i)}(s=0;\Lambda_T^{(i)})\,. \tag{4.20}$$

This uniquely fixes the scale $\Lambda_T^{(i)}$ in terms of Λ_T for any explicit wave function factor $Z_{(i)}^{-1}$. Quantitatively, the scales Λ_T and $\Lambda_T^{(i)}$ will at worst differ by 15%. We display this in Fig. 4.4.

4.2.5 Form-factor approximation

Another possible scale identification is the exchanged 4-momentum $\sqrt{s}$ so that

$$\mu^2 = s\,. \tag{4.21}$$

This choice is made in Ref. [53] along with the linear approximation (4.9). The coefficient $C(s)$ in this case remains divergent in the KK integral, and must be regulated as in effective field theory. We denote the regularized version of the KK integral as C_{KK}, so that this choice implies the factorization of the coefficient $C(s)$ as

$$C(s) = Z^{-1}(\sqrt{s})\, C_{\text{KK}}\,. \tag{4.22}$$

Furthermore, the parameter t introduced in the form-factor of Ref. [53] is related to g_* in (4.9) and the scale Λ_T as $t = (g_*)^{1/(n+2)} = \Lambda_T/M_D$. This suggest that the form-factor approximation (4.22) can be obtained from a matching (4.12) provided that a further factorization $Z(\mu(\sqrt{s},m)) \propto Z_s(\sqrt{s})\, Z_m(m)$ is realized in the relevant kinematical regime. The virtue of the matching (4.21) is that, provided an s independent regularization such as the lowest dimensional EFT

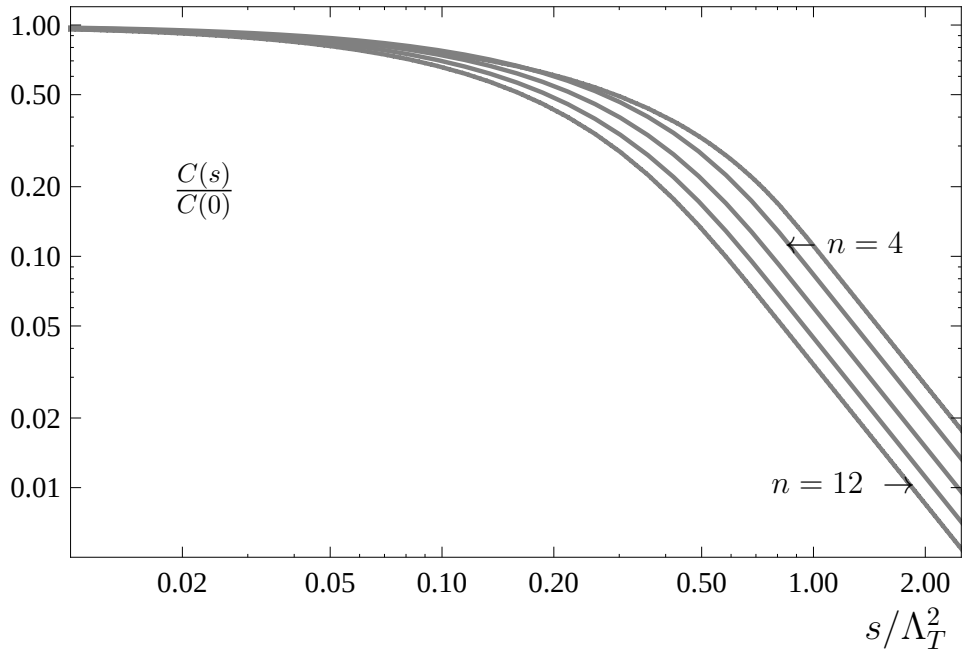

Figure 4.5: The energy-dependence of the functions $C(s)$ from (4.24) in the quenched approximation with the euclidean matching, for $n = 4, 6, 8, 10$ and 12 (top to bottom). The amplitude can become suppressed at scales significantly below Λ_T. From Ref. [1]

(3.44), the s dependence is contained solely in $C(s)$ which behaves like $s^{-n/2-1}$. Applying a regularization maintaining the dynamics of the KK integration as in (3.40) produces $\mathcal{S}(s) \sim s^{-2}$. In the next section we will see that this power behavior is a necessary condition for perturbative unitarity.

The downsides of the form-factor matching are first, that depending on the relation between Λ_T and M_*, this scaling may not be realized in the single graviton exchange process. Second, the opportunity to extract low energy contributions from quantum gravity is missed by matching a purely 4-dimensional scale such as (4.21). In the next section we will introduce a scale choice which maintains s dependence in addition to regulating the KK integral.

4.2.6 Euclidean Matching

We are interested in the behavior of amplitudes at center-of-mass energies not parametrically lower than M_* where the expansion in $\sqrt{s}/M_*$ from the previous

section is ill-suited. In this case we identify the renormalization group scale μ with the $4+n$-dimensional euclidean momentum scale

$$\mu^2 = s + m^2 \,. \tag{4.23}$$

This identification is most natural from a $4+n$-dimensional perspective as the effective single graviton amplitude is sensitive to the $4+n$-dimensional momenta running through the propagator. Using the definition for $Z(\mu)$ in (2.29), we find

$$C(s) = \int_0^\infty dx \frac{x^{n-1}}{y^2+x^2} Z^{-1}\left(\sqrt{y^2+x^2}\,\Lambda_T\right) \quad \text{with} \quad y^2 = s/\Lambda_T^2 \,. \tag{4.24}$$

The s-dependence of (4.24) originates from both the graviton propagator and the RG improved coupling. In Fig. 4.5, we compute (4.24) in the quenched approximation for various extra dimensions. For small $s/\Lambda_T^2 \ll 1$ the variation compared to $C(s=0)$ is small though increases with n. With increasing number of extra dimensions, the crossover from perturbative scaling to high-energy scaling sets in at lower energy scales $s < \Lambda_T^2$. We learn here that as the number of extra dimensions increases, the deviation from the low energy coefficient sets-in at lower energy scales. Two implications are that as the number of dimensions increase, the amplitudes become better behaved with respect to perturbative unitarity and consequently that the effective theory computation is less applicable.

For large $s/\Lambda_T^2 \gg 1$, the amplitude (4.24) is integrated analytically. Since Z is in the scaling regime for large $\sqrt{s}$ we find that $\lim_{\mu\to\infty} \mu^{n+2} Z^{-1}(\mu)$ becomes a μ-independent constant. The leading behavior reads

$$C(s) = c_n \left(\frac{\Lambda_T^2}{s}\right)^2 \,, \tag{4.25}$$

with the coefficient

$$c_n = \lim_{s\to\infty} \int_{\Lambda_T/\sqrt{s}}^\infty dz \frac{z^{n-1}}{(1+z^2)^{n/2+2}} = \frac{2}{n(n+2)} \,, \tag{4.26}$$

where we have substituted $z = m/\sqrt{s}$. The leading large-s decay (4.25) is universal and independent of the number of extra dimensions. The only evidence of the dimensionality of the underlying theory remains in the the constant c_n. Furthermore, the scaling s^{-2} in the UV implies that the effective 4-dimensional

coupling constant behaves like G_N/E^2, exactly as expected for a purely 4-dimensional fixed point. It seems that the lower dimensional theory, upon KK integration, inherits some of the general properties of asymptotically safe gravity present at the higher dimensional fixed point.

4.2.7 Pole region and virtuality

In this section, we evaluate the KK integral in the pole region, where $s \approx m^2$ and the graviton is deemed on-shell. KK gravitons can also decay into lighter particles and therefore have a non-zero decay width. We explore the implications of the graviton width in more detail in Appendix .1.2. Here, we adopt the principal value prescription. In addition, we compare the matching (4.23) with the alternative choice

$$\mu^2 = |s - m^2_{\rm KK}| \tag{4.27}$$

where the RG scale is identified with the virtuality of a KK graviton. Note that the main difference between the choice $\mu^2 = s + m^2$ from (4.23) and (4.27) relates to the pole region where $s \approx m^2$. Around the pole, (4.27) implies $\mu \approx 0$, meaning that this region is only sensitive to classical physics $G(\mu \approx 0)$, even for energies with $s, m^2 \gg M_*^2$. In contrast, the matching (4.23) leads to $\mu \approx m$ at the pole, which is sensitive to RG corrections.

For illustration, the physics content of the matching (4.27) is depicted in Fig 4.6 for a specific choice of M_* and Λ_T. Single graviton exchange is reliable for $\sqrt{s}$ below the fundamental Planck scale. For KK modes starting with masses of the order $\sqrt{s + \Lambda_T^2}$, RG corrections must be taken into account. This is denoted as the high mass region (HM) in Fig 4.6. A high energy region (HE) requiring RG effects may also exist, provided that the cross-over scale Λ_T is below the fundamental scale of gravity M_*. As the collider energy approaches M_*, we expect multi-graviton processes or the production of mini-black holes to become important. Finally, we define the pole region (P), where $s \approx m^2$ and the graviton is on-shell.

We quantify the pole contribution using the RG running in the linear approximation (4.9), together with the matching in (4.27). The KK kernel falls

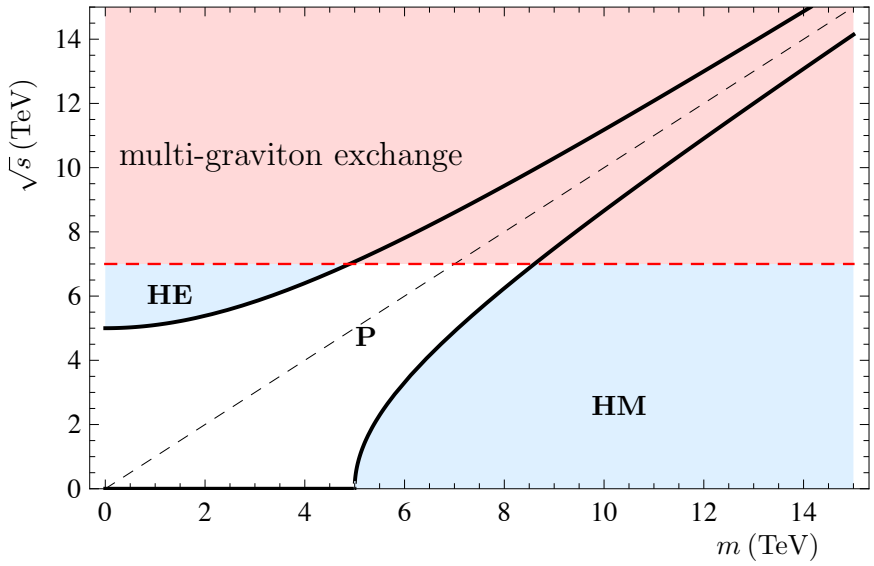

Figure 4.6: UV/IR division of integration kernel using (4.27) with $\Lambda_T = 5\,\text{TeV}$ and $M_* = 7\,\text{TeV}$ in the quenched approximation for illustration. The red region corresponds to physics above $s \geq M_*^2$ (chosen for illustrative purposes), where multi-graviton and width effects become relevant. KK states in the high mass (HM) and high energy (HE) regions are sufficiently far from their mass shell in four dimensions, and thus probe the underling $4+n$ dimensional quantum gravitational theory. The boundaries between pole, HM and HE regions are indicative, and smeared-out due to the RG running in the linear and quadratic approximation. From Ref. [1].

off sufficiently quickly as a function of m_{KK} and we can adopt the prescription

$$Z^{-1}\frac{m^{n-1}}{s-m_{\text{KK}}^2+i\epsilon} = Z^{-1}\,\text{P}\frac{m^{n-1}}{s-m_{\text{KK}}^2} + \frac{i\pi}{\sqrt{s}}m_{\text{KK}}^{n-1}\delta(\sqrt{s}-m_{\text{KK}})\,. \tag{4.28}$$

We also use the fact that $Z^{-1}=1$ at $\mu=0$ for all approximations. The second term in (4.28) is responsible for the on-shell production of KK gravitons. The principal value integration we perform analytically for all $n = 2+4i$ and integer i. For $n=2$ we obtain

$$C(s) \;=\; \text{P}\int dx \frac{x}{-s+x^2}\,Z^{-1}(\mu^2=|s-x^2|\Lambda_T^2) = \frac{1}{4}\ln\left(1+\frac{1}{s^2}\right) \tag{4.29}$$

with $x = m/\Lambda_T$, and $s \to s/\Lambda_T^2$. We note that the amplitude is well-defined for

all $s > 0$, and the result agrees with the one obtained by analytical continuation. The amplitude decays asymptotically as $\propto 1/s^2$. For comparison, effective theory gives $C_{\text{eff}}(s) = \frac{1}{2}\ln(1/s - 1)$ valid for $s/\Lambda_T^2 < 1$, which produces a logarithmic singularity at the EFT boundary [20]. We can see the cause for this as follows. In our s versus m_{KK} plane, the effective theory contribution is a box with sides Λ_T. We evaluate the principle value over the pole by essentially canceling the divergent terms on each-side. However, any cut-off we place on the m_{KK} integration automatically produces a singularity as the $\Lambda_T - \epsilon$ contribution is no longer cancelled. In the region where $s, m_{\text{KK}} \to \Lambda_T$ this is precisely the contribution giving rise to the effective field theory singularity. In our approach the principle value integration is singularity free for all energies.

Next we consider $n = 6$, where

$$C(s) = \frac{\pi\, s}{2\sqrt{2}} + \frac{s^2}{8}\ln\left(1 + \frac{1}{s^4}\right) - \left(\frac{s}{4\sqrt{2}}\ln\left(A(s) + s^2\right) - \frac{A(s)}{4}\arctan A(s) + (s \leftrightarrow -s)\right), \tag{4.30}$$

and $A(s) = 1 - \sqrt{2}s$, $x = m/\Lambda_T$, while s is again expressed in units of Λ_T^2. The result includes the terms of the Euclidean matching (4.24) after analytical continuation $s \to -s$. In the high scattering energy limit, (4.30) grows linearly with s, approaching $\pi\, s/\sqrt{2} + \mathcal{O}(1/s^2)$. We stress that the linearly growing term in s originates from the density of states at the pole region for $s, m^2 > \Lambda_T^2$. As discussed above, this behavior is an effect of the virtuality matching (4.27), which treats modes at the pole with $s, m^2 \gg \Lambda_T^2$ as classical. Essentially, for $n = 6$ we obtain sub-leading pole terms in addition to the one in (4.28). Neglecting the pole terms we obtain exactly the euclidean matched result decaying universally as $1/s^2$ in the UV. Only by incorporating the full effects of the graviton decay width can we realistically study the pole terms. In fact, Ref. [97] pointed out that gravitons produced with $m_{\text{KK}} \sim \sqrt{s}$ may actually decay outside of the detector and thus should be included in the missing energy search. From the perspective of the KK integral for virtual graviton exchange, these effects are unphysical and an artifact of the virtuality matching along with principle value prescription.

Now for illustrative purposes let us examine the quenched approximation. The additional poles prohibit a straight-forward Wick rotation of the momenta to Euclidean space. Therefore, defined in the Minkowski regime the computation

produces large contributions at the boundary between the classical and UV regions. In this case even the UV region remains sensitive to the pole and grows in general as $s^{n/2+1}$. This leads to an unphysical breakdown of perturbative unitarity at an intermediate energy scale. The purpose here is to emphasize that the quenched approximation cannot be applied in the virtuality matching in any meaningful sense. As a corollary, we find no low energy matching condition which generates scheme independence in the sense of (4.20).

To conclude, we obtain a good approximation for the amplitude (4.14) within a principal value integration via the euclidean matching (4.23). The virtual graviton KK kernel decays like s^{-2} for large s and quantitatively becomes equivalent to analytical continuation in s from (4.24). The significance of the s^{-2} scaling is that a necessary condition for perturbative unitarity is that the cross-section[2] be bounded by $1/s$. Examining the full s-channel cross-section

$$d\sigma \sim ds\, dt\, dY\, \frac{1}{s^2} s^4 |\mathcal{S}(s)|^2, \tag{4.31}$$

we see that $C(s) \sim s^{-2}$ produces exactly this behavior at the level of σ. Hence, the amplitude decays asymptotically as required by perturbative unitarity for all physically motivated matchings. For Λ_T/M_* up to the order of a few, the s-channel amplitude is unitary. In turn, for large $\Lambda_T/M_* \gg 1$, our results fall back on those from standard effective theory where perturbative unitarity is violated for center-of-mass energies approaching the fundamental Planck scale [98]. Hence, the high-energy fixed point improves s-channel unitarity of the single graviton amplitude.

4.3 Evaluation of Diagrams

Now that we understand the integral over KK propagators, we focus on the tensorial part of the amplitude for tree-level and one-loop processes. The evaluation of tree level amplitudes is straight-forward, especially in the unitary gauge where longitudinal modes of the graviton do not contribute. The KK mass kernel $\mathcal{S}(s)$ then produces an overall (energy dependent) multiplicative factor. For one-loop computations on the other hand, the loop integral essentially extends

[2]In the Standard Model, W^+W^- longitudinal scattering decays like $1/s$ only after including the propagating Higgs

to $4+n$ dimensions and must be performed at once. While this makes the scale identification very natural, it is technically more involved. We devote a sizable portion of this section to describing these details.

4.3.1 Tree-Level

Using the Feynman rules in the appendix, we compute the tree-level s-channel exchange of a virtual graviton originating from either gg or $q\bar{q}$ initial states. Using the definition of $\mathcal{S}(s)$ from (3.39), the $gg \to \mu^+\mu^-$ amplitude in the Unitary gauge is

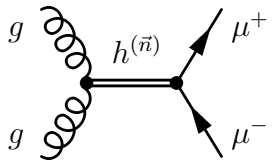

$$= \frac{i\mathcal{S}(s)}{4}\left[\epsilon_1^\alpha \epsilon_2^\beta (W_{\mu\nu\alpha\beta} + W_{\nu\mu\alpha\beta})\Delta^{\mu\nu\rho\sigma}\bar{u}_1[W_{\rho\sigma} + W_{\sigma\rho}]v_2\right].$$

Here, ϵ_1^α is the polarization of the gluon with momentum k_1, $W_{\mu\nu}$ is the $f\bar{f}h$ vertex found in the appendix, $W_{\mu\nu\alpha\beta}$ is the ggh vertex and $\bar{u}_1$ is the outgoing spinor for the muon with momentum p_1. Squaring the amplitude and noting the factor of $1/2$ in the phase space due to identical gluons we obtain [23],

$$\frac{d\sigma}{dt}(gg \to \mu^+\mu^-) = -\frac{|\mathcal{S}(s)|^2}{256\pi s^2}\left[|\mathcal{S}(s)|^2 t(s+t)(s^2+2st+2t^2)\right] \tag{4.32}$$

Here there is no tree-level interference term with the SM. For the $q\bar{q}$ initial state on the other hand there exist a SM contribution mediated by Z/γ, itself with its own interference, along with the graviton-Z/γ mixing [23].

$$\begin{aligned}\frac{d\sigma}{dt}(q\bar{q} \to \mu^+\mu^-) = \\ &\frac{u^2(|G^{LL}|^2 + |G^{RR}|^2) + t^2(|G_s^{LR}|^2 + |G_s^{RL}|^2) + s^2(|G_t^{LR}|^2 + |G_t^{RL}|^2)}{48\pi s^2} \\ &+ \frac{1}{384\pi s^2}\left[\frac{|\mathcal{S}(s)|^2}{4}(s^4 + 10s^3t + 42s^2t^2 + 64st^3 + 32t^4)\right. \\ &\left. + 2\mathrm{Re}\,\mathcal{S}(s)^*\left((G_s^{LR} + G_s^{RL})t^2(3s+4t) + (G^{LL} + G^{RR})(s+4t)u^2\right)\right]\end{aligned} \tag{4.33}$$

Here we have defined the electroweak couplings and propagators in the canonical way so that for example

$$G_s^{LL} = \sum_{i=\gamma,Z} \frac{g_L(q) g_L(\mu)}{s - m_i^2 + i m_i \Gamma_i} \tag{4.34}$$

Squaring these introduces the Z/γ mixing. Details are available in [23] and [3].

4.3.2 One-loop

While the tree-level amplitude can be quite easily separated from the KK integral, loop computations inevitably mix the two. In our computation the loop integral and the KK sum are combined and regulated at once using the D-dimensional scale matching of the previous section. To demonstrate this we compute the massive gauge boson, $W^\pm$ and Z, self-energy corrections.

Evaluation

We start with the seagull diagram in the DeDonder gauge [2]. From the Feynman rules we obtain

$\Pi_S^{\mu\nu}(p^2) =$ $\frac{1}{2}$

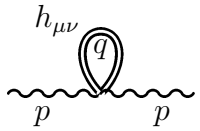

$$= -\frac{32\pi}{M_*^{2+n}} \int \frac{d^{4+n}q}{(2\pi)^{4+n}} \, \Delta_G \, \frac{3}{2} \left(p^2 \eta^{\mu\nu} - p^\mu p^\nu \right), \tag{4.35}$$

in agreement with the transverse nature of the amplitude for a massless gauge boson. Here, p is the external momentum, q is the bulk loop momentum, and Δ_G the scalar part of the graviton propagator. Furthermore, the gravi-scalar contribution in four dimensions is proportional to the trace of the energy-momentum tensor and thus can only couple to the mass term. However we find in the metric expansion that there is no term of order $M_{\rm Pl}^{-2}\phi^2$ and thus the only contribution from extra dimensions is (4.35). We will not simplify the loop

integral at this point. The rainbow diagram is

$\Pi_R^{\mu\nu}(p^2)$ = 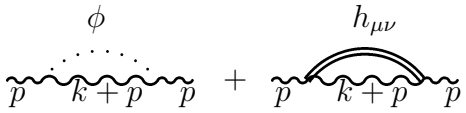

$$= \frac{32\pi}{M_*^{2+n}} \int \frac{d^{4+n}q}{(2\pi)^{4+n}} \, \Delta_G \, \frac{A^{\mu\nu}(k,p)}{(k+p)^2 - m_V^2}, \tag{4.36}$$

We have also introduced k, the brane only component of the full loop momentum. The tensor $A^{\mu\nu} \equiv A_1^{\mu\nu} + A_2^{\mu\nu} + A_3^{\mu\nu}$ contains additionally terms proportional to m_V^2 and m_V^4.

$$\begin{aligned} A_1^{\mu\nu}(k,p) = \frac{1}{2} \big[& -4p^\mu p^\nu p^2 - 4p^\mu p^\nu p \cdot k - p^\mu p^\nu k^2 - 4p^\mu k^\nu p^2 - 3p^\mu k^\nu p \cdot k \\ & + p^\nu k^\mu p \cdot k - k^\mu k^\nu p^2 + 8\eta^{\mu\nu} p^2 p \cdot k + \eta^{\mu\nu} p^2 k^2 + 4\eta^{\mu\nu} p^4 + 3\eta^{\mu\nu} (p \cdot k)^2 \big] \end{aligned} \tag{4.37}$$

$$A_2^{\mu\nu}(k,p) = 3m_V^2(\eta^{\mu\nu}(p \cdot k + p^2) - p^\mu k^\nu - p^\mu p^\nu) \tag{4.38}$$

$$A_3^{\mu\nu} = \frac{5m_V^4}{2}\eta^{\mu\nu} \tag{4.39}$$

At this point we could introduce Feynman parameters and perform a cut-off or dimensional regularization. We expect that the leading UV divergences would cancel with similar terms from the seagull diagram. However, the amplitude would retain power and logarithmic sensitivity to the cut-off scale [7]. In both cases the amplitude is UV sensitive, and the effects of quantum gravity are explicitly cut-off.

For now we tensor reduce this amplitude without making specific reference to the regulator. Additionally, the amplitude in (4.36) can be reduced to scalar integrals without any knowledge of the higher dimensional theory. Using Lorentz

invariance on the brane, we project the tensor integral onto the scalar integrals

$$\begin{aligned}
\tilde{A}_0 &= \int \frac{d^{4+n}q}{(2\pi)^{4+n}}\ \Delta_G \\
\tilde{B}_0 &= \int \frac{d^{4+n}q}{(2\pi)^{4+n}}\ \Delta_G\ \frac{1}{(k+p)^2 - m_V^2} \\
p^2\tilde{B}_1 &= \int \frac{d^{4+n}q}{(2\pi)^{4+n}}\ \Delta_G\ \frac{p\cdot k}{(k+p)^2 - m_V^2} \\
p^2\tilde{B}_2 &= \int \frac{d^{4+n}q}{(2\pi)^{4+n}}\ \Delta_G\ \frac{k^2}{(k+p)^2 - m_V^2}
\end{aligned} \tag{4.40}$$

The notation is meant to evoke the similarity to the normal basis integrals obtained in Passarino-Veltman reduction [99]. The seagull contribution simply reads

$$\Pi_S^{\mu\nu}(p^2) = -\frac{32\pi}{M_*^{2+n}}\frac{3}{2}\ \left(p^2\eta^{\mu\nu} - p^\mu p^\nu\right)\tilde{A}_0\ , \tag{4.41}$$

while the rainbow self energy in terms of the basis integrals is

$$\begin{aligned}
\Pi_R^{\mu\nu}(p^2) = \frac{16\pi}{M_*^{2+n}}\Big(&(p^2\eta^{\mu\nu} - p^\mu p^\nu)\ \Big[12m_V^2\left(\tilde{B}_1 + \tilde{B}_0\right) \\
&+3p^2\tilde{B}_2 + 16p^2\tilde{B}_1 + 8p^2\tilde{B}_0\Big] + \eta^{\mu\nu}m_V^4\left[10 + \frac{n}{2+n}\right]\tilde{B}_0\Big)\ .
\end{aligned} \tag{4.42}$$

It should be noted that we have not taken into account brane fluctuations, coupling proportional to the brane tension τ. It is not clear how one would incorporate this parameter within the framework of asymptotic safety. Moreover, we are physically justified to neglect this contribution if we restrict ourselves to rigid branes or more precisely the energy hierarchy described in Ref. [72].

Finiteness

We can heuristically show the finiteness of our calculation in the asymptotic safety framework. We apply both the quadratic (4.10) and quenched (4.11) approximations to account for the large anomalous dimension in the UV. First of all, we consider the UV portion of the seagull integral in (4.35), assuming the wave-function renormalization in the the quenched approximation (4.11). The

momentum integral is then trivial

$$\Pi_S^{\text{quenched}} \sim \int_{\Lambda_T}^{\Lambda_{\text{UV}}} \frac{dq}{q} = \log \frac{\Lambda_{\text{UV}}}{\Lambda_T} \ . \tag{4.43}$$

For the rainbow diagram we first write the brane momenta as the 4-dimensional projection of the $4+n$-dimensional momentum *i.e.* $k^2 = q^2\chi^2$. We will only display an explicit form of χ at a later point, since it is not required for showing UV finiteness. Considering small values of the external momenta, the leading divergence is

$$\Pi_R^{\text{quenched}} \sim \int_{\Lambda_T}^{\Lambda_{\text{UV}}} \frac{dq}{q} \frac{q^2\chi^2}{q^2\chi^2 + m_V^2} = \log \frac{\Lambda_{\text{UV}}}{\Lambda_T + \cdots} \ . \tag{4.44}$$

Once we properly perform the tensor reduction the seagull and rainbow diagrams acquire pre-factors $(3/2)(p^2\eta^{\mu\nu} - p^\mu p^\nu)$ with opposite signs, and the sum of (4.43) and (4.44) becomes independent of Λ_{UV} and hence finite.

It is instructive as well to consider the same integrals for the quadratic approximation. For the seagull we find

$$\Pi_S^{\text{quadratic}} \sim \frac{\Lambda_T^{n+2}}{(n+2)} \sinh^{-1} \frac{\Lambda_{\text{UV}}^{n+2}}{2\Lambda_T^{n+2}} \ . \tag{4.45}$$

We obtain the term in Λ_{UV} by expanding (4.45), finding the same leading logarithmic dependence on Λ_{UV} as in the quenched case. The rainbow we evaluate using the techniques described above, and when summed with (4.45) the result is again finite. Had either of these computations provided sub-leading divergences of any type, we would not have a sufficiently regulated theory, so the fact that the only divergences are logarithmic serves as evidence of finiteness at one-loop. We have not mentioned terms in the amplitude proportional to the m_V^2 and m_V^4. By power counting the later cannot produce a divergence, while the former can at worst admit a term proportional to $p \cdot k$ and not k^2. This can be seen by examining the momentum structure of the vertices. These terms are individually finite in asymptotically safe gravity.

The lack of sensitivity to Λ_{UV} in the self energy amplitude is of course only valid for the DeDonder gauge and will not be true for any other choice. However, also in a less appropriate gauge any physical observable must be independent

of $\Lambda_{\rm UV}$. To emphasize this point we outline the related computation in unitary gauge. The amplitude for the seagull diagram is

$$\Pi^{\mu\nu}_{S\,(\text{unitary})} = \frac{32\pi}{M_*^{2+n}} \int \frac{d^{4+n}q}{(2\pi)^{4+n}}\, \Delta_G\, \left(p^2\eta^{\mu\nu} - p^\mu p^\nu\right) \times \left(\frac{3}{2} - \frac{3}{4}\frac{k^2}{k_T^2} + \frac{1}{16}\frac{k^4}{k_T^4}\right) , \tag{4.46}$$

with a similar, albeit lengthy, expression for the rainbow. There are no higher UV divergences since upon substitution as described in the following sections the additional terms are proportional only to the ratio of the angular parts, with no q dependence. However, the cancellation of the additional logarithmic terms must also be checked. For genuine physical observables, such as the one presented later in Chapter 5, this cancellation does indeed take place and the result is finite.

Warm-up in $2+1$ dimensions

To illustrate the geometrical picture of our loop integral we consider the same integral with a (Euclidean) 2 dimensional brane and a single extra dimension. In momentum space we can easily picture the integral over brane and bulk momenta as a three dimensional integral in terms of spherical polar coordinates. For a rainbow like diagram we have

$$\begin{aligned}\Pi_{2+1}(p^2) &= \int d^3q\, \frac{1}{q^2}\frac{k_2^2}{(k_2+p)^2+m_V^2} \\ &= \int dq\, q^2 \int_0^\pi d\theta \sin\theta \int_0^{2\pi} d\phi \\ &\quad \frac{1}{q^2}\frac{q^2\sin^2\theta}{q^2\sin^2\theta + 2|p||q|\sin\theta\cos\phi + p^2 + m_V^2} ,\end{aligned} \tag{4.47}$$

where we denote the 2-dimensional brane analogy of the full momentum by k_2. The spherical coordinates we orient such that p is located at $\phi = 0$ and the dot product occurs between the brane projection $|q|\sin\theta$ with the brane external momentum p. This integral is evaluated numerically, or in this simple case analytically over the angular coordinates. The full result in $(4+n)$ dimensions is merely a higher dimensional generalization of (4.47).

Bulk Polar Coordinates

Explicitly the variable change we make is

$$\begin{aligned}
q^2 &= \bar{k}_1^2 + \cdots + \bar{k}_n^2 + k_0^2 + k_1^2 + k_2^2 + k_3^2 \\
\bar{k}_1 &= |q| \cos\phi_1 \\
\bar{k}_2 &= |q| \sin\phi_1 \cos\phi_2 \\
&\vdots \\
\bar{k}_n &= |q| \sin\phi_1 \sin\phi_2 \cdots \cos\phi_n \\
k_0 &= |q| \sin\phi_1 \sin\phi_2 \cdots \sin\phi_n \cos\phi_{n+1} \\
k_1 &= |q| \sin\phi_1 \sin\phi_2 \cdots \sin\phi_n \sin\phi_{n+1} \cos\phi_{n+2} \\
k_2 &= |q| \sin\phi_1 \sin\phi_2 \cdots \sin\phi_n \sin\phi_{n+1} \sin\phi_{n+2} \cos\phi_{n+3} \\
k_3 &= |q| \sin\phi_1 \sin\phi_2 \cdots \sin\phi_n \sin\phi_{n+1} \sin\phi_{n+2} \sin\phi_{n+3}
\end{aligned}$$

In Euclidean space we are free to orient these coordinates in the unconventional way where the $\phi_i = 0$ momenta are orthogonal to the brane. The virtue of taking these momentum space coordinates is that the brane-confined 4-momentum squared is

$$\begin{aligned}
k^2 = k_0^2 + k_1^2 + k_2^2 + k_3^2 &= q^2 \sin^2\phi_1 \sin^2\phi_2 \cdots \sin^2\phi_n \\
&\equiv q^2\phi^2.
\end{aligned} \tag{4.48}$$

For completeness we also list the form of the transverse momentum coordinates.

$$\begin{aligned}
\bar{k}_T^2 &= q^2 \left(\cos^2\phi_1 + \sin^2\phi_1 \cos^2\phi_2 + \cdots + \sin^2\phi_1 \cdots \sin^2\phi_{n-1} \cos^2\phi_n\right) \\
&\equiv q^2 \bar{\varphi}
\end{aligned} \tag{4.49}$$

We can now deduce the effects of using the unitary gauge. There is no UV enhancement as the q dependence cancels and the only difference is terms of the form $k^2/\bar{k}_T^2 = \varphi/\bar{\varphi}$. Now how do the spurious IR divergences present themselves here. For $\phi_i \to \pi/2$ this expression becomes singular and we have exactly the case which we expect; an IR divergence as we approach a 4-dimensional massless graviton.

Result in $4+n$ dimensions

Having established the finiteness of our computation in both the quenched and quadratic approximation, we can numerically evaluate the rainbow and seagull diagrams. It is clear at this point that we would like to perform the $(4+n)$-dimensional momentum integral over a radial coordinate $|q|$, but the loop momentum in the gauge boson propagator depends on only the brane projection of $|q|$. Thus our integral in $(4+n)$ dimensions must retain some angular dependence as the bulk and brane momentum are not interchangeable in the rainbow diagram.

A straightforward solution is to define a $(4+n)$ dimensional Euclidean vector $q = (k_T, k_4)$ in polar coordinates. Treating the brane momentum as the last entries in this $(4+n)$-vector allows us to make the variable change $k_4^2 + k_T^2 \equiv q^2$ which in turn requires the projection

$$k_4^2 \equiv q^2 \sin^2\phi_1 \sin^2\phi_2 \cdots \sin^2\phi_n \equiv q^2\chi^2 \,, \tag{4.50}$$

where the last step is simply a shorthand notation. The physical interpretation of the angular variables should be clear as they measure the 4-dimensional projection of q. The configuration with all $\phi_i = \pi/2$ corresponds to momenta confined to the brane, and the corresponding integral is the conventional 4-dimensional case. This simplifies our loop integrals and is easily evaluated numerically. Under the coordinate change the measure in our $(4+n)$-dimensional loop integration should be replaced as

$$\int \frac{d^{4+n}q}{(2\pi)^{4+n}} = \frac{\pi}{(2\pi)^{4+n}} \int dq\, q^{3+n} \int_0^\pi d\phi_1 \sin^{2+n}\phi_1 \cdots \int_0^\pi d\phi_n \sin^3\phi_n \int_0^{2\pi} d\phi_{3+n}. \tag{4.51}$$

The pre-factor π in front is the result of integrating over the 2-additional brane angular coordinates ϕ_{1+n} and ϕ_{2+n} which our amplitude does not depend on. For the angular measure related to χ we write $\int d\chi$, so the basis integrals from (4.40) with the renormalization group improved scalar propagator become

$$\tilde{A}_0 = \frac{2}{(2\pi)^{4+n}} \frac{\pi^{n/2+2}}{\Gamma[n/2+2]} \int dq\, q^{n+1} Z^{-1} \tag{4.52}$$

$$\tilde{B}_0 = \frac{\pi}{(2\pi)^{4+n}} \int dq\, q^{3+n} \int d\chi \int_0^{2\pi} d\phi_{3+n} \frac{Z^{-1}}{q^2} \frac{1}{q^2\chi^2 + 2|p||q|\cos\phi_{3+n}\chi + (p^2 + m_V^2)} \tag{4.53}$$

$$p^2\tilde{B}_1 = \frac{\pi}{(2\pi)^{4+n}} \int dq\, q^{3+n} \int d\chi \int_0^{2\pi} d\phi_{3+n} \frac{Z^{-1}}{q^2} \frac{|p||q|\cos\phi_{3+n}}{q^2\chi + 2|p||q|\cos\phi_{3+n} + (p^2 + m_V^2)\chi^{-1}} \tag{4.54}$$

$$p^2\tilde{B}_2 = \frac{\pi}{(2\pi)^{4+n}} \int dq\, q^{3+n} \int d\chi \int_0^{2\pi} d\phi_{3+n} \frac{Z^{-1}}{q^2 + 2|p||q|\cos\phi_{3+n}\chi^{-1} + (p^2 + m_V^2)\chi^{-2}} \tag{4.55}$$

Even though these expression are somewhat lengthy, the crucial point is that they are one-dimensional and without singularities. We can numerically compute the gauge bosons self energies in (4.35) and (4.42). The sum of the two integrals does not depend on $\Lambda_{\rm UV}$. In the next chapter we will see how this method of computing the KK integral compares with an effective theory analysis.

4.4 Conclusions

In this chapter we computed the UV complete KK integral using the fixed point consistent with asymptotic safety. We applied this first to single graviton exchange for collider energies below M_*. Therefore we neglect diagrams with for example two virtual gravitons in the intermediate state which in some way or another will eventually lead to black hole formation [100].

The KK integral was found to be finite without any additional UV regulation. For the one-loop computation we found that similarly the KK integral and loop integral could be performed to all energies without a UV cutoff. The technical aspect of this calculation led to a new method for tensor reduction, which allowed a convenient handling of the brane and bulk momentum.

We add here for completeness that there are of course completely unrelated

theories of quantum gravity or approximations which offer solutions to the cut-off dependence of the KK integral. In string theory, instead of gravitons in low scale extra dimensions, the dominant new physics contribution to virtual processes comes from higher string excitations [85][101]. The scattering mediated by these new states is well-described and obeys perturbative unitarity by virtue of an exponential suppression above the string scale $M_S \sim M_*$. There are a number of effective-theory proposals which side-step this complication by defining the integral in a cutoff independent scheme. One such treatment relates to the eikonal approximation to the $2 \to 2$ process [102], another involves introducing a finite brane thickness [103]. In this example, the gravitational coupling is exponentially suppressed above M_* by a brane rebound effect. However, neither of these models offer a compelling UV completion for the KK effective theory.

Chapter 5

Phenomenology

5.1 Introduction

In this section we analyze the experimental consequences of the previous chapter. We consider first LHC collider signatures based on virtual graviton exchange. Then we compute the contribution to an electroweak precision parameter arising from massive graviton loops. In both case we implement asymptotic safety at the level of the wave-function renormalization.

5.2 Virtual gravitons at the LHC

The LHC has several on-going searches for extra-dimensions (for recent publications see [104][105]). These include real graviton emission, black-hole production and virtual graviton exchange. Real emission searches are generally well-defined, and have little sensitivity to Planck scale physics at sub-Planckian collider energies. Similarly, black-hole production only becomes relevant at center-of-mass energies above the Planck scale. Virtual graviton exchange probes the quantum gravity effects in the ultraviolet range of the Kaluza-Klein spectrum. This makes this production process the prime candidate to test different descriptions of quantum gravity in low-scale gravity models. Hence, we apply our findings from the previous sections to gravitational processes at the LHC.

5.2.1 Kinematics and cuts

The generic prediction for virtual graviton exchange at the LHC is an enhancement of rates at increasing invariant masses. This does not include a mass peak or any kind of side-bin analysis, which means we must test the Standard-Model-only hypothesis as well as the Standard-Model-plus-graviton hypothesis on the kinematic distributions of the Drell-Yan process [19][20]. This signature may be further refined through the use of angular correlation techniques [91]. Our reference channel is $pp \to \mu^+\mu^-$ at $\sqrt{s} = 14$ TeV but other channels will show similar behavior. For the di-muon final state one advantage from the theory point of view is that we need only consider s-channel diagrams. The benefit here is that we define $\mathcal{S}(s)$ for the KK propagator depending only on s and not t/u. Based on the discussion in Sect. 4.2.7, we evaluate the relevant amplitudes in the Euclidean matching.

As model parameter we consider 2-6 extra dimensions and fix the fundamental Planck scale to $M_* = 5$ TeV. The experimental cuts which we apply throughout the section to take into account detector features are

$$p_{T,\mu} > 50 \text{ GeV}, \qquad |\eta_\mu| < 2.5. \tag{5.1}$$

where $p_{T,\mu}$ is the transverse momentum of the muon with respect to the beam pipe and $\eta_\mu = (1/2)\log(E + p_z)/(E - p_z)$ is the rapidity. The detection efficiency for muons we assume to be 100%, including triggering, as well as the energy resolution. Whenever we compare signal and background rates we require $m_{\mu\mu} > M_*/3$ to enhance the graviton signal over the Standard Model backgrounds. Combined with the cuts in (5.1) this suppresses the highly IR peaked photon and Z backgrounds which generically fall off with the partonic center-of-mass energy fast. As said above, the idea of this section is not to present a comprehensive LHC analysis, but to test our results for the behavior of the graviton KK integral at the level of LHC signals.

5.2.2 LHC signatures of the fixed point

We first compare LHC predictions from fixed point gravity with those from effective theory with the amplitude given by (4.14) [1]. We compare the total cross section from fixed point gravity using Z^{-1} from the quenched approximation

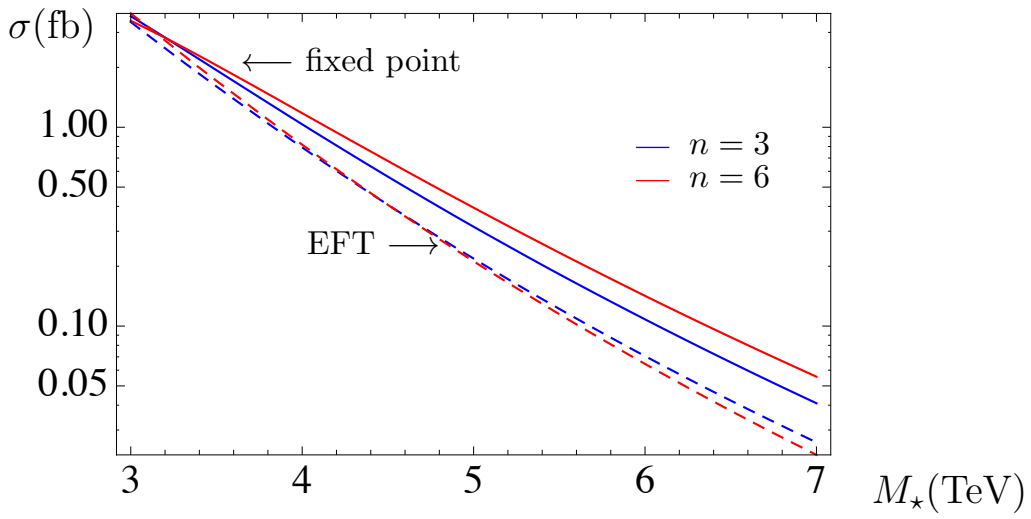

Figure 5.1: LHC total cross-section versus the fundamental scale of gravity M_* for events with $\sqrt{\hat{s}} < M_*$ for $n = 3$ (blue) and $n = 6$ (red) extra dimensions. Solid lines are asymptotically safe gravity and Dashed lines are effective theory. The difference in the total hadronic cross-section between the two persists even for higher M_*. From Ref. [1].

(4.11) with the predictions from effective theory with UV cutoffs at $m = \Lambda_T$ and at $\Lambda_s = M_*$, which we implement as $Z_{\rm eff}^{-1} = \theta(\Lambda_T - m_{\rm KK})\,\theta(M_* - \sqrt{s})$. The result is displayed in Fig. 5.1 for $\Lambda_T = M_*$. Dashed lines denote the result from effective theory, full lines stand for fixed point gravity. This figure shows that the difference between an effective theory and fixed point gravity description does not disappear as we raise the fundamental scale of gravity. We expect this based on the UV sensitivity of the KK integral. Furthermore, we see an overall enhancement of the signal for reasonable values of M_*.

This last fact is not *a priori* obvious. In effective theory the KK integral is cut-off separately in the KK mass $m_{\rm KK} < \Lambda_T$ and the graviton 4-momentum $\sqrt{s} < \Lambda_T$, and thus (after an analytic continuation) may include modes with $\sqrt{m_{\rm KK}^2 + s} > \Lambda_T$. The region outside this circle is suppressed by UV effects in our framework. On the other hand, modes with $\max(\sqrt{s}, m_{\rm KK}) > \Lambda_T$ are not included in the effective theory computation, while these modes will contribute in our computation albeit with the UV suppression provided by asymptotic safety. The answer however provided by (4.14) is that it is the UV modes in asymptotic safety which win and provide the bigger cross-section.

σ[fb]	$n=3$		$n=6$	
M_*[TeV]	5	8	5	8
a)	0.317	0.015	0.393	0.020
b)	0.320	0.015	0.394	0.020
c)	0.215	0.009	0.209	0.007
d)	0.182	0.009	0.190	0.007

Table 5.1: Comparison of total cross-sections for di-muon production via virtual graviton exchange at the LHC in different approximations. a) fixed point gravity with $\Lambda_T = M_*$, cutoff in $\sqrt{s}$ at $\Lambda_s = M_*$ b) fixed point gravity with $\Lambda_T = M_*$ (no cutoff in $\sqrt{s}$) c) effective theory with UV cut-off in both $m_{\rm KK}$ and $\sqrt{s}$ at $\Lambda = M_*$, d) form factor approximation with cutoff at $\Lambda = M_*$. From Ref [1].

In Tab. 5.1 we compare the production cross-sections in various approximations for $M_* = \Lambda_T = 5\,\text{TeV}$. For the UV contributions arising from KK modes, comparing fixed point gravity a,b) with effective theory c), we find an increase in the total rate. On the other hand, including the UV events in $\sqrt{s}$ by comparing a) with b) we find only a modest increase. Evidently, the $1/s^2$ behavior for large energies and the rapidly falling parton distribution functions makes these contributions sub-leading. The form factor approximation d) comes out below the effective theory estimate c), introducing a modest extra reduction of overall rates with energy slightly below M_*. Provided the cross-over scale takes the larger value $M_* = 8\,\text{TeV}$, we find that the LHC is only very weakly sensitive to the UV KK modes, leaving no difference between a) and b), and c) and d), respectively. Still, the difference between $a), b)$ and $c), d)$ persists, also evident from Fig. 5.1.

Next we compare the results from fixed point gravity using the linear (4.9), quadratic (4.10) and quenched (4.11) forms of the RG running, at fixed transition scale Λ_T. The variation of results under changes in the RG running allow an estimate for the 'RG scheme dependence' in the present set-up. We expect weak scheme dependence for the s-dependent amplitudes. In order to verify this we present in Fig. 5.2 and Fig. 5.3 LHC distribution for $n = 3$ and $n = 6$ extra-dimensions, respectively, for several values of the transition scale Λ_T. The variation is minute at the low-end of the spectrum but increases at higher energies. We expect this because the matching condition applies to the $s = 0$ low-energy coefficients. In all cases the uncertainty due to the scheme is smaller than uncertainties coming from QCD effects, conservatively estimated at

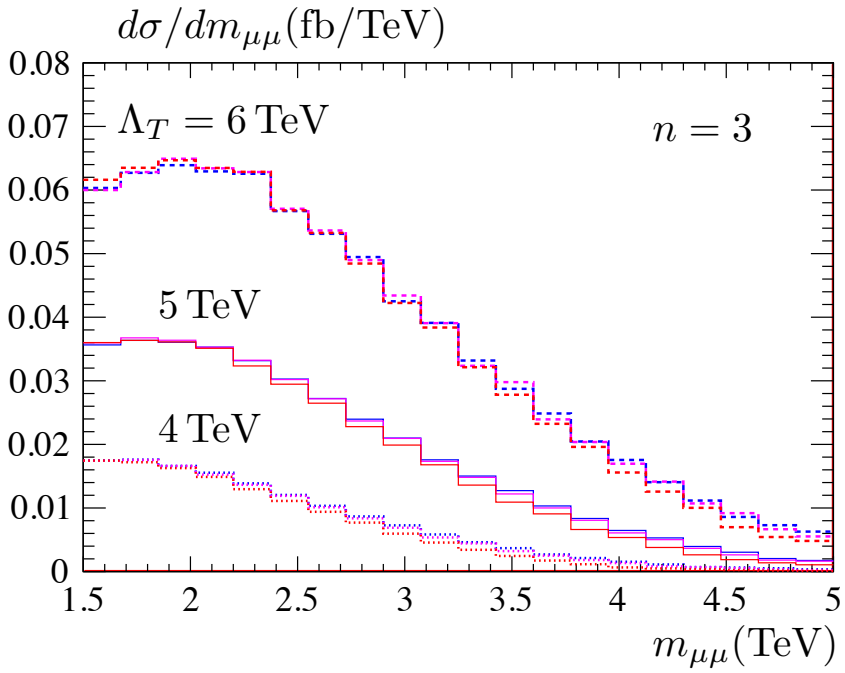

Figure 5.2: Signal distribution for di-muon production via virtual graviton exchange at the LHC with $M_* = 5$ TeV and $n = 3$ (6) extra dimensions show left (right). Comparison of several RG schemes and transition scales Λ_T: quenched (red lines), linear (blue), and quadratic (magenta) approximation with $\Lambda_T/M_* = 1.2$ (dotted lines), $\Lambda_T/M_* = 1$ (full), and $\Lambda_T/M_* = 0.8$ (dashed). With increasing Λ_T/M_*, the di-muon production rate increases. The scheme dependence is small. From Ref. [1].

$\sim 15\%$ here.

A second point illustrated in Fig. 5.4 and Fig. 5.5 is that the total rates depend strongly on the transition scale Λ_T. This is especially true for higher n, as pointed out in Sect. 4.2.3, and illustrated in the $n = 6$ plot. The reason for this is that the suppression of amplitudes due to the gravitational fixed point sets in at about Λ_T, leading to larger rates for larger Λ_T. However, the s-dependence in the signal is mostly independent of Λ_T. Therefore, in the next section we study also the normalized distributions in order to obtain a handle on the signals.

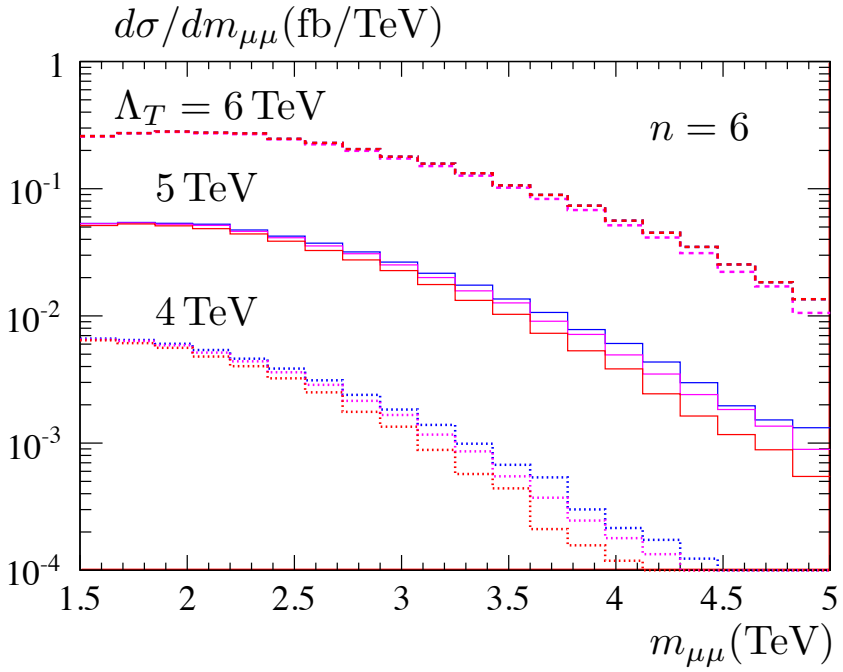

Figure 5.3: Same as FIg. 5.2 but for $n = 6$. From Ref. [1].

5.2.3 LHC Phenomenology

In this section, we discuss signatures of asymptotically safe gravity and large extra dimensions at the LHC. If not stated otherwise, we set $M_* = \Lambda_T = 5\,\text{TeV}$ and examine distributions with respect to $m_{\mu\mu}$, the invariant mass of the produced di-muon pair. We also compare our results, and in particular the $m_{\mu\mu}$-dependence, with those from effective field theory [19, 23, 93], the form-factor approximation [53], and the Standard Model background.

In Fig. 5.4 and Fig. 5.5 we compute normalized and un-normalized differential cross sections for $M_* = 5$ TeV and $\Lambda_T = M_*$ for $n = 2, 3, 6$ extra dimensions respectively. Again, we contrast fixed point gravity results with those from effective theory. Comparing the full $\sqrt{s}$-dependence from a) asymptotically safe gravity with b) effective theory (full versus dashed colored lines), we note that they essentially agree for $n = 2$. The reason for this is that the perturbative amplitude is only logarithmically divergent. For $n = 3$ and $n = 6$ the decay of the differential cross section with invariant mass becomes more pronounced within fixed point gravity. Here, the difference is due to the UV divergence of

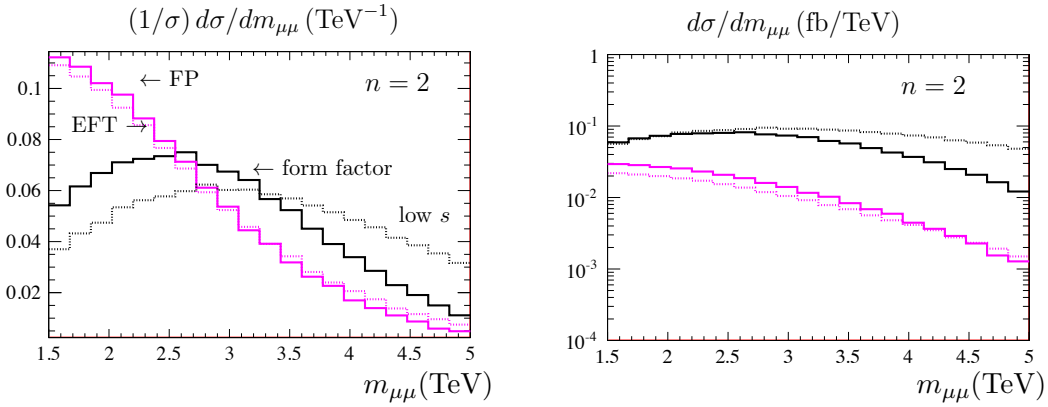

Figure 5.4: Normalized differential cross sections $(1/\sigma)\, d\sigma/dm_{\mu\mu}$ (left column) and un-normalized ones $d\sigma/dm_{\mu\mu}$ (right column) for gravitational di-muon production at the LHC for $n = 2$ with $M_* = 5$ TeV and cross-over scale $\Lambda_T = 5$ TeV. a) fixed point gravity (FP) with full s-dependence (full magenta/blue/red lines); b) fixed point gravity in the form factor approximation with UV cutoff at $m = \Lambda_T$ (full black lines); c) effective theory (EFT) with UV cutoff at Λ_T (dotted magenta/blue/red lines); d) effective theory in the $s = 0$ approximation (low s) and UV cutoff at Λ_T (dotted grey lines). From Ref. [1].

the perturbative amplitude. Note in particular that with increasing number of extra dimensions n, the difference between a) and b) grows. Turning to the low-s approaches, we note that the differential cross section decays more slowly within the form-factor approximation c) (full black lines) for all n. This comes about because a dynamical suppression with energy sets in only close to $\sqrt{s} \approx \Lambda_T$, unlike a). Also, the form-factor approximation c) deviates from the effective theory approximation (with $s = 0$) d) only close to Λ_T. Overall, we see that fixed point gravity falls off most quickly with increasing energy $\sqrt{s}$. Technically, this results from the powers of s in the denominator of the RG improved KK sum, not present in the lowest dimensional operator from effective theory.

In Fig. 5.6 we present for the first time a comparison of our data including the SM background from (4.32) and (4.33). For larger values of $m_{\mu\mu} \sim M_*/2$ signal to background S/B becomes of order 1. Note that the cross section for $n = 2, 3$ and $n = 6$ are very close to each other. This near-degeneracy is a consequence of our choice $\Lambda_T = M_*$, which is lifted as soon as $\Lambda_T \neq M_*$, see Fig. 4.3. In view of perturbative unitarity, our calculations in (4.25) and the behavior in Fig. 5.4-**??** indicate a clear improvement over effective theory.

Phenomenologically, for the LHC we now know that the on-set of fixed point

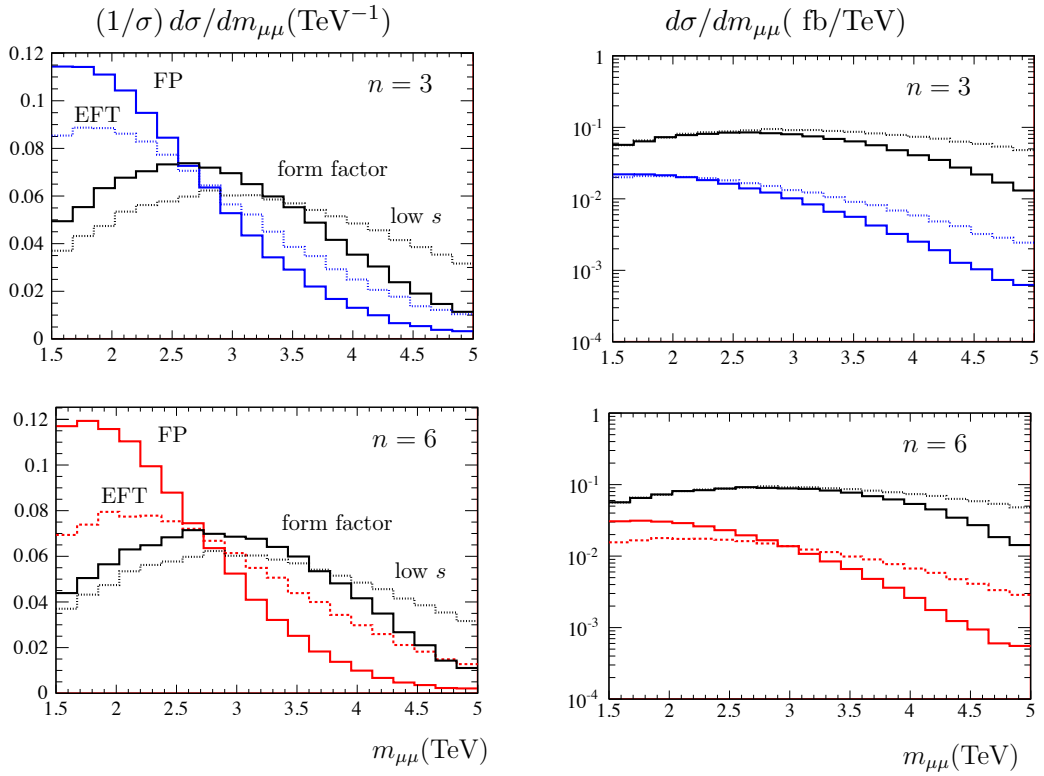

Figure 5.5: Same as Fig. 5.4 with $n = 3$ (top) and $n = 6$ (bottom). From Ref. [1].

scaling should be distinguishable from effective field theory descriptions. Turning this argument around, the ad hoc assumption of an effective field theory is not well suited to analyze LHC data which should be expected to strongly depend on ultraviolet effects. This is even more obvious for string theory signatures [101][85] with their peak structure dictated by the Veneziano amplitude. Therefore, the two existing descriptions of quantum gravity at the LHC, fixed point gravity and string theory could not look more different in their predictions for the $m_{\mu\mu}$ distribution. Fig. 5.6 provides a realistic signature for asymptotic safety. Moreover, the differential cross section as a function of $m_{\mu\mu}$ can be used to distinguish our effect uniquely and study in some detail the transition from the classical to the quantum gravity regime. Although the cross-sections can be small, with 1000 fb^{-1} at 14TeV it is entirely possible to delineate such a distribution.

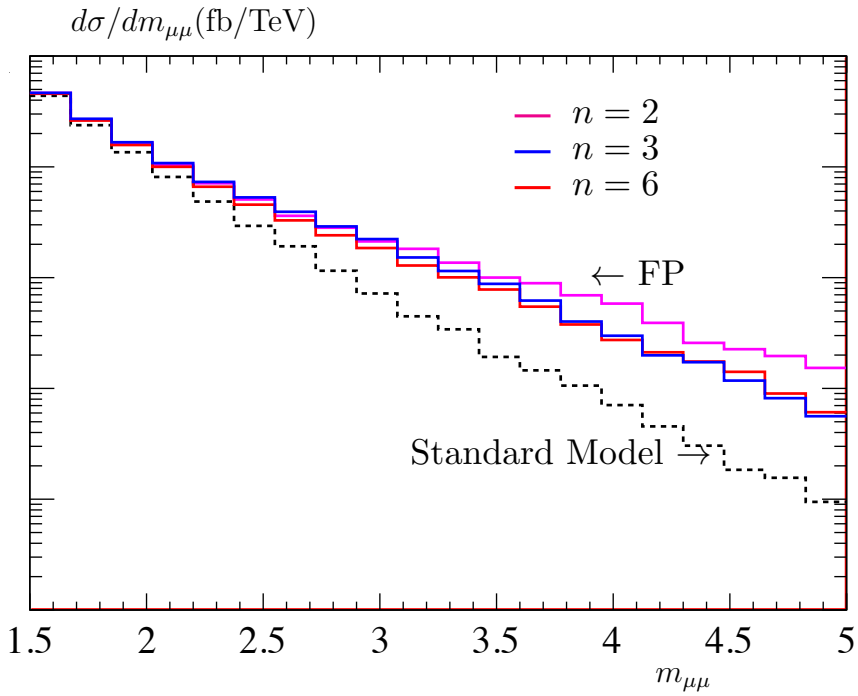

Figure 5.6: Differential cross-sections (in fb/TeV) for di-muon production within fixed point gravity (FP) for $n = 2$ (magenta), $n = 3$ (blue) and $n = 6$ (red) extra dimensions, in comparison with Standard Model background (black dashed line). From Ref. [1].

5.3 Electroweak Precision Constraints

We now discuss indirect constraints on asymptotic safety, based on measurments mostly at high luminosity e^+e^- colliders. In order to constrain new physics based on precision measurements it is typical to use either the oblique parameter set $\{S, T, U\}$ [82] or the ϵ parameterization [106]. However, the former are not well suited for gravitons, which in general will modify more than just gauge boson self-energies. The later can be related to the weak mixing angle s_0, c_0 to define the leading corrections

$$\rho - 1 \simeq \bar{\epsilon} = \epsilon_1 - \epsilon_2 - \frac{s_0^2}{c_0^2}\epsilon_3 \,, \tag{5.2}$$

quantifying the violation of custodial symmetry [107, 108]. The individual observables ϵ_1, ϵ_2 and ϵ_3 in the context of gravity require additional computations

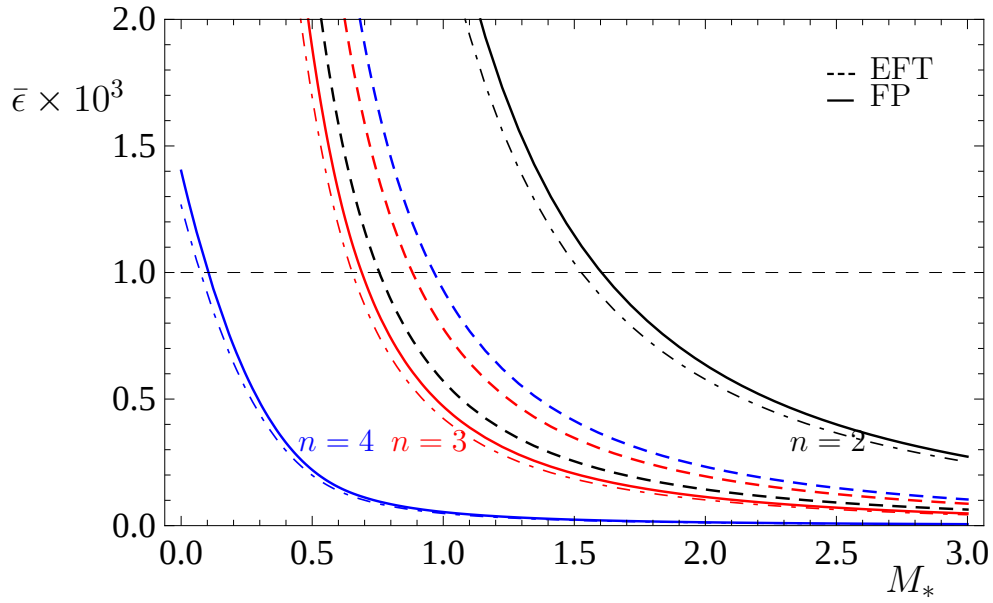

Figure 5.7: Contribution to $\bar{\epsilon} \simeq 1 - \rho$ from extra dimensions computed in asymptotically safe gravity in linear (4.9) (dot-dashed), quadratic (4.10) (solid) and in effective theory (dashed) from Ref. [7]. Values above the dashed horizontal curve are in tension with data. For all asymptotic safety curves we have taken $M_* = \Lambda_T$. From Ref. [2].

beyond the self-energies, but the specific linear combination

$$\bar{\epsilon} = \frac{\Pi(m_W^2)}{m_W^2} - \frac{\Pi(m_Z^2)}{m_Z^2} \tag{5.3}$$

has to be smaller than roughly 10^{-3}, assuming a light Standard Model Higgs boson [109]. The exact central value depends on the Higgs mass, but the uncertainty of $\bar{\epsilon}$ also ranges around 10^{-3}. We treat this value a generic upper bound on new physics effects. The effective theory result for gravity contributions from Ref. [7] in our notation reads

$$\Delta\rho \simeq \Delta\bar{\epsilon} = \frac{s^2 m_Z^2}{M_*^2} \left(\frac{\Lambda_{\text{eft}}}{M_*}\right)^n \frac{1}{\Gamma(2+n/2)} \frac{5(8+5n)}{48\pi^{2-n/2}} , \tag{5.4}$$

for $m_{\text{KK}} \gg m_Z$. Here, Λ_{eft} is the effective theory cut-off scale. In Figure 5.7 we compare this result to our computation as described in the previous chapter. The numerical results are similar for $n = 3$, where fundamental Planck masses below $M_* \lesssim 1$ TeV are forbidden. In asymptotically safe gravity the limits are

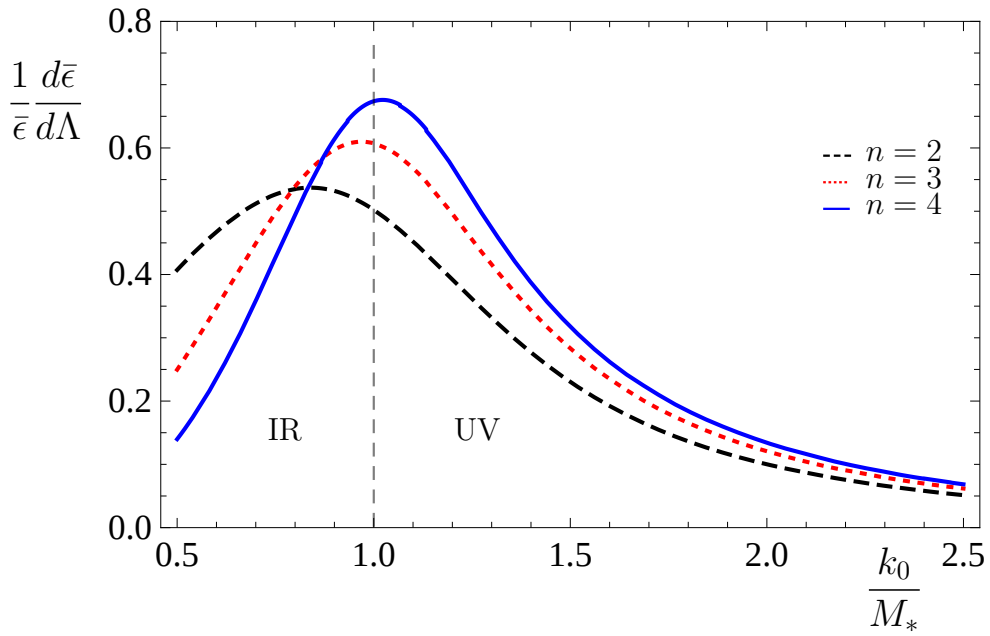

Figure 5.8: Contribution to $\bar{\epsilon}$ as a function of the highest momentum mode $q < k_0$ in the $(4 + n)$-dimensional integration. We see the approximate pattern of Eq. (5.5) in the ratio of IR to UV contributions. From Ref. [2].

significantly weakened when we increase the number of extra dimensions, which is not the case for the effective theory computation in Eq. (5.4). In other words, once we take the higher dimensional quantum effects seriously there are essentially no limits on large extra dimensions with $n > 3$ from electroweak precision data.

The explanation for this discrepancy is the following: in effective theory, the amplitudes are dominated by modes with both k and $m_{\rm KK}$ near the cut-off, *i.e.* in the corner of a square in the k vs $m_{\rm KK}$ plane. However, in our picture of asymptotic safety with $|\mu| = \sqrt{k^2 + m_{\rm KK}^2}$ this region is outside the central circle which means it is suppressed. For higher numbers of extra dimensions this effect is more pronounced, as shown by the lessening contribution to $\bar{\epsilon}$ as n increases.

To confirm our observation of an increasing impact from the UV regime we need to study the distribution of the momentum modes contributing to $\bar{\epsilon}$. More specifically, we would like to know the size of the contribution to the observable for UV momentum modes with $|q| > \Lambda_T$. In the quenched approximation we can easily estimate this fraction. Neglecting terms of order m_V/Λ_T the leading

momentum integrals are of the form

$$\begin{aligned}\bar{\epsilon}\Big|_{\rm IR} &\sim \int_0^{\Lambda_T} dq\; q^{3+n}\; \frac{1}{q^2}\; \frac{1}{q^2+\cdots} \approx \frac{\Lambda_T^n}{n} \\ \bar{\epsilon}\Big|_{\rm UV} &\sim \int_{\Lambda_T}^{\infty} dq\; q^{3+n}\; \frac{\Lambda_T^{2+n}}{q^{4+n}}\; \frac{1}{q^2+\cdots} \approx \frac{\Lambda_T^n}{2}\;. \end{aligned} \tag{5.5}$$

This expansion in m_V/Λ_T is well validated, for example compared with LHC tree level virtual graviton exchange where $\sqrt{s}/\Lambda_T$ can easily become $\mathcal{O}(1)$. For $n = 2$ approximately 50% of the combined integral comes from the quantum gravity regime, and for a larger number of extra dimensions this fraction increases. Numerically, Fig. 5.8 shows that the exact results follow the pattern delineated in (5.5). The UV region becomes the dominant contribution already for $n > 2$ extra dimensions.

This can be contrasted with the case of LHC tree level graviton exchange in the previous section, where in a similar limit the UV graviton contribution becomes dominant only for $n > 6$ [95]. This is not surprising though as the integral in the tree-level exchange is over four less directions in momentum space, and thus we see the rough equivalence of the $n = 6$ case in tree-level with the $n = 2$ case at one-loop.

5.4 Conclusions

In this chapter we quantified observable consequences of asymptotic safety. First we found that at the level of the cross-section, the LHC signal may be dominated by the fixed point regime of gravity even for collider energies below M_*. Moreover, the total cross-section while not depending largely on the scheme, does in fact depend greatly on the scale Λ_T. For this purpose we considered normalized distributions and found that the scaling with $\sqrt{s}$ depends the scale identification. We looked at the form-factor $\sqrt{s}$, low energy $m_{\rm KK}$ and D-dimensiona $s + m_{\rm KK}$ matching and found the later to be the most appealing. Note that the D-dimensional scheme is equivalent to the virtuality matching for $n = 2$ and $n = 6$ extra dimensions provided that we abandon the pole terms. Most importantly, we found that the kinematic distribution with respect to invariant mass in the di-muon channel, behaves very differently compared with effective field theory.

This is the strategy currently used by LHC experimentalists to exclude large extra dimensions.

By computing the contribution to the $\bar{\epsilon}$ parameter we found significantly weakened constraints on higher numbers of extra dimensions. The explanation given in terms of regions in the $\sqrt{s}$ versus m_{KK} plane also applies to the results of the total cross-section, for example depicted in Fig. 5.1. An additional contrast between the tree-level and one-loop result is depicted in Fig. 5.8, namely that the amplitude becomes UV dominated already in $n > 2$ extra dimensions.

Chapter 6

Conclusions

In this thesis we explored the possibility of asymptotic safety existing in large extra dimensional scenarios where the fundamental scale of gravity is around the TeV. The motivation for this was primarily that that virtual gravitons in these models inevitably probe the UV regime of quantum gravity. Applying the effects of asymptotic safety though a running coupling and the resulting large anomalous dimension, we found that there are several possible choices for identifying the RG scale. The best choice was found to be the euclidean scale $\mu^2 = s + m_{\rm KK}^2$, and in cases where it could be evaluated analytically via contour integration, the virtuality matching $\mu^2 = |s - m_{\rm KK}^2|$. In LHC Drell-Yan production, these choices led to amplitudes behaving much differently than effective field theory and still show a sizable deviation from the standard model for the chosen model parameters, namely $M_* = 5\,\text{TeV}$. At the one-loop level we found stronger bounds on $n = 2$ models compared with effective field theory, and in general weakening bounds for higher n. However, there still remains some open questions and further directions which we now discuss.

On the experimental side, we did not present exclusion bounds based on the virtual graviton process at the LHC, but in principle this should be possible in a three-parameter fit for the number of extra dimension n, the transition scale Λ_T and the fundamental scale of gravity M_*. With the LHC running at full energy, we expect these bounds somewhere above the 10 TeV range. It would be interesting, though rather long and tedious, using likelihood methods to combine the results from all search channels, including real emission, into single exclusion bounds. Furthermore, the one-loop amplitude we computed provides a method

for evaluating general loop-integral involving KK gravitons. This can in principle be extended to many phenomenologically interesting applications, for example the muon $g-2$. In principle our methods should be applicable to all higher order effects.

Theoretically, there are still questions to be answered regarding the computation of the principle value of the KK integral in the virtuality matching in particular regarding the effect of a physical decay width. The sub-leading pole terms which grow as a function of energy in the $n = 6$ computation are still not fully understood, although perhaps the most remarkable result of the thesis is that in the linear approximation the virtuality matching factorizes into a pole terms plus the exact euclidean matched result. In the appendix we discuss one example of a 5-dimensional theory where the effect of the KK width can be understood analytically.

We did not consider the effects of asymptotic safety in warped scenarios. Although KK gravitons are generically observable in RS like realizations, the fundamental scale of gravity where naively quantum gravitational effects become relevant is still close to $M_{\rm Pl}$. Whether the "warping" down of the KK gravitons and other fields might nevertheless be sensitive to asymptotic safety like effects requires additional investigation. Similarly, another known low-scale gravity mechanism due to the RG running of a large number of additional (though strictly 4-dimensional) fields may be experimentally distinguishable from large extra dimensions for the following reason. In the 4-dimensional case the anomalous dimension at the UV fixed point would remain exactly -2 to all orders. It would be useful to add this insight to for example the study of Ref. [92]. On the more technical side, we only included the Einstein-Hilbert term in this work, and including the cosmological constant changes the running of g_N. We know from experimental results that this term should be included and its effects on the RG well studied. Nevertheless, it would be interesting to include the cosmological constant in the running of g_N and repeat our computations. FInally, we did not consider vertex corrections due to the fixed point. The influence of the fixed point on matter-graviton vertices was considered in some approximations in Ref. [49], but it is not clear how to implement this analysis in our framework.

Although there is currently no evidence for low scale extra dimensions, they continue to be an intriguing possibility for beyond the standard model physics. If

and when the LHC sees a non-resonant excess it will be very important to study the scaling behavior of this excess. In this thesis, we demonstrate a systematic way that asymptotic safety can be studied in this situation.

.1 Appendix

.1.1 Feynman rules and Amplitudes

Starting with the minimally coupled interaction Lagrangian

$$\mathcal{L} = \sqrt{-g}\left(i\bar{\psi}\gamma^{\mu}\mathcal{D}_{\mu}\psi - \frac{1}{4}g^{\mu\nu}g_{\alpha\beta}F_{\mu\alpha}F_{\nu\beta} + \frac{m_V^2}{2}g^{\mu\nu}V_{\mu}V_{\nu}\right). \tag{1}$$

we derive the vertices by first expanding out the metric to order h^2 in the graviton field. Defining the gravitational coupling constant $\kappa_D = 32\pi/M_*^{n+2}$ we have

$$(\sqrt{-g}g^{\mu\nu})_h = \kappa_D\left(-h^{\mu\nu} + \frac{1}{2}h\eta^{\mu\nu}\right) + \frac{\kappa_D^2}{2}\left(2h^{\mu\alpha}h^{\alpha\nu} - \frac{1}{2}h^{\alpha\beta}h_{\alpha\beta}\eta^{\mu\nu} - hh^{\mu\nu} + \frac{1}{4}h^2\eta^{\mu\nu}\right) \tag{2}$$

$$\begin{aligned}(\sqrt{-g}g^{\mu\nu}g^{\alpha\beta})_h = \kappa_D(-h_{\mu\nu}\eta_{\alpha\beta} - h_{\alpha\beta}\eta_{\mu\nu} + \frac{1}{2}h\eta_{\mu\nu}\eta_{\alpha\beta}) \; + \; \kappa_D^2\left(h_{\mu\nu}h_{\alpha\beta} + h_{\mu\gamma}h_{\gamma\nu}\eta_{\alpha\beta}\right.\\ \left. + h_{\alpha\gamma}h_{\gamma\beta}\eta_{\mu\nu} - \frac{1}{2}hh_{\mu\nu}\eta_{\alpha\beta} - \frac{1}{2}hh_{\alpha\beta}\eta_{\mu\nu} + \frac{1}{8}\eta_{\mu\nu}\eta_{\alpha\beta}\left(h^2 - 2h_{\sigma\rho}h_{\sigma\rho}\right)\right).\end{aligned} \tag{3}$$

In addition our weak field expansion in (3.19) implies that scalar component ϕ also couples to the 4-dimensional brane confined energy momentum tensor. Therefore we also require

$$(\sqrt{-g}g^{\mu\nu})_{\phi} = -\frac{\kappa_D}{2}\eta^{\mu\nu}\phi, \tag{4}$$

$$(\sqrt{-g}g^{\mu\nu}g^{\alpha\beta})_{\phi} = -\kappa_D\eta^{\mu\nu}\eta^{\alpha\beta}\phi + \frac{\kappa_D^2}{2}\eta^{\mu\nu}\eta^{\alpha\beta}\phi^2. \tag{5}$$

We will not write the fully expanded Lagrangian, but using the FORM [110] symbolic manipulation package it is a simple matter to derive the following vertices. We list only the terms proportional to the mass, as the others may be found in Ref. [111] for example. The relevant terms in the $VVhh$ and VVh

vertices are,

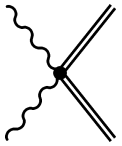

$$= \frac{m_V^2}{2}\kappa_D^2 \left(-\eta^{\mu\nu}\eta^{\alpha\beta}\eta^{\gamma\sigma} + \eta^{\mu\nu}\eta^{\alpha\gamma}\eta^{\beta\sigma} + \eta^{\mu\nu}\eta^{\alpha\sigma}\eta^{\beta\gamma}\right.$$
$$- \eta^{\mu\alpha}\eta^{\nu\beta}\eta^{\gamma\sigma} + \eta^{\mu\alpha}\eta^{\nu\gamma}\eta^{\beta\sigma} + \eta^{\mu\alpha}\eta^{\nu\sigma}\eta^{\beta\gamma} + \eta^{\mu\beta}\eta^{\nu\alpha}\eta^{\gamma\sigma} - 2\eta^{\mu\gamma}\eta^{\nu\alpha}\eta^{\beta\sigma}$$
$$\left.+\eta^{\mu\gamma}\eta^{\nu\beta}\eta^{\alpha\sigma} + \eta^{\mu\gamma}\eta^{\nu\sigma}\eta^{\alpha\beta} - 2\eta^{\mu\sigma}\eta^{\nu\alpha}\eta^{\beta\gamma} + \eta^{\mu\sigma}\eta^{\nu\beta}\eta^{\alpha\gamma} + \eta^{\mu\sigma}\eta^{\nu\gamma}\eta^{\alpha\beta}\right) \tag{6}$$

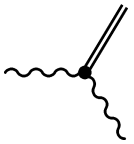

$$= \frac{m_V^2}{2}\kappa_D \left(\eta^{\mu\nu}\eta^{\alpha\beta} - \eta^{\mu\beta}\eta^{\nu\alpha} - \eta^{\mu\alpha}\eta^{\nu\beta}\right). \tag{7}$$

The final rule needed is the $f\bar{f}h$ vertex for massless fermions. Taken all momenta as incoming we have

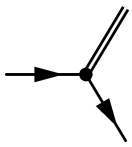

$$= \kappa_D \left[(k_1 - k_2)_\mu \gamma_\nu + (k_1 - k_2)_\nu \gamma_\mu\right]. \tag{8}$$

.1.2 KK Width

In order to justify the virtuality matching, we discuss the narrow-width assumption for KK gravitons. This aspect is independent of the UV sector, and also applies within standard effective theory. Using a Breit-Wigner propagator in the KK sum means we ignore interference between KK states. In terms of the KK mass splitting this requires

$$\delta_{\mathrm{KK}} \gg \Gamma, \tag{9}$$

for $m_{\mathrm{KK}} \sim \sqrt{s}$ where δ_{KK} is the spacing between consecutive KK modes. It is simple to compute the lowest order graviton decay width to Standard Model particles, as it appears in (9). This decay is suppressed by $1/M_{\mathrm{Pl}}^2$ since it occurs only on the brane. A calculation based on the Feynman rules given in Ref. [20]

yields

$$\begin{aligned}\Gamma_{\rm SM}(m_{\rm KK}) &= \gamma\gamma + gg + f\bar{f} + q\bar{q} + ZZ + W^+W^- + HH \\ &= \frac{m_{\rm KK}^3}{\bar{M}_P^2\pi}\left[\frac{1}{80} + 8\frac{1}{80} + 6\frac{1}{160} + 6\frac{3}{160} + \frac{13}{12}\left[\frac{1}{80} + \frac{1}{40}\right] + \frac{1}{480}\right] \\ &= \frac{293}{960\pi}\,\frac{m_{\rm KK}^3}{M_{\rm Pl}^2}\,. \end{aligned} \tag{10}$$

We may also consider on-shell decays of a single massive graviton to two other (less) massive gravitons. This contribution would produce a much larger decay width, suppressed only by factors of $1/M_*$. However, extra-dimensional momentum conservation persists as KK number conservation in the compactified theory (also the basis for dark matter in UED models [112]). The occupation vectors of all gravitons participating in an interaction must sum to zero at any vertex. When combined with energy momentum conservation $|\vec{n}_1|^2 > |\vec{n}_2|^2 + |\vec{n}_3|^2$, the on-shell decay amplitude vanishes for all graviton self interactions. In fact, the next contribution to the decay width will come from higher orders in the expanded action

$\Gamma \sim \mathrm{Im}\Big[$ 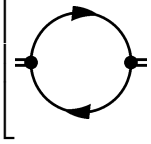 $+$ 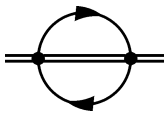 $+$ 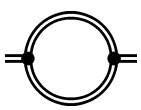 $+ \cdots \Big]$

$$\sim \quad \Big[\quad \frac{m_{\rm KK}^3}{M_{\rm Pl}^2} \quad + \quad \frac{m_{\rm KK}^3}{M_{\rm Pl}^2}\frac{m_{\rm KK}^{n+2}}{M_*^{n+2}} \quad + \quad 0 \quad + \cdots \Big], \tag{11}$$

based on power counting. We emphasize again the null contribution due to self-interactions. The second diagram includes a sum over the intermediate graviton as KK number is not conserved due to the matter coupling. Indeed, below M_* the graviton width is tiny, but at this scale the resummation quickly breaks down and the width in general exceeds the spacing. Therefore, we have little reason to extend our classical results in the pole region above the scale M_*. We emphasize that the gravitons contributing in this case probe IR physics. A rephrasing of this physical picture is that multi-graviton exchange such as the second diagram in (11) becomes relevant at the scale M_*. It is still possible to use perturbation

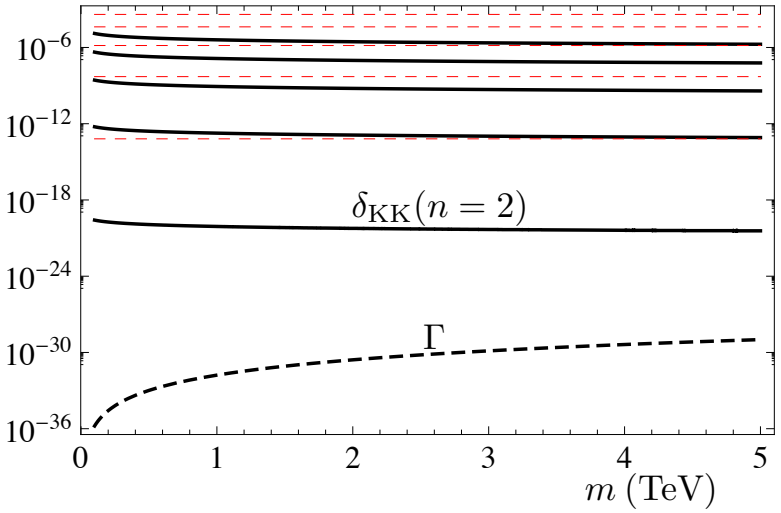

Figure 1: KK mass splitting $\delta_{\rm KK}$ (solid black) and the KK width Γ (dashed black) as a function of $m_{\rm KK}$, using $M_* = 5$ TeV. The red dashed curves indicate the spacing $1/R$. Starting from the bottom counting upwards we have $n = 2 - 6$. From Ref. [1].

theory in the pole region above Λ_T as long as we have a hierarchy $\Lambda_T < M_*$.

The KK mass spacing is often estimated using $\delta_{\rm KK} = 1/R$ [113]. We improve this estimate to assure that the narrow-width condition in (9) does not break down at scales significantly below M_*. To that end, we consider a state $\vec{n}_i$ where $\vec{n}_i^2 \equiv N$ is some integer. In general, there will exist another state $\vec{n}_{i-1}$ such that $\vec{n}_{i-1}^2 = N - 1$. If there is no state satisfying this relation then the spacing will be larger than our estimate, leaving intact (9). The integer N fixes $m_{\rm KK} = \sqrt{N}/R$ so that for two non-degenerate KK modes the spacing is at least

$$\delta_{\rm KK} \geq \frac{\sqrt{N} - \sqrt{N-1}}{R} = \left(\frac{(2\pi)^n M_*^{n+2}}{M_{\rm Pl}^2}\right)^{1/(2n)} \times \left[\sqrt{m_{\rm KK}} - \sqrt{m_{\rm KK} - \left(\frac{(2\pi)^n M_*^{n+2}}{M_{\rm Pl}^2}\right)^{1/n}}\,\right]. \quad (12)$$

We note that (12) is sensitive to the equality of the radii of the extra dimensions. For the case of unequal radii, the lower bound may be set by choosing the largest radius.

In Fig. 1 we see that this lower bound for the spacing is much larger than the

lowest order graviton width for any number of extra dimension $n \geq 2$ and for all energy scales relevant to LHC physics. For example, for $n = 2$ and $M_* = 5\,\text{TeV}$ we expect the lines to cross only around $m_{\text{KK}} \sim 1000$ TeV, far above the scale at which the leading order approximation width breaks down. For the LHC observables computed in the following, (12) confirms the hierarchy between the tiny KK width and the level spacing.

Although the spacing between modes is much larger than the width, we have not discussed how the decay width manifests itself in the KK sum. For this purpose it will prove useful to specialize to 5 dimensions. For a completely stable particle, the KK sum is performed explicitly and leads to equally spaced single particle poles as expected.

$$\sum \frac{1}{s - n^2/R^2} = \frac{\pi R \cot(\pi R\sqrt{s})}{\sqrt{s}} \tag{13}$$

The principle value integration over each particle pole is well defined in this sense as the analytically continued result is obtained from (13) by replacing the cotangent function with its hyperbolic counterpart.

Now if we add a Breit-Wigner decay width of the form icm^3/M_{Pl}^2 as in (10), the KK sum must be recomputed. After some trivial redefinitions the resulting sum is,

$$\mathcal{S}(s)_5 = \frac{R^2}{M_{\text{Pl}}^2} \sum_{n=1}^{\infty} \frac{1}{a^2 - n^2 + ibn^4} \tag{14}$$

where we define dimensionless variables $a = \sqrt{sR}$ and $b = c/(M_{\text{Pl}}^2 R)$. Physically, the last term in (14) resemble a damped oscillator with the critical damping condition given by a simple relation between a and b. We find that the exponentially damped oscillation persist up to the point $a_{\text{crit}} \sim b^{-1/3}$. In terms of the physical parameters this corresponds to $\sqrt{s}_{\text{crit}} \sim M_* c^{-1/3}$. Most importantly this number is independent of M_{Pl} even though M_{Pl} appears explicitly in $\Gamma(m_{\text{KK}})$. In other words, after summing over all modes the physical size of Γ has completely dropped out. To see this we evaluate (14) analytically. The full solution is lengthy

but the oscillatory behavior is contained in the term

$$\begin{aligned}\mathcal{S}(s)_5 &\sim \frac{b\cot\left[\frac{\pi}{\sqrt{2b}}\sqrt{i(\sqrt{1-4a^2b}-1}\right]}{\sqrt{i(\sqrt{1-4a^2b}-1}} \\ &\equiv \frac{b}{u}\cot\left[\frac{\pi}{\sqrt{2b}}u\right] \end{aligned} \tag{15}$$

Expanding out the term u for small a^2, and b not too large

$$u \equiv \sqrt{i(\sqrt{1-4a^2b}-1)} \approx \sqrt{2a^2b}\left(1+i\frac{a^2b}{2}+\cdots\right) \tag{16}$$

Now the squared amplitude $|\mathcal{S}(s)_5|^2$ is in fact the observable quantity we desire, so from (15) and (16) we have

$$\begin{aligned}|\mathcal{S}(s)_5|^2 &\sim \frac{e^{-2\pi a^3 b}+e^{\pi a^3 b}\cos 2\pi a+1}{e^{-2\pi a^3 b}-e^{\pi a^3 b}\cos 2\pi a+1} \\ &\approx \frac{1}{1-e^{-\pi a^3 b}\cos 2\pi a}. \end{aligned} \tag{17}$$

We see that the oscillating cosine term is exponentially damped. Moreover if we solve for example for the half life of the decay, we obtain the relation as previously stated that $a_{\text{crit}} \sim b^{-1/3}$.

Now taken at face value, the form of this propagator has three distinct regions. First for $\sqrt{s} < M_* c^{-1/3}$, there are large oscillations due to the insufficient dampening turn provided by the width. Next, for intermediate energies the principle value integral well approximates the damped oscillating term, and in this region our assumptions are well justified. Now at some energy, typically around but not exactly at M_* the geometric series needed to define the width in the propagator no longer convergences and more powerful techniques are needed. The propagator in this region naively behaves like $1/s^2$ here, but this prospect is never physically realized.

Finally, for higher numbers of extra dimensions we can no longer analytically compute the KK sum. Within a numerical implementation we find that there is no simple relation between the coefficient in the width and the damping, as now in general the position of $\sqrt{s}_{\text{crit}}$ depends on M_{Pl}, M_* and c.

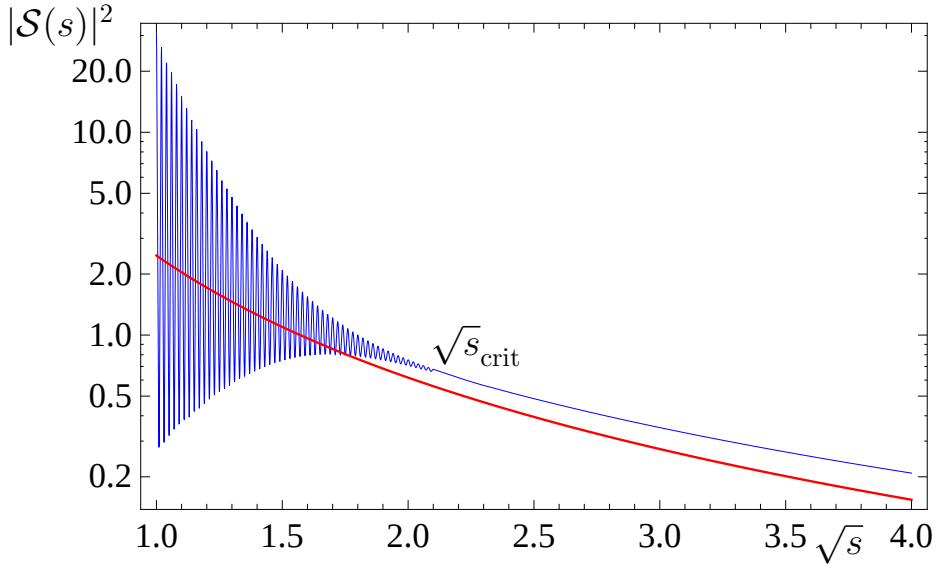

Figure 2: Squared KK kernel in the 5-D width given in blue plotted as a function of $\sqrt{s}$. Given for comparison is the analytic result computed by taking the principle value of the width-less propagator in the integral approximation. Phenomenological parameters taken for this plot are $M_* = 2\,\text{TeV}$ and $c = 1.5$. For clarity $M_{\rm Pl} = 20\,\text{TeV}$ so that the individual oscillations can be identified graphically. The difference in the blue and red curve above $\sqrt{s}_{\rm crit} \approx 2.28\,\text{TeV}$ vanishes for $M_{\rm Pl} \to \infty$.

.1.3 Monte Carlo Numerical Integrator

A VEGAS numerical integration routine is one important technique for calculating collider signatures. The internals of VEGAS will not be described in detail here, but essentially by linearizing the given function it obtains an efficient method of numerical integration. For the purposes of calculating LHC cross-sections, it is necessary to evaluate the integral,

$$\sigma_{had}(p+p\to Y) = \int_0^1 dx_1 \int_0^1 dx_2 \sum_{fl} f_f(x_1) f_{\bar{f}}(x_2)\, \sigma(q_f(x_1P) + \bar{q}_f(x_2P) \to Y) \tag{18}$$

For a $2 \to 2$ process there will be one additional integration over the phase space in the partonic cross-section. The vegas routine employed integrates over the the momentum fractions x_1 and x_2, as well as the angle θ from phase space integration. In addition, the user may numerically integrate over the KK mass $m_{\rm KK}$, provided that a chosen scale matching does not contain singularities. The

angle θ is defined in the partonic center of mass. The boost which transforms from the partonic to hadronic center-of-mass is solely along the beam axis and is given in terms of x_1 and x_2 as

$$\Lambda^{\nu}_{\mu} = \Lambda^{\nu}_{\mu}\left(\gamma(x_1,x_2),\beta(x_1,x_2)\right) \tag{19}$$

$$\gamma(x_1,x_2) = \sqrt{\frac{(x_1+x_2)^2}{4x_1x_2}} \tag{20}$$

$$\beta(x_1,x_2) = \frac{x_1-x_2}{x_1+x_2} \tag{21}$$

Note that transverse momentum of the initial state is neglected. Kinematic cuts can then be applied, and for most purposes this amounts to ignoring dilepton pairs with invariant mass less than 20 GeV. The squared and averaged matrix element can then be calculated using the momenta in either frame. This is passed first to the PDF function. The PDF used is cteq6ll [114], with the factorization scale set equal to p_t, which returns a weight equal to the probability of finding the initial partons with momentum fractions $x_1 + dx_1$ and $x_2 + dx_2$. Finally the phase space integrator computes the total cross-section as

$$\sigma_{par} = \int\int \frac{|\bar{\mathcal{M}}|^2}{2E_1 2E_2 |v_1 - v_2|} \frac{d^3p_3}{(2\pi)^3 2E_3} \frac{d^3p_4}{(2\pi)^3 2E_4} (2\pi)^4 \delta() \tag{22}$$

$$= \int d\theta \frac{|\bar{\mathcal{M}}|^2 \sin\theta}{64\pi E_1 E_2} \frac{E_3}{E_4} \tag{23}$$

where the delta function expresses overall energy momentum conservation. This integral is evaluated in the partonic center-of-mass frame due to the definition of θ. The value returned is then multiplyed by the VEGAS weight, produced internally in VEGAS when linearizing the function, which gives the contribution to the total cross-section for a particular iteration. Histogramming the partonic invariant COM energy with the associated weights for each iteration, give a distribution of $d\sigma/dm^2$ as a function of m^2. This can be seen by considering rewriting the total cross-section (18)

$$\sigma_{had} = \sum \Delta m^2 \sum_n d\sigma(m^2) \rightarrow \frac{\partial\sigma}{\partial m^2} = \sum_n d\sigma(m^2) \tag{24}$$

where the n represents contributions with $m_0^2 + n\Delta m^2 < m^2 < m_0^2 + (n+1)\Delta m^2$. The background results for the total cross-section and distribution were verified using the MadGraph and MadEvent package [115].

.1.4 Generating Functional

In this section we review functional renormalization techniques needed to study gravity in the non-perturbative regime. In particular we derive the exact renormalization group equation for the average effective action from [43]. The fundamental quantity we wish to evaluate in any generic quantum field theory is the partition function

$$Z[J] = \int [d\varphi] e^{-S[\varphi]+J\cdot\varphi}, \tag{25}$$

where ϕ is a scalar field for simplicity. Contained in the functional Z are all n-point Green functions, and solving for them explicitly deems the theory completely known. Related to the functional Z is the generator of connected Green functions.

$$W[J] = \ln Z[J] \tag{26}$$

Functionally differentiating $W[J]$ n-times with respect to the sources J therefore generates the connected n-point Green Functions. Differentiating with respect to only one source we obtain

$$\frac{\delta}{\delta J(x)} W[J] = -\frac{\int [d\varphi] e^{i\int(\mathcal{L}+J\varphi)}\varphi(x)}{\int [d\varphi] e^{i\int(\mathcal{L}+J\varphi)}} = \langle\varphi\rangle_J \;\equiv\; \phi(x). \tag{27}$$

In the final step we have defined the classical field ϕ as the expectation value of the quantum fluctuations φ. In other words, the weighted average of all the quantum effects is precisely the field which we measure in experiment ϕ. Therefore the final functional we use is the effective action $\Gamma[\phi]$; making use of this new field ϕ. This is simply the Legendre Transform of $W[J]$.

$$\Gamma[J] \equiv -W[J] - J\cdot\phi \tag{28}$$

In analogy to the equation of motion for the classical action,

$$\frac{\delta S[\phi]}{\delta\phi(x)} = J(x) \tag{29}$$

we can compute the equation of motion for the action of our full quantum theory.

$$\begin{aligned}\frac{\delta}{\delta\phi(x)}\Gamma[\phi] &= -\frac{\delta}{\delta\phi(x)}W[J] - \int d^d y \frac{\delta J(y)}{\delta\phi(x)}\phi(y) \; - J(x) \\ &= -\int d^d y \frac{\delta J(y)}{\delta\phi(x)}\frac{\delta W[J]}{\delta J(y)} - \int d^d y \frac{\delta J(y)}{\delta\phi(x)}\phi(y) \; - J(x) \\ &= -J(x) \end{aligned} \tag{30}$$

We have made use of (27) in the final step. For the functionals Z, W and Γ it is often too ambitious to include a measure which contains field modes with arbitrarily large and small momenta. Therefore, it is typical to cut-off the path integration in some manner and the theory is analysed in a particular momentum regime. The simplest implementation of this idea is called the Wilsonian cutoff,

$$Z_k[J] = \int [d\varphi]_{p^2>k^2} e^{-S[\varphi]+J\cdot\varphi} \tag{31}$$

where the integration is only carried out for field modes with momenta larger that k. This is a similar idea to the Wilsonian effective action, except in that case the cutoff is on UV modes, and the path integration is not carried out. Instead the UV cutoff is expected to modify the classical theory by the generation of higher dimensional operators, introducing new interactions at low energy.

The modern implementation for restricting the path integral is to cut-off field modes in a smooth way by inserting a mode suppression operator ΔS_k, and leaving the measure unchanged.

$$Z_k[J] = \int [d\varphi] e^{-S[\varphi]+J\cdot\phi-\Delta S_k[\varphi]} \tag{32}$$

The functional $\Delta S_k[\phi]$ has the form of a mass term with variable coefficient,

$$\Delta S_k[\varphi] = \frac{1}{2}\varphi \cdot R_k \cdot \varphi \tag{33}$$

where R_k has certain restrictions. R_k is large for modes with momenta less than k in order to suppress the path integral. For large momenta in the path integral,

R_k goes to 0 so that the region $q^2 >> k^2$ is not affected.

$$\lim_{\frac{q^2}{k^2}\to 0} R_k(q^2) = 0, \qquad \lim_{\frac{k^2}{q^2}\to 0} R_k(q^2) > 0 \tag{34}$$

At first it may seem surprising that $R_k(q^2) > 0$ when $k^2/q^2 \to 0$ is sufficient to eliminate IR divergences. Effectively, a non-zero R_k acts as a mass term, and this alone cures any IR pathology in the same way as a non-zero photon mass eliminate IR singularities in QED. In order for the path integral to fully suppress all modes with momentum less that k^2 it is necessary to stipulate that $R_k \to k^2$ for $q^2 < k^2$ since in effect we have introduced a mass gap in our theory of order k^2. Now we must confront the problem that in general, our functionals do not have explicit UV regulation. However, it turns out that we may still study certain aspects of our theory. Varying the cut-off scale k, induces a change in our functional which can be traced back to the effect of slightly higher or lower momentum modes. This leads to genuine physical behaviour of our theory at different energy scales. The quantity we wish to calculate in this framework is the k-derivative of the relevant generating functional.

$$k\frac{\partial}{\partial k} Z_k[J] = -k\frac{\partial}{\partial k}\langle \Delta S_k \rangle = -\int_q k\frac{\partial}{\partial k} R_k \langle \varphi(q)\varphi(-q)\rangle \tag{35}$$

since the only k dependence is in the cutoff function. In practice it is simpler to first define the smoothly cutoff effective action,

$$\Gamma_k[\phi] = -\ln Z_k[J] + J\cdot\phi - \Delta S_k[\phi] \tag{36}$$

here and henceforth known as the *effective average action*. This quantity has a very intuitive physical meaning. This can be seen by considering the limits as we take the cut-off either to 0 or very large. In the first case, taking $k \to 0$ removes the cut-off all together, and we are left with the unregulated quantum action $\Gamma[\phi]$. In the second case, if our theory is endowed with a physical UV cut-off Λ, taking $k \to \Lambda$ removes all quantum fluctuations in the theory. This is the classical action $S[\phi]$. Therefore, the average effective action can be seen as interpolating between a fully quantum and classical theory. The crucial observation for our purposes though is that when we take the UV cut-off $\Lambda \to \infty$ we are asking whether or not very high momentum modes render the path integral ill-defined. The action

which results from this procedure is thus defined $\Gamma_\star = \Gamma_{\Lambda\to\infty}$. There are three possibilities,

- $\Gamma_\star$ does not exist, we know immediately that Γ is not a renormalizable theory.
- $\Gamma_\star = S_{cl}$ in which case the theory is perturbatively renormalizable and asymptotically free.
- $\Gamma_\star$ exist as some non-trivial theory, where it is said to be non-perturbatively renormalizable.

For the second case, the analogy of QCD is instructive. Asymptotic freedom at high energies implies that QCD is non-interacting, and the action is neatly described by $\mathcal{L} = -\frac{1}{4}F_{\mu\nu}F^{\mu\nu}$. The asymptotic safety scenario is predicated on the possibility that gravity will fit into the third category. In any case, defining

$$k\frac{\partial}{\partial k} = \frac{\partial}{\partial \ln k} \equiv \frac{\partial}{\partial t} = \partial_t, \tag{37}$$

we compute the derivative of (36)

$$\partial_t \Gamma_k[\phi] = \frac{1}{2}\int_q \partial_t R_k(q^2)\left[\langle\varphi(q)\varphi(-q)\rangle - \phi(q)\phi(-q)\right], \tag{38}$$

where now we have the term in brackets $\langle\varphi(q)\varphi(-q)\rangle - \langle\varphi(q)\rangle\langle\varphi(-q)\rangle$ compared to (35). This is just the connected corralator.

$$\langle\varphi(q)\varphi(-q)\rangle - \langle\varphi(q)\rangle\langle\varphi(-q)\rangle = \frac{\delta^2 W_k[J]}{\delta J \delta J} \tag{39}$$

We would like to have our differential equation (38) completely in terms of $\Gamma_k[\phi]$. Hence, we start with the quantum equation of motion (30), and take the functional derivative with respect to $J(y)$ on both sides,

$$\begin{aligned}\delta(x-y) &= -\frac{\delta}{\delta J(y)}\frac{\delta\Gamma_k}{\delta\phi(x)} \\ &= \int d^d z \frac{\delta\phi(z)}{\delta J(y)}\frac{\delta^2\Gamma_k}{\delta\phi(z)\delta\phi(x)}\end{aligned} \tag{40}$$

where in the second line we have used the chain rule and introduced a dummy integration over z. Now, we replace $\phi(z)$ with its definition in (27). Our final

expression then is

$$\delta(x-y) = \int d^d z \frac{\delta^2 W_k[J]}{\delta J(y)\delta J(z)} \frac{\delta^2 \Gamma_k[J]}{\delta\phi(z)\delta\phi(x)}\,, \tag{41}$$

and it is clear that the two terms are functional inverses. Therefore, (38) turns into a functional differential equation containing only $\Gamma_k[\phi]$

$$\partial_t \Gamma_k[\phi] = \frac{1}{2}\int_q \partial_t R_k \left(\frac{\delta^2\Gamma_k[J]}{\delta\phi\delta\phi} + R_k\right)^{-1}. \tag{42}$$

It is typical to generalize the integration to include a sum over all internal indices in the theory, and represent this as a trace. In final form, the flow equation for the average effective action is,

$$\partial_t \Gamma_k[\phi] = \frac{1}{2}\mathrm{Tr}\left[\left(\frac{\delta^2\Gamma_k[J]}{\delta\phi\delta\phi} + R_k\right)^{-1}\partial_t R_k\right] \tag{43}$$

This result was originally derived in [43]. First of all, the second derivative of the effective action is the exact propagator. Thus, as a Feynman diagram the RHS of this equation is a single loop for the exact propagator, with insertions at the vertex corresponding to regulator terms. The crucial point though is that the function R_k appears in (43) as a multiplicative factor $\partial_t R_k$. By construction, the function $R_k(q^2) \to 0$ for large q^2, and this is enough to guarantee that $\partial_t R_k$ will go to 0 as well. If $R_k \to 0$ at an exponential rate, the flow equation (43) is UV finite even when $\Gamma_k[\phi]$ is not. All UV modes in this case are exponentially suppressed. Our point of interest though is the case when the flow ends on a UV fixed point. It is in this (and only this) case that we can define our $\Gamma[\phi]$ as representing a fundamental theory.

We are always at liberty to integrate our flow equation, starting at some well defined boundary action Γ_Λ. With our a foot in the door so to speak, we can apply the (finite) flow equation to define our theory Γ as,

$$\Gamma = \Gamma_\Lambda + \int_\Lambda^0 \frac{dk}{k}\frac{1}{2}\Gamma_k \frac{\partial_t R_k}{\Gamma_k^{(2)} + R_k} \tag{44}$$

without making any reference to the path integral itself. Essentially, we have differentiated then re-integrated (36) and in doing so have defined a sufficient

regularization scheme.

Perturbation theory is easily reproduced from the flow equation, and in the case of small coupling accurately describes our theory. The first step is to replace $\Gamma_k[\phi]$ with the classical action $S[\phi]$ on the left hand side of (43). Since the only k dependence in the trace is contained in the R_k we can rewrite this as

$$\partial_t \Gamma_k = \partial_t \frac{1}{2} \mathrm{Tr} \ln \left[\frac{\delta^2 S}{\delta\phi(z)\delta\phi(x)} + R_k \right]. \tag{45}$$

Integrating gives the one loop effective action,

$$\begin{aligned} \Gamma_k^{\text{1-loop}} &= \frac{1}{2} \mathrm{Tr} \ln \left[S^{(2)} + R_k \right] \Big|_{k=\Lambda}^{k=0} \\ &= S[\phi] + \frac{1}{2} \mathrm{Tr} \ln \left[S^{(2)} \right] \end{aligned} \tag{46}$$

where $R_0 = 0$ since no modes will be suppressed in that case. We use the fact that for the momentum integral over $(S^{(2)} + R_\Lambda)^{-1}$, there is a mass gap $m^2 \sim \Lambda^2$, so that only S_{cl} remains. The result (46) is the normal one-loop equation derived from Schwinger-Dyson methods.

As the goal of the renormalization group flow equation is to provide a type of non-perturbative description of a theory, it is useful to formulate an ordering scheme of the effective action which does not rely on a small coupling. The derivative expansion is commonly used and involves ordering all terms with no derivatives first, all terms with two (for the case of a scalar theory) second, and so on. Schematically,

$$\Gamma_k[\phi] = \int d^d x \left(U_k(\phi) + Z_k \phi (\partial\phi)^2 + \cdots + Y_k(\phi) \phi \partial^4 \phi + \cdots \right) \tag{47}$$

U_k is the exact potential function in this case, and using the flow equation it is possible to calculate the flow for each coefficient function $Z_k[\phi]$ for example. Obviously any term which violate the symmetries of the underlying theory is disallowed, in this scheme and any other. A second ordering scheme for the average effective action is called the vertex expansion. This involves ordering operators by the number of field.

$$\Gamma_k[\phi] = \sum_n \frac{1}{n!} \Gamma_k^{(n)}(x_1, \cdots x_n) \phi(x_1) \cdots \phi(x_2) \tag{48}$$

where the $\Gamma_k^{(n)}$ is the average effective action for all invariants with n powers of the fields. A final point, is that in some sense the vertex expansion and the derivative expansion are orthogonal, since the first term in the derivative expansion for example, contains terms from all orders of the vertex expansion, and vice versa. In gravity, we use mainly the derivative expansion.

.1.5 ERG Formalism of Gravity

In order to apply RG methods to quantum gravity it is necessary to formulate a fully quantum effective action. The RG flow equation will then be used to determine whether such an action is free of UV singularities. Equivalently, the effective action exists if the RG trajectory ends on an UV fixed point. These steps for quantizing gravity were first carried out in Ref. [45]. The structure and some of the main results are from Ref. [4].

The Asymptotic safety scenario states that the metric, a dimensionless second rank tensor, carries the degrees of freedom of the gravitational field in both the IR and UV. However, it is also expected to be a fluctuating field in accordance with quantum theory, and in effect, off-shell geometries must also be included in the path integral. We define the quantum metric analogous to φ in our previous discussions as $\gamma_{\mu\nu}$. The combined average effects of this fluctuating metric produce the classical field $g_{\mu\nu} = \langle\gamma_{\mu\nu}\rangle$. The original symmetries of the theory are maintained in the path integral by using the background field method. To implement this we introduce the background field $\bar{g}^{\mu\nu}$ so that $\Gamma[g_{\mu\nu}] \to \Gamma[\bar{g}_{\mu\nu}, g_{\mu\nu}]$. The field $\bar{g}_{\mu\nu}$ is non-propagating and can be identified with the physical field $g_{\mu\nu}$ following quantization. With this definition, we define the quantum metric $\gamma_{\mu\nu} = \bar{g}_{\mu\nu} + h_{\mu\nu}$ where $\bar{g}_{\mu\nu}$ is not necessarily flat, but is constant, and the field $h_{\mu\nu}$ contains all quantum effects. This replacement means that path integration over $\gamma_{\mu\nu}$ can be replaced by integration over $h_{\mu\nu}$.

The metric is required to be invariant under changes in the space time coordinates $\delta x_\mu = \xi_\mu(x)$. It is important now to examine how our diffeomorphism transformation acts on our fields $g_{\mu\nu}$, $\bar{g}_{\mu\nu}$, $h_{\mu\nu}$ and $\gamma_{\mu\nu}$. First of all, the dynamical field in the path integral transforms under δ as,

$$\delta\gamma_{\mu\nu} = \mathcal{L}_\xi(\bar{g}_{\mu\nu} + h_{\mu\nu}) \tag{49}$$

$$\delta\bar{g}_{\mu\nu} = 0 \tag{50}$$

However under the background variation,

$$\bar{\delta} h_{\mu\nu} = \mathcal{L}_\xi h_{\mu\nu} \tag{51}$$

$$\bar{\delta} \bar{g}_{\mu\nu} = \mathcal{L}_\xi \bar{g}_{\mu\nu} \tag{52}$$

Thus the quantum symmetry is realized by a non-linear and trivial transformation of $h_{\mu\nu}$ and $\bar{g}_{\mu\nu}$ respectively. The background symmetry transforms both fields linearly. In effect we have merely divided the symmetry in different proportions in the background case. The crucial consequence for our purposes is that δ and $\bar{\delta}$ act identically on $\gamma_{\mu\nu}$.

In analogy to the quantization of non-Abelian gauge theories, field configurations related by diffeomorphism are counted an infinite number of times in the path integral. Hence we introduce a gauge fixing term (harmonic gauge).

$$S_{gf} = \frac{1}{2\alpha} \int d^d x \sqrt{g} \bar{g}^{\mu\nu} F_\mu F_\nu \tag{53}$$

where

$$F_\mu = \sqrt{64\pi G_N} [\delta^\beta_\mu \bar{g}^{\alpha\gamma} \bar{\mathcal{D}}_\gamma - \frac{1}{2} \bar{g}^{\alpha\beta} \bar{\mathcal{D}}_\mu] h_{\alpha\beta} \tag{54}$$

and $\bar{\mathcal{D}}_\gamma$ is the covariant derivative defined with respect to $\bar{g}_{\mu\nu}$. Evaluation of the Faddeev-Popov determinant also produces ghost terms with field C_μ. Although we have not shown it explicitly, the combined quantum and background variation of the effective action $\Gamma[g, \bar{g}]$ is,

$$(\delta + \bar{\delta}) \Gamma(g, \bar{g})|_{\bar{g}=g} = 0 \tag{55}$$

modulo terms coming explicitly from the gauge fixing. Therefore, the action is invariant under diffeomorphism,

$$\Gamma[\phi + \mathcal{L}_\xi \phi] = \Gamma[\phi] \tag{56}$$

where $\phi = \{g_{\mu\nu}, \bar{g}_{\mu\nu}, C_\mu, \bar{C}_\mu\}$. The action we use is

$$\Gamma_k = \int d^d x \sqrt{g} \left\{ \frac{1}{16\pi G_N} (-R + 2\Lambda_k) + \mathcal{O}(R^2) + \mathcal{L}_{matter} + \mathcal{L}_{gf} + \mathcal{L}_{gh} \right\}, \tag{57}$$

in the RG flow equation (43) and in order to see evidence for Asymptotic safety it is only necessary to include the Einstein-Hilbert term with cosmological constant. Thus, we neglect all matter interactions.

$$\Gamma_k = \int d^d x \sqrt{g} \left\{ \frac{1}{16\pi G_N}(-R + 2\Lambda_k) + \mathcal{L}_{gf} + \mathcal{L}_{gh} \right\} \tag{58}$$

Solving the flow equation and extracting the β-functions even for this simple action is technically involved and we will not present the details. Instead we quote results for the beta functions of the dimensionless couplings g and λ,

$$\beta_g = (d - 2 + \eta)g \tag{59}$$

$$\beta_\lambda = (-2 + \eta)\lambda + g\left(a_1(\lambda) - \eta a_2(\lambda)\right) \tag{60}$$

$$\eta = \frac{g b_1(\lambda)}{1 + g b_2(\lambda)} \tag{61}$$

Writing out a_1, a_2, b_1 and b_2 and η explicitly

$$\beta_g = (d-2)g + \frac{2(d-2)(d+2)g^2}{2(d-2)g - (1-2\lambda)^2} \tag{62}$$

$$\beta_\lambda = -2\lambda + \frac{g}{2} d(d+2)(d+5) - d(d+2)g \frac{(d-1)g - \frac{1}{d-2}\left(1 - 4\frac{d-1}{d}\lambda\right)}{2g - \frac{1}{d-2}(1-2\lambda)^2}, \tag{63}$$

where the g is rescaled with a factor $c_d = \Gamma\left(\frac{d}{2} + 2\right)(4\pi)^{d/2-1}$. Gauge fixing dependency is responsible for the relative complexity of (62) and (63) compared with (59) and (60), which are valid for any gauge fixing condition.

There are several interesting results contained in (62) and (63). First and foremost, these equations have UV fixed points with non-vanishing λ and g in $d = 4$ dimensions. More precisely both β-functions vanish for $(g_\star, \lambda_\star) = (\frac{1}{64}, 14)$ although these are not physical and depends on the gauge fixing as well as the cut-off scheme. We will refer to such quantities as being *non-universal*.

What is physically relevant though, is that the FP in $d = 4$ is continuously connected to the Gaussian FP known to exist in $d = 2$ gravity. A second physical point is that the phase diagram for λ and g exhibits a *separatix* trajectory, which connects the Gaussian and non-gaussian FP. All other trajectories are repelled from the Gaussian FP, so that for example, in the IR these trajectories flow towards values of $g = 0$ and $\lambda = \pm\infty$. Connecting physics around the Gaussian

FP with perturbation theory, we say that λ is a relevant perturbation. The actual position of our universe on the $\lambda - g$ phase diagram is argued in Ref. [54] to just miss the separatix trajectory and flow towards $+\infty$ in the IR. While the position of FP show a fairly strong cut-off scheme and gauge fixing dependence, their existence is considered a universal quantity. Another set of universal quantities are the critical exponents θ in the vicinity of a particular FP. The eigenvalues of the stability matrix are defined as $-\theta_i$. From inspection of (62) and (63) the matrix $M_{ij} = \frac{\partial \beta_j}{\partial g_i}$ will have non-vanishing components in every entry. An explicit calculations in $d = 4$ shows that the critical exponents are a complex-conjugate pair parametrized as $\theta = \theta' \pm i\theta''$ with $\theta' = 1.1 - 2.3$ and $\theta'' = 2.4 - 7.0$. These number show a small variation due to scheme dependence, but are numerically relatively stable. Most importantly, varying the gauge fixing and cut-off do not change the signs of the critical exponent (nor do they destroy the FP altogether).

The final aspect of the Asymptotic safety scenario we would like to address with our analysis using the RG, is whether it predicts explicit anti-screening effects to G_N in the UV. If we expand the generic form of β_g and η in (59) to order g^2, and set $\lambda = 0$, we obtain.

$$\beta_g = (d-2)g - (d-2)\omega g^2 + \mathcal{O}(g^3, g^2\lambda) \tag{64}$$

The constant $\omega \equiv \frac{c_d b_1(0)}{2-d}$ where c_d is defined in (63), and $b_1(0)$ is in general scheme dependent. The replacement $g \to G\mu^{d-2}$ leads to,

$$\beta_G = -(d-2)\omega G^2 \mu^{d-2} \tag{65}$$

This equation is easily integrated to obtain

$$G_k = \frac{G_\Lambda}{1 - \omega G_\Lambda(\Lambda^{d-2} - k^{d-2})} \tag{66}$$

where Λ is some reference scale, and k is the energy of our process. If we take $\Lambda = 0$ then our reference scale is G_N and we obtain a one loop formula for the the running of G_N,

$$G_k = \frac{G_0}{1 + \omega G_0 k^{d-2}} \tag{67}$$

which is the resummation of the one loop contribution to the gravitational coupling previously derived using effective theory techniques in (2.27). Formally, this is equivalent to the linear approximation defined in (4.9). Since ω is universally positive (its magnitude however is non-universal), the gravitational coupling show signs of anti-screening as one moves away from the Gaussian FP.

This does not a constitute a proof that gravity is a finite theory. As we saw in perturbative calculations, higher derivative invariants play a crucial role in the action and it may be that the fixed point does not remain after the inclusion of these terms. In addition to being a more robust test of the asymptotic safety scenario, the inclusion of higher order invariant allow us to judge the stability of numerical results. In general, we require that the addition of new couplings in the theory does not change significantly θ' and θ''. Using similar computational methods to the ones used for Einstein-Hilbert action, the β-functions can be calculated for the action,

$$\Gamma_k = \int d^d x \sqrt{g} \left\{ \frac{1}{16\pi G_N}(-R + 2\Lambda_k) + c_2 R^2 + \mathcal{L}_{gf} + \mathcal{L}_{gh} \right\} \tag{68}$$

The results in Ref. [116] show that c_3 is also a UV attractive coupling. The critical exponent θ_2 shows a rather large scheme dependence but the physically relevant sign in unchanged by varying the gauge fixing condition. Therefore, it should be included in any fundamental theory of gravity in the formal sense. It is also speculated that the other term $R_{\mu\nu}R^{\mu\nu}$ will have a UV attractive coupling.

Further polynomial invariants R^n have been included in the effective action and the numerical results are in [48]. The results show not only that θ' and θ'' are stable, but also that the higher order critical exponents θ^n for $n \geq 3$ are negative, and thus these terms are UV repulsive. This is encouraging for our requirement that the theory be predictive. UV repulsive couplings do not need to be specified for the theory to have a well defined UV limit. Of course these terms may have non-trivial effects away from the non-Gaussian FP.

The addition of minimally coupled matter, especially in the R^2 truncation, provides a non-trivial test for Asymptotic Safety. This is particularly interesting since gravitational interactions with matter were shown to be divergent at the R^2 level, with no hope for renormalization or field redefinition. The computation in [50] reveals that not only does the fixed point survive this inclusion, but the

critical exponents are affected in a fairly trivial manner; Evidence perhaps that the underlying physics probed by the ERG is truly non-perturbative.

.1.6 Toy RG Model of Gravity

In this section we outline some explicit calculation in a simplified model of gravity presented in Ref. [4]. The stability matrix (2.35) is essential for gaining physical insight about our theory. In order to demonstrate the variety of qualitatively different fixed point behaviours, we will compute explicitly this matrix for a simple gravitational action. Furthermore, quantum corrections to the β-functions will be estimated on a very heuristic level. The theory we will study is the gravitational action,

$$\mathcal{L} = \sqrt{g}Z(-R + 2\Lambda) \tag{69}$$

in $D = 4$ Euclidean dimensions. The parameter $Z = G_N^{-1}$ and the factor 16π has been absorbed into G for convenience. In addition we will consider $U = 2\Lambda Z$ as the vacuum energy. In order for the Lagrangian to have mass dimension 4, we have $[G] = -2$, $[Z] = 2$, $[\Lambda] = 2$ and $[U] = 4$. However, as already mentioned, the physically relevant parameters are dimensionless so we define,

$$g = G_N\mu^2 \qquad z = Z\mu^{-2} \qquad \lambda = \Lambda\mu^{-2} \qquad u = U\mu^{-4} \tag{70}$$

with β-functions,

$$\beta_g = 2g \qquad \beta_z = -2Z \qquad \beta_\lambda = -2\lambda \qquad \beta_u = -4u \tag{71}$$

Since there are only two independent parameters, it is only necessary to compute M_{ij} twice. At the Gaussian fixed point we have,

$$M^{(\lambda,g)} = \begin{pmatrix} 2 & 0 \\ 0 & -2 \end{pmatrix} \quad M^{(g,u)} = \begin{pmatrix} 2 & 0 \\ 0 & -4 \end{pmatrix} \quad M^{(z,u)} = \begin{pmatrix} -2 & 0 \\ 0 & -4 \end{pmatrix} \tag{72}$$

which are stability matrices for a classically scaling theory. However, there is a qualitatively different Gaussian fixed point for our theory described by (g, u) and (g, z). This can be seen from the last two stability matrices, where the first has $M^{(g,u)}$ has one IR stable directions and $M^{(z,u)}$ has two unstable IR directions.

Quantum effects are expected to modify the simple scaling region of the

classical theory. The one loop modification to the dimensionful β-functions can be guessed by dimensional analysis

$$\beta_U = a\mu^4, \quad \beta_Z = b\mu^2. \tag{73}$$

By making the replacement $U \to u\mu^4$, and similarly for Z, we can derive β_u and β_z

$$\beta_u = -4u + a, \quad \beta_z = -2z + b. \tag{74}$$

The effect of the quantum fluctuations then is to shift the previously Gaussian fixed point to a new value $(z, u) = (b/2, a/4)$. The stability matrix remains the same as (72).

What is more physically apparent for gravity is the behaviour of the β-functions for g and λ. These can be derived from β_z for example as

$$\mu\frac{d}{d\mu}z = \mu\frac{dg}{d\mu}\frac{d}{dg}\frac{1}{g} = -2z + b, \tag{75}$$

so that

$$\beta_g = 2g - bg^2. \tag{76}$$

A similar computation reveals

$$\beta_\lambda = -2\lambda + \frac{ag}{2} - bg\lambda. \tag{77}$$

In addition to the trivial fixed point there is a non-trivial one for $(g, \lambda) = (2/b, a/(4b))$. We have two stability matrices to calculate,

$$M^{(Gaussian)} = \begin{pmatrix} 2 & 0 \\ a/2 & -2 \end{pmatrix} \quad M^{(NG)} = \begin{pmatrix} -2 & 0 \\ a/4 & -4 \end{pmatrix} \tag{78}$$

The flow in the vicinity of each fixed point is tilted due to the off-diagonal components of the stability matrix. Instead of having straight line solutions which lie on the axes, the new straight line solutions are the eigenvectors of M_{ij} denoted v_1 and v_2. In fact $v_i^G = v_i^{NG}$ so that in order for there to be exactly 2 fixed points, the non-gaussion FP must lie on the straight line trajectory emanating from the Gaussian FP. The genuine physics is encoded in the eigenvalues of (78) where we see that the quantum effects at the NG fixed point overcome the canonical

dimension and render g an UV attractive direction. The UV critical surface is thus two dimensional.

In order to analyze quantum effects in gravity quantitatively, more powerful techniques are required. The functional renormalization group picture from the previous section is necessary for us to move beyond these simple manipulations.

Bibliography

[1] Erik Gerwick, Daniel Litim, and Tilman Plehn. Asymptotic safety and Kaluza-Klein gravitons at the LHC. *Phys.Rev.*, D83:084048, 2011, 1101.5548.

[2] Erik Gerwick. Asymptotically Safe Gravitons in Electroweak Precision Physics. *Eur.Phys.J.*, C71:1676, 2011, 1012.1118.

[3] Erik Gerwick and Tilman Plehn. Extra Dimensions and their Ultraviolet Completion. 2009, 0912.2653.

[4] Daniel F. Litim. News from quantum gravity. *Lectures at the Heidelberg Graduate School*, 2009.

[5] Erik Gerwick, Tilman Plehn, and Steffen Schumann. Understanding Jet Scaling and Jet Vetos in Higgs Searches. 2011, 1108.3335.

[6] D.J. Kapner, T.S. Cook, E.G. Adelberger, J.H. Gundlach, Blayne R. Heckel, et al. Tests of the gravitational inverse-square law below the dark-energy length scale. *Phys.Rev.Lett.*, 98:021101, 2007, hep-ph/0611184.

[7] Roberto Contino, Luigi Pilo, Riccardo Rattazzi, and Alessandro Strumia. Graviton loops and brane observables. *JHEP*, 0106:005, 2001, hep-ph/0103104.

[8] Greg Landsberg. Collider Searches for Extra Spatial Dimensions and Black Holes. 2008, 0808.1867.

[9] Peter W. Higgs. Broken symmetries, massless particles and gauge fields. *Phys.Lett.*, 12:132–133, 1964.

[10] F. Englert and R. Brout. Broken Symmetry and the Mass of Gauge Vector Mesons. *Phys.Rev.Lett.*, 13:321–322, 1964.

[11] Daniele Alves, Nima Arkani-Hamed, Sanjay Arora, Yang Bai, Matthew Baumgart, et al. Simplified Models for LHC New Physics Searches. 2011, 1105.2838. * Temporary entry *.

[12] T. Moroi, H. Murayama, and Masahiro Yamaguchi. Cosmological constraints on the light stable gravitino. *Phys.Lett.*, B303:289–294, 1993.

[13] M. Bolz, A. Brandenburg, and W. Buchmuller. Thermal production of gravitinos. *Nucl.Phys.*, B606:518–544, 2001, hep-ph/0012052.

[14] Ignatios Antoniadis, Nima Arkani-Hamed, Savas Dimopoulos, and G.R. Dvali. New dimensions at a millimeter to a Fermi and superstrings at a TeV. *Phys.Lett.*, B436:257–263, 1998, hep-ph/9804398.

[15] Nima Arkani-Hamed, Savas Dimopoulos, and G. R. Dvali. The hierarchy problem and new dimensions at a millimeter. *Phys. Lett.*, B429:263–272, 1998, hep-ph/9803315.

[16] Lisa Randall and Raman Sundrum. A Large mass hierarchy from a small extra dimension. *Phys.Rev.Lett.*, 83:3370–3373, 1999, hep-ph/9905221.

[17] Lisa Randall and Raman Sundrum. An Alternative to compactification. *Phys.Rev.Lett.*, 83:4690–4693, 1999, hep-th/9906064.

[18] Thomas Appelquist, Hsin-Chia Cheng, and Bogdan A. Dobrescu. Bounds on universal extra dimensions. *Phys.Rev.*, D64:035002, 2001, hep-ph/0012100.

[19] Gian F. Giudice, Riccardo Rattazzi, and James D. Wells. Quantum gravity and extra dimensions at high-energy colliders. *Nucl. Phys.*, B544:3–38, 1999, hep-ph/9811291.

[20] Tao Han, Joseph D. Lykken, and Ren-Jie Zhang. On Kaluza-Klein states from large extra dimensions. *Phys. Rev.*, D59:105006, 1999, hep-ph/9811350.

[21] L. Vacavant and I. Hinchliffe. Signals of models with large extra dimensions in ATLAS. *J.Phys.G*, G27:1839–1850, 2001.

[22] J. L. Hewett. Phenomenology of extra dimensions. Prepared for Les Houches Summer School on Theoretical Physics: Session 84: Particle Physics Beyond the Standard Model, Les Houches, France, 1-26 Aug 2005.

[23] Gian F. Giudice, Tilman Plehn, and Alessandro Strumia. Graviton collider effects in one and more large extra dimensions. *Nucl.Phys.*, B706:455–483, 2005, hep-ph/0408320.

[24] Steven Weinberg. ULTRAVIOLET DIVERGENCES IN QUANTUM THEORIES OF GRAVITATION. In *Hawking, S.W., Israel, W.: General Relativity*, 790- 831.

[25] Charles W. Misner, K. S. Thorne, and J. A. Wheeler. Gravitation. San Francisco 1973, 1279p.

[26] L.F. Abbott. Introduction to the Background Field Method. *Acta Phys.Polon.*, B13:33, 1982.

[27] Gerard 't Hooft and M. J. G. Veltman. One loop divergencies in the theory of gravitation. *Annales Poincare Phys. Theor.*, A20:69–94, 1974.

[28] Marc H. Goroff and Augusto Sagnotti. The Ultraviolet Behavior of Einstein Gravity. *Nucl. Phys.*, B266:709, 1986.

[29] K. S. Stelle. Classical Gravity with Higher Derivatives. *Gen. Rel. Grav.*, 9:353–371, 1978.

[30] Joaquim Gomis and Steven Weinberg. Are Nonrenormalizable Gauge Theories Renormalizable? *Nucl. Phys.*, B469:473–487, 1996, hep-th/9510087.

[31] Tirthabir Biswas, Anupam Mazumdar, and Warren Siegel. Bouncing universes in string-inspired gravity. *JCAP*, 0603:009, 2006, hep-th/0508194.

[32] John F. Donoghue. Leading quantum correction to the Newtonian potential. *Phys. Rev. Lett.*, 72:2996–2999, 1994, gr-qc/9310024.

[33] C. P. Burgess. Quantum gravity in everyday life: General relativity as an effective field theory. *Living Rev. Rel.*, 7:5, 2004, gr-qc/0311082.

[34] David J. Gross and Andre Neveu. Dynamical Symmetry Breaking in Asymptotically Free Field Theories. *Phys.Rev.*, D10:3235, 1974.

[35] Baruch Rosenstein, Brian J. Warr, and Seon H. Park. The Four Fermi Theory Is Renormalizable in (2+1)-Dimensions. *Phys.Rev.Lett.*, 62:1433–1436, 1989.

[36] Daniel F. Litim. Fixed Points of Quantum Gravity and the Renormalisation Group. 2008, 0810.3675.

[37] J. Ambjorn, J. Jurkiewicz, and R. Loll. Spectral dimension of the universe. *Phys. Rev. Lett.*, 95:171301, 2005, hep-th/0505113.

[38] Roberto Percacci. Asymptotic Safety. 2007, 0709.3851. to appear in 'Approaches to Quantum Gravity: Towards a New Understanding of Space, Time and Matter' ed. D. Oriti, Cambridge University Press.

[39] S. M. Christensen and M. J. Duff. QUANTUM GRAVITY IN TWO + epsilon DIMENSIONS. *Phys. Lett.*, B79:213, 1978.

[40] Toshiaki Aida, Yoshihisa Kitazawa, Jun Nishimura, and Asato Tsuchiya. Two loop renormalization in quantum gravity near two- dimensions. *Nucl. Phys.*, B444:353–380, 1995, hep-th/9501056.

[41] Lee Smolin. A FIXED POINT FOR QUANTUM GRAVITY. *Nucl.Phys.*, B208:439, 1982.

[42] Wataru Souma. Nontrivial ultraviolet fixed point in quantum gravity. *Prog.Theor.Phys.*, 102:181–195, 1999, hep-th/9907027.

[43] Christof Wetterich. Exact evolution equation for the effective potential. *Phys. Lett.*, B301:90–94, 1993.

[44] Tim R. Morris. The Exact renormalization group and approximate solutions. *Int.J.Mod.Phys.*, A9:2411–2450, 1994, hep-ph/9308265.

[45] M. Reuter. Nonperturbative Evolution Equation for Quantum Gravity. *Phys. Rev.*, D57:971–985, 1998, hep-th/9605030.

[46] M. Niedermaier. The asymptotic safety scenario in quantum gravity: An introduction. *Class. Quant. Grav.*, 24:R171, 2007, gr-qc/0610018.

[47] Max Niedermaier and Martin Reuter. The Asymptotic Safety Scenario in Quantum Gravity. *Living Rev.Rel.*, 9:5, 2006.

[48] Alessandro Codello, Roberto Percacci, and Christoph Rahmede. Investigating the Ultraviolet Properties of Gravity with a Wilsonian Renormalization Group Equation. *Annals Phys.*, 324:414–469, 2009, 0805.2909.

[49] Roberto Percacci and Daniele Perini. Asymptotic safety of gravity coupled to matter. *Phys.Rev.*, D68:044018, 2003, hep-th/0304222.

[50] Dario Benedetti, Pedro F. Machado, and Frank Saueressig. Taming perturbative divergences in asymptotically safe gravity. 2009, 0902.4630.

[51] Peter Fischer and Daniel F. Litim. Fixed points of quantum gravity in extra dimensions. *Phys. Lett.*, B638:497–502, 2006, hep-th/0602203.

[52] Daniel F. Litim and Tilman Plehn. Virtual Gravitons at the LHC. 2007, 0710.3096.

[53] JoAnne Hewett and Thomas Rizzo. Collider Signals of Gravitational Fixed Points. *JHEP*, 0712:009, 2007, 0707.3182.

[54] A. Bonanno and M. Reuter. Cosmology of the Planck era from a renormalization group for quantum gravity. *Phys. Rev.*, D65:043508, 2002, hep-th/0106133.

[55] Mark Hindmarsh, Daniel Litim, and Christoph Rahmede. Asymptotically Safe Cosmology. *JCAP*, 1107:019, 2011, 1101.5401.

[56] Alfio Bonanno and Martin Reuter. Renormalization group improved black hole spacetimes. *Phys. Rev.*, D62:043008, 2000, hep-th/0002196.

[57] A. Bonanno and M. Reuter. Spacetime structure of an evaporating black hole in quantum gravity. *Phys. Rev.*, D73:083005, 2006, hep-th/0602159.

[58] Kevin Falls, Daniel F. Litim, and Aarti Raghuraman. Black holes and asymptotically safe gravity. 2010, 1002.0260.

[59] Changrim Ahn, Chanju Kim, and Eric V. Linder. From Asymptotic Safety to Dark Energy. 2011, 1106.1435. * Temporary entry *.

[60] Theodor Kaluza. On the Problem of Unity in Physics. *Sitzungsber.Preuss.Akad.Wiss.Berlin (Math.Phys.)*, 1921:966–972, 1921. Often incorrectly cited as Sitzungsber.Preuss.Akad.Wiss.Berlin (Math. Phys.) K1,966. In reality there is no volume number, so SPIRES used the year in place of a volume number.

[61] O. Klein. Quantum Theory and Five-Dimensional Theory of Relativity. (In German and English). *Z.Phys.*, 37:895–906, 1926.

[62] Ignatios Antoniadis. A Possible new dimension at a few TeV. *Phys.Lett.*, B246:377–384, 1990.

[63] Petr Horava and Edward Witten. Eleven-dimensional supergravity on a manifold with boundary. *Nucl.Phys.*, B475:94–114, 1996, hep-th/9603142.

[64] Joseph Polchinski. Dirichlet Branes and Ramond-Ramond charges. *Phys.Rev.Lett.*, 75:4724–4727, 1995, hep-th/9510017.

[65] Nima Arkani-Hamed and Martin Schmaltz. Hierarchies without symmetries from extra dimensions. *Phys. Rev.*, D61:033005, 2000, hep-ph/9903417.

[66] G. R. Dvali and Mikhail A. Shifman. Families as neighbors in extra dimension. *Phys. Lett.*, B475:295–302, 2000, hep-ph/0001072.

[67] E.G. Adelberger, Blayne R. Heckel, Seth A. Hoedl, C.D. Hoyle, D.J. Kapner, et al. Particle Physics Implications of a Recent Test of the Gravitational Inverse Sqaure Law. *Phys.Rev.Lett.*, 98:131104, 2007, hep-ph/0611223.

[68] E.G. Adelberger, Blayne R. Heckel, and A.E. Nelson. Tests of the gravitational inverse square law. *Ann.Rev.Nucl.Part.Sci.*, 53:77–121, 2003, hep-ph/0307284.

[69] C.D. Hoyle, U. Schmidt, Blayne R. Heckel, E.G. Adelberger, J.H. Gundlach, et al. Submillimeter tests of the gravitational inverse square law: a search for 'large' extra dimensions. *Phys.Rev.Lett.*, 86:1418–1421, 2001, hep-ph/0011014.

[70] M. Fierz and W. Pauli. On relativistic wave equations for particles of arbitrary spin in an electromagnetic field. *Proc. Roy. Soc. Lond.*, A173:211–232, 1939.

[71] Raman Sundrum. Effective field theory for a three-brane universe. *Phys.Rev.*, D59:085009, 1999, hep-ph/9805471.

[72] Dietmar Ebert, Jan Plefka, and Andreas Rodigast. Gravitational Contributions to the Running Yang-Mills Coupling in Large Extra-Dimensional Brane Worlds. *JHEP*, 0902:028, 2009, 0809.0624.

[73] Herbert W. Hamber. Quantum gravitation: The Feynman path integral approach. 2009.

[74] Hsin-Chia Cheng. 2009 TASI Lecture – Introduction to Extra Dimensions. 2010, 1003.1162.

[75] Steen Hannestad and Georg G. Raffelt. Stringent neutron star limits on large extra dimensions. *Phys.Rev.Lett.*, 88:071301, 2002, hep-ph/0110067.

[76] Lawrence J. Hall and David Tucker-Smith. Cosmological constraints on theories with large extra dimensions. *Phys.Rev.*, D60:085008, 1999, hep-ph/9904267.

[77] Steen Hannestad. Strong constraint on large extra dimensions from cosmology. *Phys.Rev.*, D64:023515, 2001, hep-ph/0102290.

[78] Stephen J. Asztalos, Leslie J. Rosenberg, Karl van Bibber, Pierre Sikivie, and Konstantin Zioutas. Searches for astrophysical and cosmological axions. *Ann.Rev.Nucl.Part.Sci.*, 56:293–326, 2006.

[79] M.L. Graesser. Extra dimensions and the muon anomalous magnetic moment. *Phys.Rev.*, D61:074019, 2000, hep-ph/9902310.

[80] Prasanta Das and Sreerup Raychaudhuri. Rho parameter constraints on models with large compact dimensions. 1999, hep-ph/9908205.

[81] Tao Han, Danny Marfatia, and Ren-Jie Zhang. Oblique parameter constraints on large extra dimensions. *Phys.Rev.*, D62:125018, 2000, hep-ph/0001320.

[82] Michael E. Peskin and Tatsu Takeuchi. A New constraint on a strongly interacting Higgs sector. *Phys.Rev.Lett.*, 65:964–967, 1990.

[83] Paul R. Archer and Stephan J. Huber. Electroweak Constraints on Warped Geometry in Five Dimensions and Beyond. *JHEP*, 1010:032, 2010, 1004.1159.

[84] Paul R. Archer and Stephan J. Huber. Reducing Constraints in a Higher Dimensional Extension of the Randall and Sundrum Model. *JHEP*, 1103:018, 2011, 1010.3588.

[85] Schuyler Cullen, Maxim Perelstein, and Michael E. Peskin. TeV strings and collider probes of large extra dimensions. *Phys. Rev.*, D62:055012, 2000, hep-ph/0001166.

[86] W.T. Giele, E.W.Nigel Glover, and David A. Kosower. Higher order corrections to jet cross-sections in hadron colliders. *Nucl.Phys.*, B403:633–670, 1993, hep-ph/9302225.

[87] Tilman Plehn. LHC Phenomenology for Physics Hunters. pages 125–180, 2008, 0810.2281.

[88] Tao Han, David L. Rainwater, and D. Zeppenfeld. Drell-Yan plus missing energy as a signal for extra dimensions. *Phys.Lett.*, B463:93–98, 1999, hep-ph/9905423.

[89] King-man Cheung and Greg L. Landsberg. Drell-Yan and diphoton production at hadron colliders and low scale gravity model. *Phys.Rev.*, D62:076003, 2000, hep-ph/9909218.

[90] JoAnne L. Hewett. Indirect collider signals for extra dimensions. *Phys. Rev. Lett.*, 82:4765–4768, 1999, hep-ph/9811356.

[91] Kaoru Hagiwara, Qiang Li, and Kentarou Mawatari. Jet angular correlation in vector-boson fusion processes at hadron colliders. *JHEP*, 0907:101, 2009, 0905.4314.

[92] Xavier Calmet, Stephen D.H. Hsu, and David Reeb. Quantum gravity at a TeV and the renormalization of Newton's constant. *Phys.Rev.*, D77:125015, 2008, 0803.1836.

[93] Gian Francesco Giudice and Alessandro Strumia. Constraints on extra dimensional theories from virtual graviton exchange. *Nucl. Phys.*, B663:377–393, 2003, hep-ph/0301232.

[94] Daniel F. Litim. Fixed points of quantum gravity. *Phys.Rev.Lett.*, 92:201301, 2004, hep-th/0312114.

[95] Daniel F. Litim and Tilman Plehn. Signatures of gravitational fixed points at the LHC. *Phys. Rev. Lett.*, 100:131301, 2008, 0707.3983.

[96] A. Zee. Quantum field theory in a nutshell. Princeton, UK: Princeton Univ. Pr. (2010) 576 p.

[97] Roberto Franceschini, Pier Paolo Giardino, Gian F. Giudice, Paolo Lodone, and Alessandro Strumia. LHC bounds on large extra dimensions. *JHEP*, 1105:092, 2011, 1101.4919. * Temporary entry *.

[98] Michael Atkins and Xavier Calmet. Unitarity bounds on low scale quantum gravity. *Eur.Phys.J.*, C70:381–388, 2010, 1005.1075.

[99] G. Passarino and M. J. G. Veltman. One Loop Corrections for e+ e- Annihilation Into mu+ mu- in the Weinberg Model. *Nucl. Phys.*, B160:151, 1979.

[100] Steven B. Giddings, Maximilian Schmidt-Sommerfeld, and Jeppe R. Andersen. High energy scattering in gravity and supergravity. *Phys.Rev.*, D82:104022, 2010, 1005.5408.

[101] E. Accomando, Ignatios Antoniadis, and K. Benakli. Looking for TeV scale strings and extra dimensions. *Nucl.Phys.*, B579:3–16, 2000, hep-ph/9912287.

[102] W.J. Stirling, E. Vryonidou, and J.D. Wells. Eikonal regime of gravity-induced scattering at higher energy proton colliders. *Eur.Phys.J.*, C71:1642, 2011, 1102.3844.

[103] Masako Bando, Taichiro Kugo, Tatsuya Noguchi, and Koichi Yoshioka. Brane fluctuation and suppression of Kaluza-Klein mode couplings. *Phys.Rev.Lett.*, 83:3601–3604, 1999, hep-ph/9906549.

[104] S.V. Shmatov. Searches for extra dimensions in the CMS experiment at the Large Hadron Collider (LHC). *Phys.Atom.Nucl.*, 74:490–495, 2011.

[105] Serguei Chatrchyan et al. Search for Large Extra Dimensions in the Diphoton Final State at the Large Hadron Collider. *JHEP*, 1105:085, 2011, 1103.4279. * Temporary entry *.

[106] Guido Altarelli and Riccardo Barbieri. Vacuum polarization effects of new physics on electroweak processes. *Phys.Lett.*, B253:161–167, 1991.

[107] James D. Wells. TASI lecture notes: Introduction to precision electroweak analysis. pages 41–64, 2005, hep-ph/0512342.

[108] Roberto Tenchini and Claudio Verzegnassi. The physics of the Z and W bosons. 2008.

[109] Precision electroweak measurements on the Z resonance. *Phys.Rept.*, 427:257–454, 2006, hep-ex/0509008.

[110] J.A.M. Vermaseren. New features of FORM. 2000, math-ph/0010025.

[111] Dietmar Ebert, Jan Plefka, and Andreas Rodigast. Absence of gravitational contributions to the running Yang-Mills coupling. *Phys.Lett.*, B660:579–582, 2008, 0710.1002.

[112] Geraldine Servant and Timothy M.P. Tait. Is the lightest Kaluza-Klein particle a viable dark matter candidate? *Nucl.Phys.*, B650:391–419, 2003, hep-ph/0206071.

[113] Graham D. Kribs. Phenomenology of extra dimensions. 2006, hep-ph/0605325.

[114] H.L. Lai, J. Botts, J. Huston, J.G. Morfin, J.F. Owens, et al. Global QCD analysis and the CTEQ parton distributions. *Phys.Rev.*, D51:4763–4782, 1995, hep-ph/9410404.

[115] Johan Alwall, Pavel Demin, Simon de Visscher, Rikkert Frederix, Michel Herquet, et al. MadGraph/MadEvent v4: The New Web Generation. *JHEP*, 0709:028, 2007, 0706.2334.

[116] Alessandro Codello, Roberto Percacci, and Christoph Rahmede. Ultraviolet properties of f(R)-gravity. *Int. J. Mod. Phys.*, A23:143–150, 2008, 0705.1769.

Publications

Gerwick. Asymptotically Safe Gravitons in Electroweak Precision Physics. arXiv:1012.1118, Published in Eur.Phys.J.C71:1676, 2011.

Gerwick, Litim and Plehn. Kaluza-Klein Gravitons at the LHC. arXiv:1101.5548, published in Phys.Rev.D83:084048, 2011.

Gerwick and Plehn. UV Completions of Extra Dimensions. arXiv:0912.2653, In Proceedings of Science, 2009.

Gerwick, Plehn and Schumann. Understanding Jet Vetos and Jet Scaling in Higgs Searches. arXiv:0912.2653